

5-2011

## Developmental And Cellular Functions Of Delta-Catenin

Dongmin Gu

Follow this and additional works at: [https://digitalcommons.library.tmc.edu/utgsbs\\_dissertations](https://digitalcommons.library.tmc.edu/utgsbs_dissertations)



Part of the [Cell Biology Commons](#), and the [Developmental Biology Commons](#)

---

### Recommended Citation

Gu, Dongmin, "Developmental And Cellular Functions Of Delta-Catenin" (2011). *Dissertations and Theses (Open Access)*. 114.

[https://digitalcommons.library.tmc.edu/utgsbs\\_dissertations/114](https://digitalcommons.library.tmc.edu/utgsbs_dissertations/114)

This Dissertation (PhD) is brought to you for free and open access by the MD Anderson UTHealth Houston Graduate School at DigitalCommons@TMC. It has been accepted for inclusion in Dissertations and Theses (Open Access) by an authorized administrator of DigitalCommons@TMC. For more information, please contact [digcommons@library.tmc.edu](mailto:digcommons@library.tmc.edu).

**DEVELOPMENTAL AND CELLULAR FUNCTIONS OF DELTA-CATENIN**

by

**Dongmin Gu, M.D., M.S.**

---

**Pierre D. McCrea, Ph.D.  
Supervisory Professor**

---

**Michelle C. Barton, Ph.D.**

---

**Amy K. Sater, Ph.D.**

---

**Lei Li, Ph.D.**

---

**Warren S. Liao, Ph.D.**

**APPROVED:**

---

**Dean  
The University of Texas  
Health Science Center at Houston  
Graduate School of Biomedical Sciences**

**DEVELOPMENTAL AND CELLULAR FUNCTIONS OF DELTA-CATENIN**

**A**

**DISSERTATION**

**Presented to the Faculty of**

**The University of Texas**

**Health Science Center at Houston**

**Graduate School of Biomedical Sciences**

**And**

**The University of Texas**

**M.D. Anderson Cancer Center**

**In Partial Fulfillment**

**of the Requirements**

**for the Degree of**

**DOCTOR OF PHILOSOPHY**

**by**

**Dongmin Gu, M.D., M.S.**

**Houston, Texas**

**May, 2011**

## **DEDICATION**

I dedicate this work to my wife Ying Liu, whose love, trust, patience and encouragement have made it all possible.

## ACKNOWLEDGEMENTS

First and foremost, I would like to thank my mentor Pierre D. McCrea, Ph.D. for his guidance and support in science. Aside from being a great advisor, Dr. McCrea has also been a good friend and helped much with my life. His consideration, patience, forgiveness and numerous other virtues have shaped me into a better person. For those, I am truly indebted.

I also wish to acknowledge members of my Advisory, Candidacy Exam and Supervisory Committees: Michelle C. Barton, Ph.D., Amy K. Sater, Ph.D. (University of Houston), Warren S.-L. Liao, Ph.D., Lei Li, Ph.D., Andreas Bergmann, Ph.D., and Milan Jamrich, Ph.D. (Baylor College of Medicine). Their insight and guidance helped to keep me on the right track with my progress. I also express my gratitude to Malgorzata Kloc, Ph.D. (Methodist Hospital Research Institute), who joined the meetings of McCrea Laboratory and offered her wisdom and knowledge of *Xenopus*.

I further thank members of McCrea Laboratory, past and present, for their contributions to my work and friendship: Hong Ji, Jon P. Lyons, Ph.D., Jae-II Park, Ph.D., Kyucheol Cho, Ph.D., Ji-Yeon Hong, Rachel K. Miller, Ph.D., William A. Munoz and Moonsup Lee.

I also appreciate the Genes and Development Graduate Program (Program Manager: Elisabeth Lindheim) and the Department of Biochemistry and Molecular Biology for providing an exceptional research environment and wonderful administrative assistance (Ruby S. Desiderio and Jodie Polan).

I am especially grateful to my family for their endless love and support: my wife, Ying Liu, my parents: Jianchang Gu and Chuanzhen Dai, My mother-in-law: Ping Ding, and my daughter: Grace L. Gu, who truly delighted my life.

This work was supported by the National Institutes of Health Research Grant (RO1-GM52112), a Texas ARP Grant, and the March of Dimes (1-FY-07-461-01).

# DEVELOPMENTAL AND CELLULAR FUNCTIONS OF DELTA-CATENIN

Publication No. \_\_\_\_\_

Dongmin Gu, Ph.D.

Supervisory Professor: Pierre D. McCrea, PhD.

Catenins have diverse and powerful roles in embryogenesis, homeostasis or disease progression, as best exemplified by the well-known beta-catenin. The less studied delta-catenin likewise contains a central Armadillo-domain. In common with other p120 sub-class members, it acts in a variety of intracellular compartments and modulates cadherin stability, small GTPase activities and gene transcription. In mammals, delta-catenin exhibits neural specific expression, with its knock-out in mice correspondingly producing cognitive defects and synaptic dysfunctions.

My work instead employed the amphibian, *Xenopus laevis*, to explore delta-catenin's physiological functions in a distinct vertebrate system. Initial isolation and characterization indicated delta-catenin's expression in *Xenopus*. Unlike the pattern observed for mammals, delta-catenin was detected in most adult *Xenopus* tissues, although enriched in embryonic structures of neural fate as visualized using RNA in-situ hybridization. To determine delta-catenin's requirement in amphibian development, I employed anti-sense morpholinos to

knock-down its gene products, finding that delta-catenin depletion results in developmental defects in gastrulation, neural crest migration and kidney tubulogenesis, phenotypes that were specific based upon rescue experiments. In biochemical and cellular assays, delta-catenin knock-down reduced cadherin levels and cell adhesion, and impaired activation of RhoA and Rac1, small GTPases that regulate actin dynamics and morphogenetic movements. Indeed, exogenous C-cadherin, dominant-negative RhoA or dominant-active Rac1, significantly rescued delta-catenin depletion. Thus, my results indicate delta-catenin's essential roles in *Xenopus* development, with contributing functional links to cadherins and Rho family small G proteins.

In examining delta-catenin's nuclear roles, I identified delta-catenin as an interacting partner and substrate of the caspase-3 protease, which plays critical roles in apoptotic as well as non-apoptotic processes. Delta-catenin's interaction with and sensitivity to caspase-3 was confirmed using assays involving its cleavage in vitro, as well as within *Xenopus* apoptotic extracts or mammalian cell lines. The cleavage site, a highly conserved caspase consensus motif (DELD) within Armadillo-repeat 6 of delta-catenin, was identified through peptide sequencing. Cleavage thus generates an amino- (1-816) and carboxyl-terminal (817-1314) fragment each containing about half of the central Armadillo-domain. I found that cleavage of delta-catenin both abolishes its association with cadherins,



and impairs its ability to modulate small GTPases. Interestingly, the carboxyl-terminal fragment (817-1314) possesses a conserved putative nuclear localization signal that I found is needed to facilitate delta-catenin's nuclear targeting. To probe for novel nuclear roles of delta-catenin, I performed yeast two-hybrid screening of a mouse brain cDNA library, resolving and then validating its interaction with an uncharacterized KRAB family zinc finger protein I named ZIFCAT. My results indicate that ZIFCAT is nuclear, and suggest that it may associate with DNA as a transcriptional repressor. I further determined that other p120 sub-class catenins are similarly cleaved by caspase-3, and likewise bind ZIFCAT. These findings potentially reveal a simple yet novel signaling pathway based upon caspase-3 cleavage of p120 sub-family members, facilitating the coordinate modulation of cadherins, small GTPases and nuclear functions.

Together, my work suggested delta-catenin's essential roles in *Xenopus* development, and has revealed its novel contributions to cell junctions (via cadherins), the cytoskeleton (via small G proteins), and the nucleus (via ZIFCAT). Future questions include the larger role and gene targets of delta-catenin in the nucleus, and identification of upstream signaling events controlling delta-catenin's activities in development or disease progression.

## TABLE OF CONTENTS

Approval Page	i
Title Page	ii
Dedication	iii
Acknowledgements	iv
Abstract	vi
Table of Contents	ix
List of Illustrations	xiii

### **Chapter I: Introduction**

Cadherins and catenins	2
P120-catenin sub-family	6
Delta-catenin	8
Caspases	12
KRAB zinc finger proteins	14

### **Chapter II: Results**

#### **Part I: Developmental characterization of delta-catenin in *Xenopus laevis*** 16

<i>Xenopus</i> delta-catenin cDNA isolation	17
Delta-catenin temporal expression in <i>Xenopus</i> embryos	22

Xenopus delta-catenin spatial characterization	25
Delta-catenin sub-cellular localization in Xenopus embryos	29
Delta-catenin anti-sense morpholinos	32
Delta-catenin depletion results in developmental phenotypes in gastrulation, neural crest migration and kidney tubulogenesis	33
Delta-catenin depletions are rescued with delta- or p120-catenin	38
Delta-catenin depletion impairs cadherin-dependent adhesive functions	45
Depletion of delta-catenin perturbs Rho and Rac activities	55
<b>Part II: Exploring the roles of delta-catenin in the nucleus</b>	<b>58</b>
Delta-catenin is a novel caspase-3 substrate	59
Caspase-3 cleaves delta-catenin at DELD816 consensus motif	63
Cleavage of delta-catenin abolishes cadherin binding	64
Cleaved delta-catenin fragments are impaired in Rho and Rac modulation	65
An NLS within delta-catenin's Armadillo-repeat 6 enhances 817-1314 nuclear localization	66
Delta-catenin had no detectable effect upon chemical-induced apoptosis	71
ZIFCAT is a novel KRAB zinc finger protein associating with delta-catenin and ARVCF	72
ZIFCAT associates with chromosomal DNA, and may act as a transcriptional repressor	85

### **Chapter III: Discussion**

<b>Part I: Developmental characterization of <i>Xenopus</i> delta-catenin</b>	94
<b>Part II: Exploring the roles of delta-catenin in the nucleus</b>	101

### **Chapter IV: Materials and Methods**

DNA cloning	112
Antibodies and chemicals	112
Cell culture, transfection and luciferase assays	113
Yeast two-hybrid screening	114
PCR oligos and morpholinos	114
Co-immuno-precipitation and immuno-blotting	115
Caspase-3 cleavage and apoptotic assays	116
Manipulation of <i>Xenopus</i> embryos and micro-injection	116
Cell dissociation, re-aggregation and in vitro adhesion assays	118
Immuno-fluorescence and antibody staining	118
In vitro DNA association assay	119
Rho and Rac activation assays	119
Fractionation methods	120
Alcian blue staining	120
Whole mount RNA in-situ hybridization	121
Biostatistics	121

**Chapter V: Bibliography**

123

**Vita**

149

## LIST OF ILLUSTRATIONS

<b>Figure 1.</b> Schematic diagram of the catenin super-family	4
<b>Figure 2.</b> Catenins in the adherens junction and their signaling roles	5
<b>Figure 3.</b> Summary of known delta-catenin protein interactions	10
<b>Figure 4.</b> Primary sequence alignment of <i>Xenopus</i> , human and mouse delta-catenins	19
<b>Figure 5.</b> Phylogenetic analysis and predicted <i>Xenopus</i> delta-catenin isoforms	20
<b>Figure 6.</b> Jpred secondary structure prediction of delta-catenin splicing variants	21
<b>Figure 7.</b> Characterization of delta-catenin alternative pre-mRNA splicings	23
<b>Figure 8.</b> Endogenous delta-catenin protein expression in <i>Xenopus</i> embryos	24
<b>Figure 9.</b> Whole mount in-situ RNA hybridization of delta-catenin	27
<b>Figure 10.</b> Delta-catenin expression profile in adult <i>Xenopus</i> tissues	28
<b>Figure 11.</b> Delta-catenin associates with classical cadherins	30
<b>Figure 12.</b> Membrane-cytosolic fractionation	31
<b>Figure 13.</b> Delta-catenin anti-sense morpholino oligos (splice type)	34
<b>Figure 14.</b> Immuno-blotting evaluation of delta-catenin knock-down	35
<b>Figure 15.</b> Gastrulation phenotypes of <i>Xenopus</i> embryos upon delta-catenin depletion	39

<b>Figure 16.</b> Delta-catenin depletion does not affect dorsal convergent-extension	40
<b>Figure 17.</b> Delta-catenin depletion in presumptive neural ectoderm causes eye and craniofacial defects	41
<b>Figure 18.</b> Delta-catenin depletion perturbs neural crest migration	42
<b>Figure 19.</b> Delta-catenin depletion impairs pronephric kidney tubulogenesis	43
<b>Figure 20.</b> Synergism between delta- and p120-catenin depletions in <i>Xenopus</i>	46
<b>Figure 21.</b> Delta-catenin depletion-rescue experiments	47
<b>Figure 22.</b> Over-expression of delta-catenin produces delays in blastopore closure	48
<b>Figure 23.</b> Delta-catenin depletion leads to reduced cadherin functions	49
<b>Figure 24.</b> C-cadherin effectively rescues delta-catenin depletion in <i>Xenopus</i> embryos	52
<b>Figure 25.</b> Characterization of delta-catenin $\Delta$ ARM1-5 construct-I	53
<b>Figure 26.</b> Characterization of delta-catenin $\Delta$ ARM1-5 construct-II	54
<b>Figure 27.</b> Delta-catenin depletion results in activation of RhoA and inhibition of Rac1	57
<b>Figure 28.</b> Delta-catenin is cleaved by caspase-3 in vitro	61
<b>Figure 29.</b> Delta-catenin is cleaved in apoptotic extracts	62
<b>Figure 30.</b> Identification of caspase-3 consensus motif within delta-catenin	67

<b>Figure 31.</b> Caspase cleavage site verified via site-directed mutagenesis	68
<b>Figure 32.</b> P120-catenin is cleaved by caspase-3 in vitro	69
<b>Figure 33.</b> Cleaved delta-catenin fragments fail to associate with cadherins	70
<b>Figure 34.</b> Cleaved delta-catenin fragments exhibit impaired small GTPase regulation	73
<b>Figure 35.</b> The NLS within Armadillo-repeat 6 enhances 817-1314 localization to 293T cell nuclei	74
<b>Figure 36.</b> Sub-cellular localizations of delta-catenin constructs in MDA-MB-435 melanoma cells	75
<b>Figure 37.</b> Cytosolic-nuclear fractionation	76
<b>Figure 38.</b> The NLS within Armadillo-repeat 6 enhances 817-1314 localization to nuclei	77
<b>Figure 39.</b> Cell death detection ELISA-I	78
<b>Figure 40.</b> Cell death detection ELISA-II	79
<b>Figure 41.</b> Diagram of delta-catenin protein interactions identified through yeast two-hybrid screening	81
<b>Figure 42.</b> Phylogenetic tree of ZIFCAT and related proteins	82
<b>Figure 43.</b> Primary sequence analysis of novel KRAB zinc finger protein ZIFCAT	83
<b>Figure 44.</b> ZIFCAT associates with delta-catenin	88
<b>Figure 45.</b> ZIFCAT associates with ARVCF-catenin	89



<b>Figure 46.</b> ZIFCAT is a DNA-associating nuclear protein	90
<b>Figure 47.</b> The amino-terminal region of ZIFCAT represses UAS-luciferase activity	91
<b>Figure 48.</b> Neither delta-, nor ARVCF-catenin, have a notable impact upon the transcriptional repression conferred by Gal4DBD-ZIFCAT	92

# **CHAPTER I**

## **INTRODUCTION**

## **Cadherins and catenins**

Cadherins are calcium dependent transmembrane glycoproteins best known to mediate cell adhesion. Together with catenins, which associate with cadherin intracellular portions, and indirectly and dynamically with the actin cytoskeleton, cadherins play essential roles to establish adherens junctions and participate in the maintenance of tissue architecture or morphogenesis (Gumbiner, 2005; Harris and Tepass, 2010; Yap and Kovacs, 2003). Mis-regulation in adherens junction structure or function are thus associated with many pathological processes, including tumor progression and metastasis (Jeanes et al., 2008; Reynolds and Carnahan, 2004).

Catenins are related to the *Drosophila* Armadillo protein, and were first isolated in complex with cadherins at cell borders (Gumbiner, 2005; Lien et al., 2006). All catenins (with the exception of alpha-catenin) contain a central Armadillo-domain composed of nine or twelve repeats (each about 42 amino acids). Such repeats fold into a super-helix of helices and bear crucial binding interfaces for multiple protein interactions including those with cadherins (Huber et al., 1997; Xing et al., 2008). Certain catenins encode a carboxyl-terminal PDZ (PSD95, DlgA and ZO-1) domain interaction motif and are capable of binding a large number of PDZ proteins. Based upon the Armadillo-domain, overall sequence similarity and the binding positions on cadherins, the catenin family was divided into three sub-families referred to by a representative member:

beta-catenin, p120-catenin and plakophilin (Anastasiadis, 2007; Anastasiadis and Reynolds, 2001; McCrea and Gu, 2010) (Figure 1). Beta-catenin sub-family catenins (beta-catenin or plakoglobin/ gamma-catenin) associate with the carboxyl-termini of classical cadherins, while the membrane-proximal region of cadherins binds p120-catenin (p120-, delta-, Armadillo Repeat Protein Deleted in Velo-Cardio-Facial Syndrome/ ARVCF- and p0071-catenin) and plakophilin-catenin (plakophilin 1, 2 and 3) sub-family members. Beta-catenin and plakoglobin further indirectly associate with the intracellular actin cytoskeletons. Through such associations, catenins participate in junctional assembly and maintenance, and assist with cadherin dependent morphogenesis.

In addition to cadherin-binding at the cell membrane, catenins transduce intracellular signals critical for many cellular, developmental or pathological events (McCrea et al., 2009; McCrea and Park, 2007; Reynolds, 2007) (Figure 2). For example, Wnt ligands associate with the membrane receptor Frizzled and co-receptor LRP (Low Density Lipoprotein Receptor Related Protein). Such association directs membrane localization of Dishevelled and inactivation of the intracellular destruction complex (composed of Glycogen Synthase Kinase 3/ GSK3beta, Axin, Adenomatous Polyposis Coli/ APC, etc.), which would otherwise basally degrade the signaling pool of beta-catenin. This allows the signaling pool of beta-catenin to accumulate in the cytoplasm and enter the nucleus. In the nuclear compartment, beta-catenin associates with LEF/ TCF (Lymphoid Enhancer Factor/ T Cell Factor) transcription factors and activates

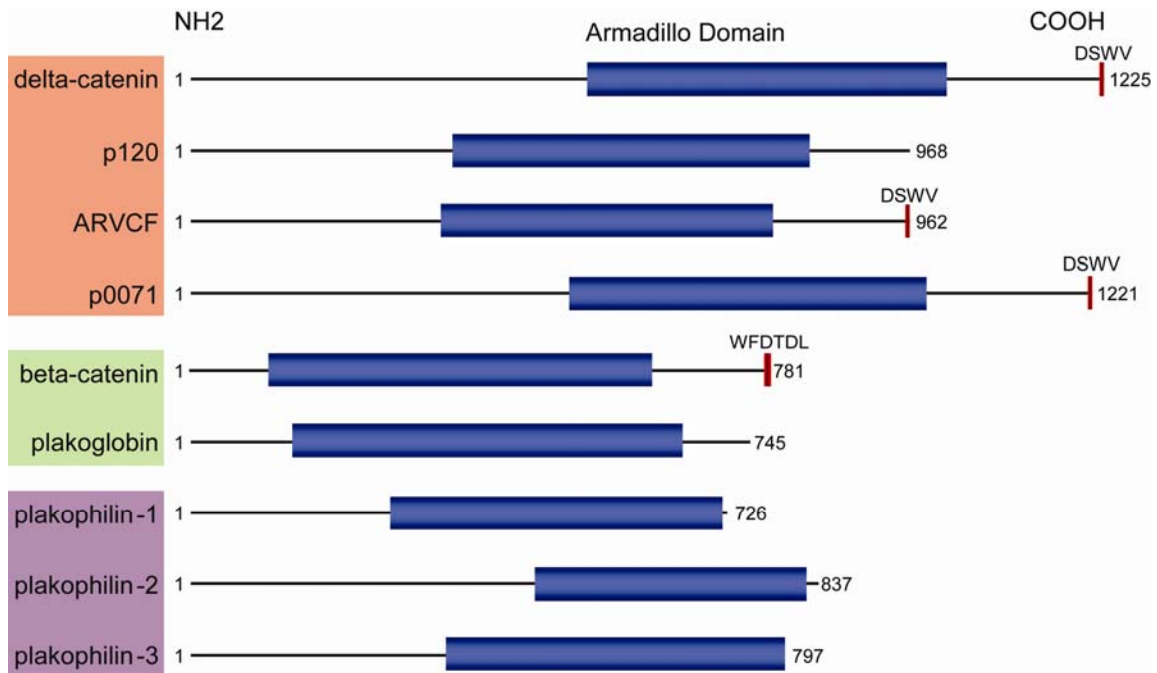


Figure 1. Schematic diagram of the catenin super-family.

Depicted are catenins of human source. The beta-catenin sub-family (beta-catenin and plakoglobin) catenins contain 12 repeats within their Armadillo domain, while members of the p120-catenin and plakophilin sub-families (all others) contain 9 characteristically spaced repeats and have more divergent amino- and carboxyl-terminal regions. Type I PDZ-binding motifs are present at the carboxyl-termini of certain catenins. Peptide lengths and positioning of domains/ motifs are drawn to scale.

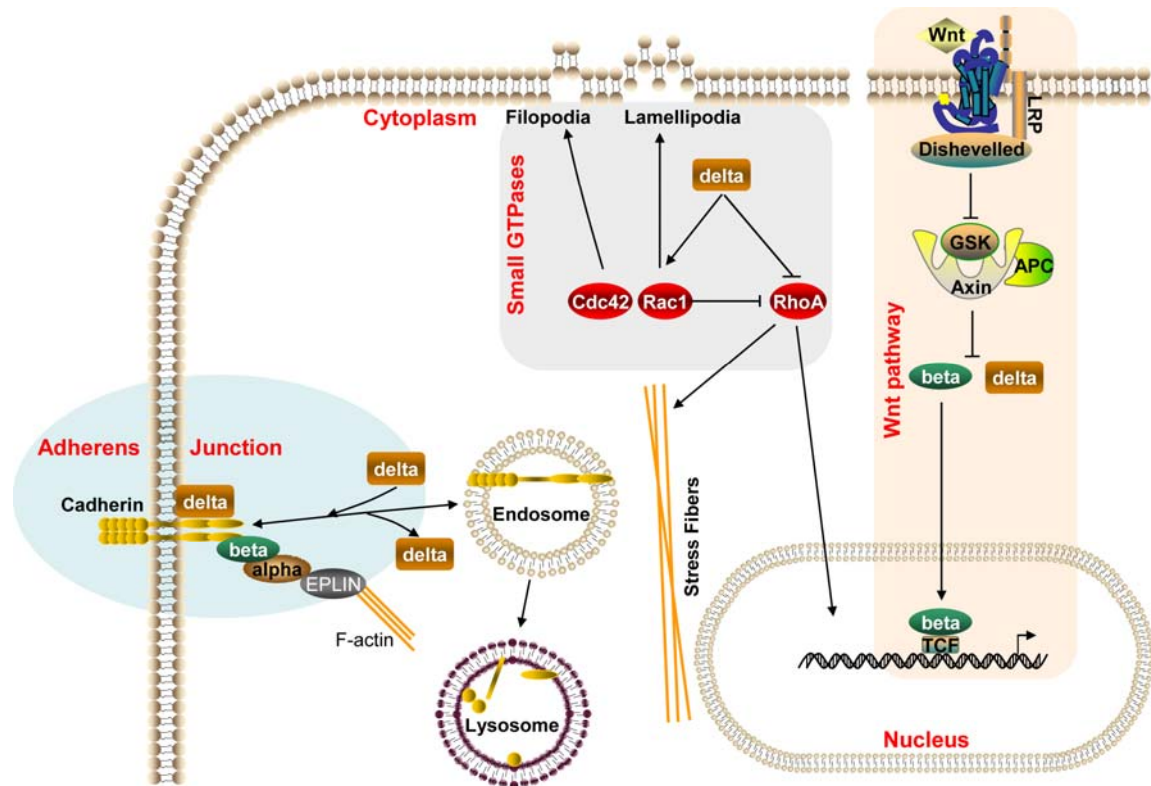


Figure 2. Catenins in the adherens junction and their signaling roles.

Beta-catenin is directly involved in adherens junction assembly by associating with the carboxyl-termini of classical cadherins and linking cadherin complexes to actin filaments. Delta-catenin and other p120 sub-family catenins bind the cadherin membrane-proximal region and are capable of regulating cadherin metabolic stability and lateral clustering, and thereby adhesive strength. Most catenins are believed to have nuclear functions, with beta-catenin being the best example to date. In the presence of Wnt stimuli, beta-catenin is protected from the degradation complex and proteasome, and enters the nucleus to convert LEF/TCF into transcriptional activators. Delta-catenin and other p120-catenin sub-family members have additional roles modulating Rho family small GTPase functions. These activities contribute to a wide spectrum of downstream effects including actin remodeling, membrane dynamics, cytokinesis and transcriptional regulations.

Wnt target genes. Varied downstream outcomes are affected as a result, extending for example from pluripotency to terminal differentiation, and from cell proliferation to apoptosis (Cadigan and Peifer, 2009; Logan and Nusse, 2004; Willert and Jones, 2006).

### **P120-catenin sub-family**

As mentioned earlier, the p120-catenin sub-family (p120-, delta-, ARVCF- or p0071-catenin) differs from beta-catenin in having nine characteristically-spaced Armadillo repeats, and binding the cadherin juxta-membrane region/ JMR. P120-catenins do not directly anchor cadherins to actin filaments. Rather, they regulate cadherin lateral surface clustering and inhibit cadherin endocytosis (Davis et al., 2003; Kowalczyk and Reynolds, 2004). Thus, p120 sub-family catenins contribute to cadherin-dependent cell adhesion, polarity and motility, and consequently to tissue homeostasis and developmental morphogenesis (Figure 2) (Anastasiadis, 2007; Anastasiadis and Reynolds, 2001; McCrea and Gu, 2010).

P120 sub-family catenins have some intriguing properties that beta-catenin lacks. One such prominent activity is the modulation of Rho family small G proteins, including RhoA, Rac1 and Cdc42 (Figure 2). Maintaining small GTPases in an active/ GTP-bound versus inactive/ GDP-bound is influenced by many positive and negative effectors (Bustelo et al., 2007; Popoff and Geny,

2009). P120-catenin sub-family catenins associate with certain GEFs (Guanine Nucleotide Exchange Factors) (e.g., Vav2), or with GAPs (GTPase Activating Proteins) (e.g., p190 Rho GAP), facilitating activation of Rac1 or Cdc42 (Noren et al., 2000; Wildenberg et al., 2006). Further, intrinsic GDI (Guanine Nucleotide Dissociation Inhibitors) activities of p120-catenin may allow its direct binding to RhoA, blocking GDP/ GTP exchange and this resulting in Rho inhibition (Anastasiadis et al., 2000; Castano et al., 2007). The downstream effects of Rho activation/ inhibition may be context-dependent given that they function in multiple cellular capacities. Focusing on cytoskeletal regulation, RhoA activation generally leads to ROCK (Rho Associated Protein Kinase) activation, and thus the formation of stress fibers and cellular contractility, while activation of Rac1 or Cdc42 often results in heightened membrane protrusions such as lamellipodia and filopodia, respectively (Hall, 1998; Popoff and Geny, 2009).

The seemingly contrasting role of p120-catenin in cell adhesion versus motility has led to the hypothesis of various p120-catenin sub-cellular pools. When bound to cadherins at the cell membrane, p120-catenin protects cadherins from endocytosis and degradation by lysosomes, thereby enhancing cell adhesion. Conversely, when dissociated from cadherins and present in the cytoplasm, p120-catenin exhibits more pronounced small GTPase effects, associated with motile states. This view is relevant to either physiologic scenarios or pathologic contexts. For example, one can envisage an epithelial-mesenchymal transition (EMT) is promoted upon p120-catenin release from



cadherins, resulting in both reduced adhesion and increased motility, thereby promoting developmental morphogenesis such as neural crest migration, or alternatively, that of primary tumor cells losing cadherin-mediated polarity and metastasize distally (Reynolds and Roczniak-Ferguson, 2004; van Hengel and van Roy, 2007).

Beyond the presence at cell contacts and in the cytosol, p120-catenins have also been observed in the nucleus. In the nuclear compartment, p120-catenin binds and relieves the transcription repression of Kaiso, a Poxvirus Zinc Finger/ POZ zinc finger protein (Daniel, 2007; Ilioka et al., 2009; van Roy and McCrea, 2005). In common with beta-catenin but employing a different mechanism, p120-catenin de-represses select canonical Wnt targets (Siamois et al., 2004; Park et al., 2006; Park et al., 2005). Intriguingly, recent findings indicate that p120 sub-family catenins are metabolically stabilized in response to upstream Wnt stimulation. Activation of the canonical Wnt pathway results in greater p120-catenin de-repression of Kaiso and associated with gene activation (Casagolda et al., 2010; Hong et al., 2010; Oh et al., 2009).

### **Delta-catenin**

Delta-catenin was initially isolated in a search for proteins with homology to Plakophilin-1 (Neural Plakophilin Related Armadillo Repeat Protein, NPARP),

or in yeast two-hybrid screenings for interacting partners of Presenilin-1 (CTNND2) (Levesque et al., 1999; Paffenholz and Franke, 1997; Tanahashi and Tabira, 1999; Zhou et al., 1997). Characterization of delta-catenin revealed its predominant expression in neural tissues of mammalian species, including the central nervous system and a number of neuro-secretory tissues (Ho et al., 2000; Paffenholz and Franke, 1997). Hemizygous deletion of the human chromosomal region (5p) containing delta-catenin is associated with mental retardation in Cri-du-Chat syndrome, a rare genetic disorder characterized by high-pitched cries, mental and growth retardation and distinctive facial features (Medina et al., 2000). Further more direct evidence regarding delta-catenin's neural functions came from gene targeting studies, wherein its knock-out in mice caused severe impairments in brain cognition and abnormal synaptic plasticity (Israely et al., 2004; Matter et al., 2009).

Delta-catenin binds multiple proteins at neural adherens or synaptic junctions (Figure 3). Most of these interactions occur through delta-catenin's central Armadillo-domain or its carboxyl-terminal PDZ binding motif (Arikkath et al., 2008; Deguchi et al., 2000; Fujita et al., 2004; Ide et al., 1999; Izawa et al., 2002; Jones et al., 2002; Kim et al., 2006; Laura et al., 2002; Lu et al., 2002; Mackie and Aitken, 2005; Martinez et al., 2003; Munoz et al., 2007; Silverman et al., 2007). Although the functions of most such associations remain unclear at present, delta-catenin was presumed to contribute scaffolding activities and exert roles as a sensor for synaptic functions in neurons (Kosik et al., 2005).

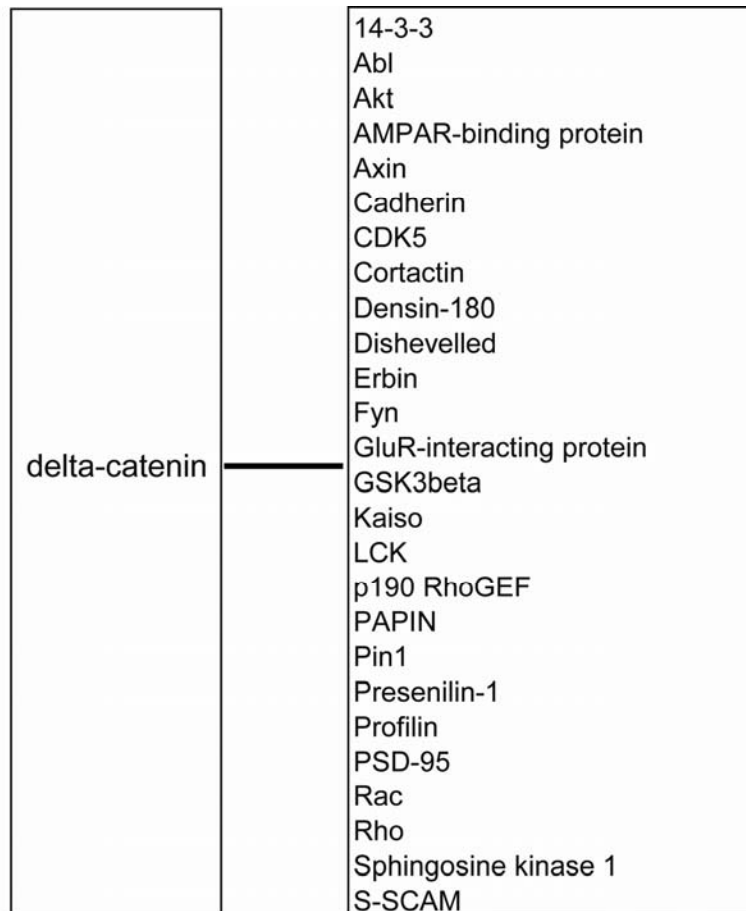


Figure 3. Summary of known delta-catenin protein interactions.

Most interactions occur through delta-catenin's Armadillo domain or the PDZ-binding motif.

As a member of the p120-catenin sub-family, delta-catenin possesses certain shared functions with p120-, ARVCF- or p0071-catenin (Hatzfeld, 2005; Kosik et al., 2005; McCrea and Park, 2007). Delta-catenin interacts with cadherin juxta-membrane regions and stabilizes the larger adhesion complex by reducing its rate of internalization (Lu et al., 1999; Xiao et al., 2007). In primary hippocampal neurons, delta-catenin promotes branching of dendrites and protrusion of spines, while similarly in fibroblasts inducing cytoskeletal reorganization and process extension (Arikkath et al., 2008; Kim et al., 2002; Lu et al., 2002; Lu et al., 1999). These effects rely mainly upon delta-catenin's direct or indirect associations with small GTPases and/ or their downstream effectors (Abu-Elneel et al., 2008; Kim et al., 2007; Kim et al., 2008a; Kim et al., 2008b; Martinez et al., 2003). Aside from its roles at the adherens junction of plasma membrane, and in the cytoplasm with small GTPases, delta-catenin is intriguingly also present within the nuclei of certain tissues. For example, delta-catenin binds Kaiso in the nucleus of neural-muscular junctions and activates the transcription of Rapsyn, which participates in anchoring and stabilizing the nicotinic acetylcholine receptor at synaptic sites (Rodova et al., 2004).

From the perspective of human disease, delta-catenin is over-expressed in prostate, lung and breast carcinomas, with the relationship to prostate cancer being best established (Burger et al., 2002; Kim et al., 2008c; Lu et al., 2005; Lu et al., 2008; Wang et al., 2008; Zhang et al., 2010b). Prostate adenocarcinoma is the most prevalent non-cutaneous cancer and the second leading cause of

cancer-related death of US males. Aberrant high-expression of delta-catenin in prostate cancer is associated with a decrease in E-cadherin protein levels (Lu et al., 2005). Further studies indicate that delta-catenin is capable of promoting expansion of prostate adenocarcinoma cells; while conversely, its haplo-insufficiency impaired pathological angiogenesis and reduced tumor growth (DeBusk et al., 2010; Zeng et al., 2009). Although delta-catenin's relationship to tumorigenesis is just beginning to be investigated, its conjectured nuclear activities is likely to be pursued by workers in the field, given that in gene profiling studies, delta-catenin over-expression results in altered transcription of survival and cell cycle regulators (Lu, 2010; Zeng et al., 2009).

## **Caspases**

Apoptosis or programmed cell death is a physiologically controlled process of cell suicide. Activated caspases cleave specific cellular substrates at defined motifs, with dying cells presenting characteristic morphological features (Kumar, 2007; Lockshin and Zakeri, 2007). It has been long appreciated that caspases have many roles apart from apoptosis, such as in immune defense, proliferation, fate determination, terminal differentiation, cell migration and neuro-degeneration, etc. In tumorigenesis, apoptosis pathways are often active in attempts to remove defective cells. Loss of caspase activity is associated with unchecked cell proliferation and the progression of cancer. However, caspases have also been observed to be aberrantly activated while promoting cancer

progression and metastasis. The mechanisms by which caspases exert these 'non-traditional' functions are still under active investigation, yet likely relate to their temporally, spatially and quantitatively controlled enzymatic activations (Feinstein-Rotkopf and Arama, 2009; Kuranaga and Miura, 2007).

Interestingly, many cadherins and catenins are targeted by caspases, yielding varied downstream outcomes (Brancolini et al., 1997; Cirillo et al., 2008; Dusek et al., 2006; Herren et al., 1998; Hunter et al., 2001; Kessler and Muller, 2009; Ling et al., 2001; Senthivinayagam et al., 2009; Steinhusen et al., 2000; Steinhusen et al., 2001; Weiske and Huber, 2005). Although the underlining mechanisms and consequences of cadherin and catenin proteolysis remain under study, with regards to epithelial apoptosis, the dismantling of cell-cell contacts likely assists dying cells in detaching themselves, and/ or in being removed by surrounding or recruited scavenger cells (Ferber et al., 2008; McCusker and Alfandari, 2009; Parisiadou et al., 2004; Suzanne and Steller, 2009; Zheng et al., 2009). Given that adherens junctions are dynamic structures, as made evident in development and wound repair (etc.), this regulated proteolysis of catenins may permit rapid junctional (as well as small GTPases) responses to upstream signaling events, with the generated catenin fragments conceivably having further gene regulatory activities (Steinhusen et al., 2000).

## **KRAB zinc finger proteins**

KRAB (Kruppel-Associated Box) zinc finger proteins comprise the largest sub-family of zinc finger transcription factors and are present only in tetrapod vertebrates. Such proteins feature a carboxyl-terminal C2H2 type zinc finger region that binds DNA (and proteins), and an amino-terminal KRAB motif associating with transcriptional cofactors such as KAP1 (KRAB Associated Protein 1) to modulate gene repression (Groner et al., 2010; O'Geen et al., 2007). Although the functions of most family members have not been well studied, a few examples suggested they contribute to transcriptional repression at RNA polymerase I, II, and III promoters, binding and splicing of RNA, and control of nucleolus function. As such, KRAB zinc finger proteins exert a wide variety of functions in cell differentiation, cell proliferation, apoptosis, and neoplastic transformation (Looman et al., 2002; Urrutia, 2003).

## **CHAPTER II**

### **RESULTS**



## **Part I: Developmental characterization of delta-catenin in *Xenopus laevis***

**Summary:** Earlier work in mouse indicated that delta-catenin knock-out affected synaptic functions leading to deficits in learning and memory, but otherwise few effects on embryonic development. To explore delta-catenin's physiological functions in a distinct vertebrate system, I employed the amphibian *Xenopus laevis* (African clawed frog). The *Xenopus* system is recognized for its experimental advantages in developmental and cell biology, including rapid external embryonic development, large embryos to facilitate microinjections, an established fate-map, the capability to work with explants *ex vivo*, and the ability to address mechanistic hypotheses via rescue analysis (Sive et al., 2000). As Part I of my dissertation, I report the isolation and characterization of *Xenopus* delta-catenin. I found that delta-catenin is regularly transcribed in *Xenopus* embryos, with at least three alternatively-spliced forms. Consistent with p120-catenin, there exist a number of alternative translation start sites for delta-catenin, suggesting structural and functional complexity. Unlike the neural-restricted expression of mammalian orthologs, delta-catenin is detected in most adult *Xenopus* tissues, although is enriched in neural structures when evaluated using *in-situ* hybridization. In addition to the fraction that binds cadherins, delta-catenin displays non-plasma membrane pools that may be implicated in cytoplasmic and/ or nuclear functions.

To determine delta-catenin's functions in amphibian development, I

employed anti-sense morpholino oligos to knock-down its gene products. Delta-catenin depletion caused developmental defects in gastrulation, neural crest migration and kidney tubulogenesis, phenotypes that were specific based upon rescue experiments. Delta-catenin depletion phenotypes in gastrulation were further enhanced by co-depletion of p120-catenin. Conversely, defects were significantly rescued by p120-catenin, suggesting roles shared by these catenins. In biochemical assays, delta-catenin knock-down reduced cadherin levels and cell adhesion and impaired activation of RhoA and Rac1, small GTPases that regulate actin dynamics and morphogenetic movements. As expected, C-cadherin, dominant-negative RhoA (N19) or dominant-active Rac1 (V12) significantly rescued delta-catenin depletion. Collectively, my experiments indicate that delta-catenin plays an essential role in amphibian development, with contributing functional links to cadherins and Rho family small G proteins.

### **Xenopus delta-catenin cDNA isolation**

To isolate the cDNA for *Xenopus* delta-catenin, I performed Rapid Amplification of cDNA Ends/ RACE PCR employing total RNA extracted from adult *Xenopus* brain. In conjunction, I referred to the available *Xenopus* sequence resources from the Ensembl genome, Xenbase and *Xenopus* Developmental Biology database/ XDB. PCR products of full-length delta-catenin migrating at the predicted size were resolved on agarose gels, purified and ligated into the cloning vector (Invitrogen). Approximately thirty potential delta-

catenin clones were sequenced. The longest cDNA isolated contains 3942 base pairs and encodes 1314 amino acids (predicted molecular weight of 144 kDa). *Xenopus* delta-catenin shows strong sequence homology (90%) with mammalian (human or mouse) orthologs. In common with p120-catenin, I identified four conserved methionines, which may serve as alternative translation start sites (Figure 4, marked with asterisks).

Furthermore, alignment of all sequenced clones identified three sequence elements (A, B and C) of *Xenopus* delta-catenin that were recognized in mammals. Conversely, mouse delta-catenin contains a splicing variant (D) that I did not identify in *Xenopus* (Kawamura et al., 1999). These variants are likely to result from alternative splicing, since they occur precisely within predicted exon junctions (Figure 4). Consistent with other p120 sub-family members, the multiple predicted translation initiation sites and alternative splicing events would be expected to generate multiple protein isoforms of delta-catenin in *Xenopus*, possibly having distinct functional attributes (Paredes et al., 2007; Yanagisawa et al., 2008). Figure 5 illustrates the phylogenetic tree of delta-catenin and its major potential protein isoforms. In Figure 6, I employed the Jpred program to predict the structural outcomes of delta-catenin splicing variants. Element A is located towards the amino-terminus of delta-catenin, and when examined in silico as an isolated unit, is predicted to form a helical structure. Splicing variants B and C are located towards delta-catenin's carboxyl-terminus and potentially

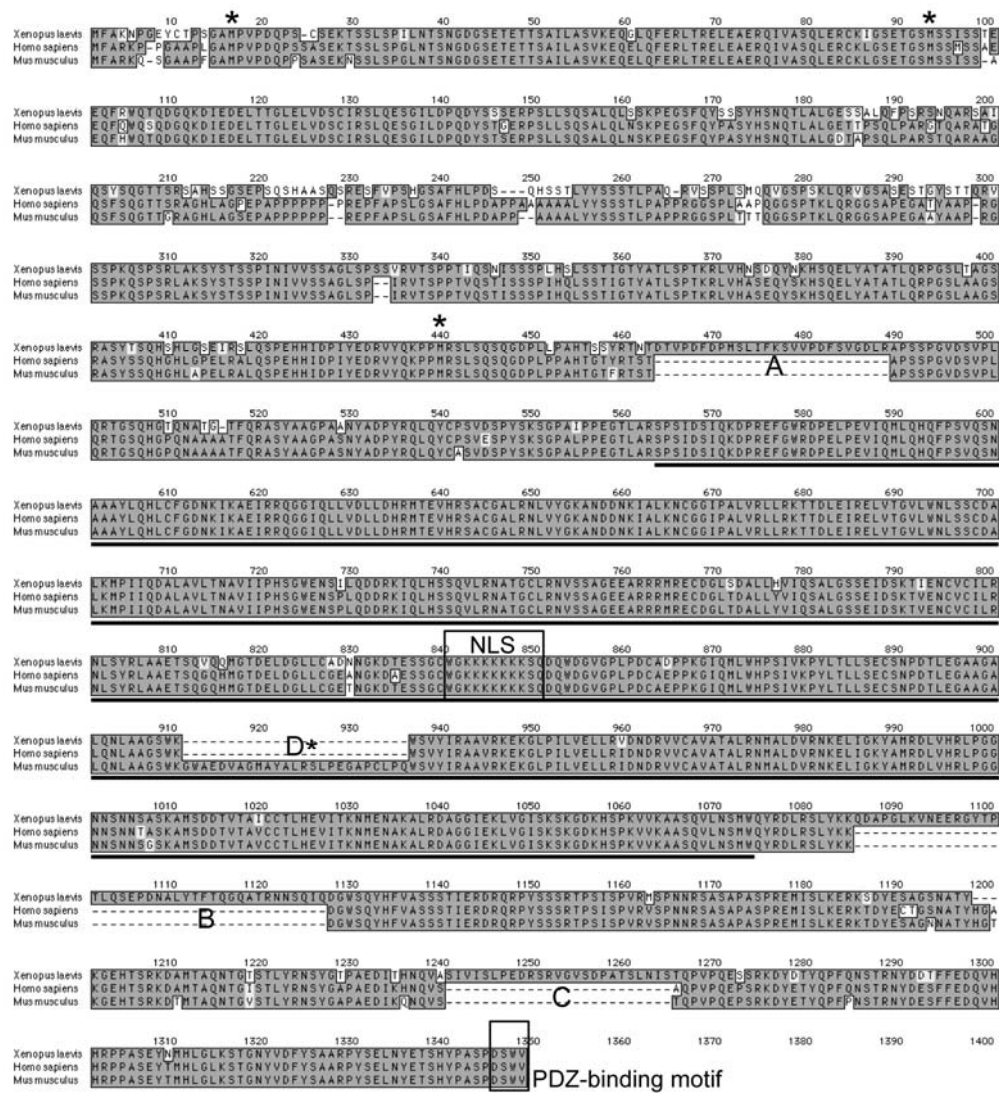


Figure 4. Primary sequence alignment of *Xenopus*, human and mouse delta-catenins.

*Xenopus* delta-catenin exhibits strong homology with human and mouse orthologs. Three alternative splicing events identified in *Xenopus* are labeled A-C (with D reported in mouse). The central Armadillo domain is underlined, while black boxes outline the putative Nuclear Localization Sequence (NLS) or the PDZ-binding motif. Asterisks mark the three methionines potentially serving as alternative translation initiation sites.

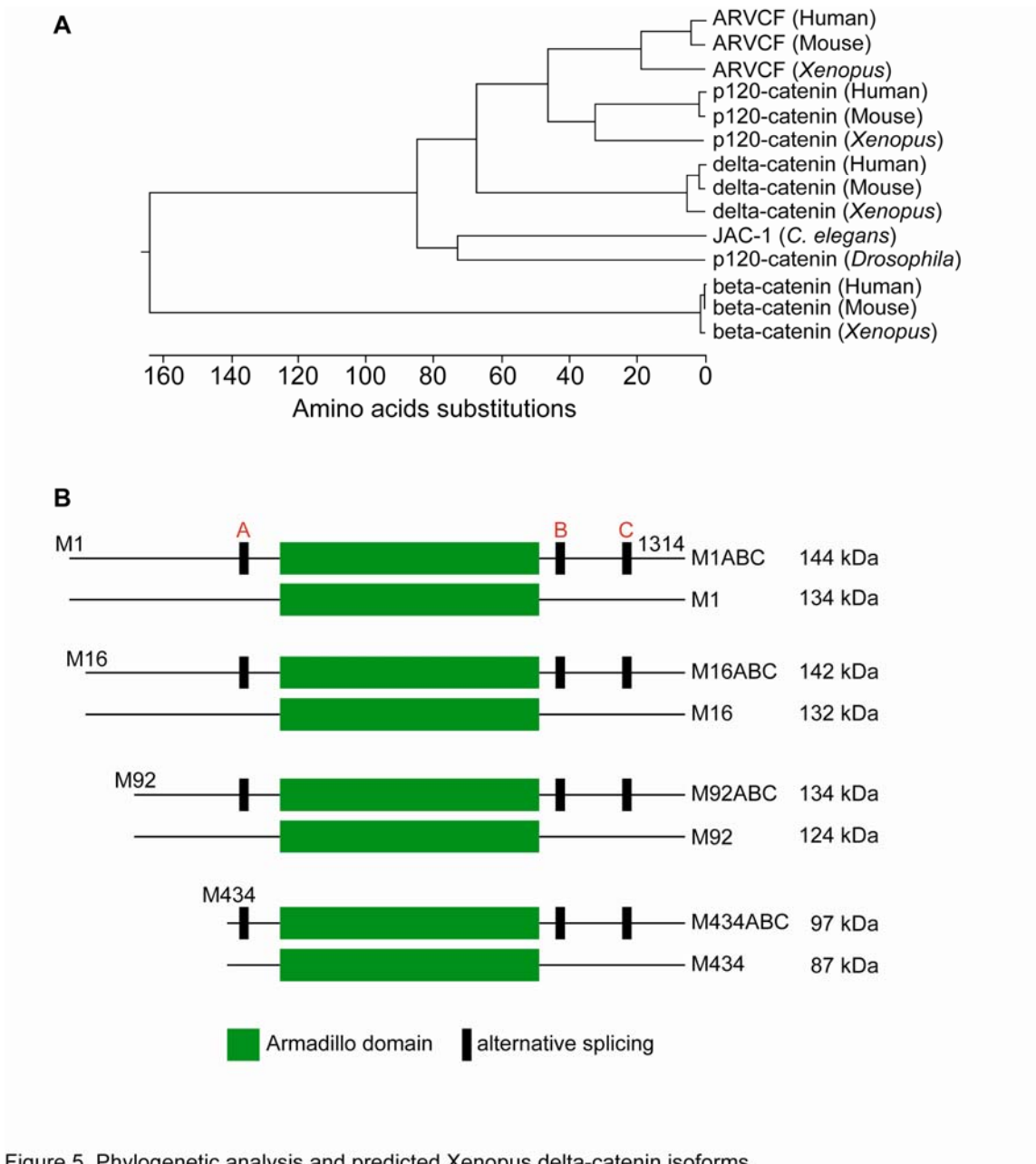


Figure 5. Phylogenetic analysis and predicted *Xenopus* delta-catenin isoforms.

A. Phylogenetic tree of select catenins, obtained using Clustal W alignment of DNASTAR package. B. Schematic illustration of potential *Xenopus* delta-catenin protein isoforms generated from alternative translation start sites and pre-RNA splicing.

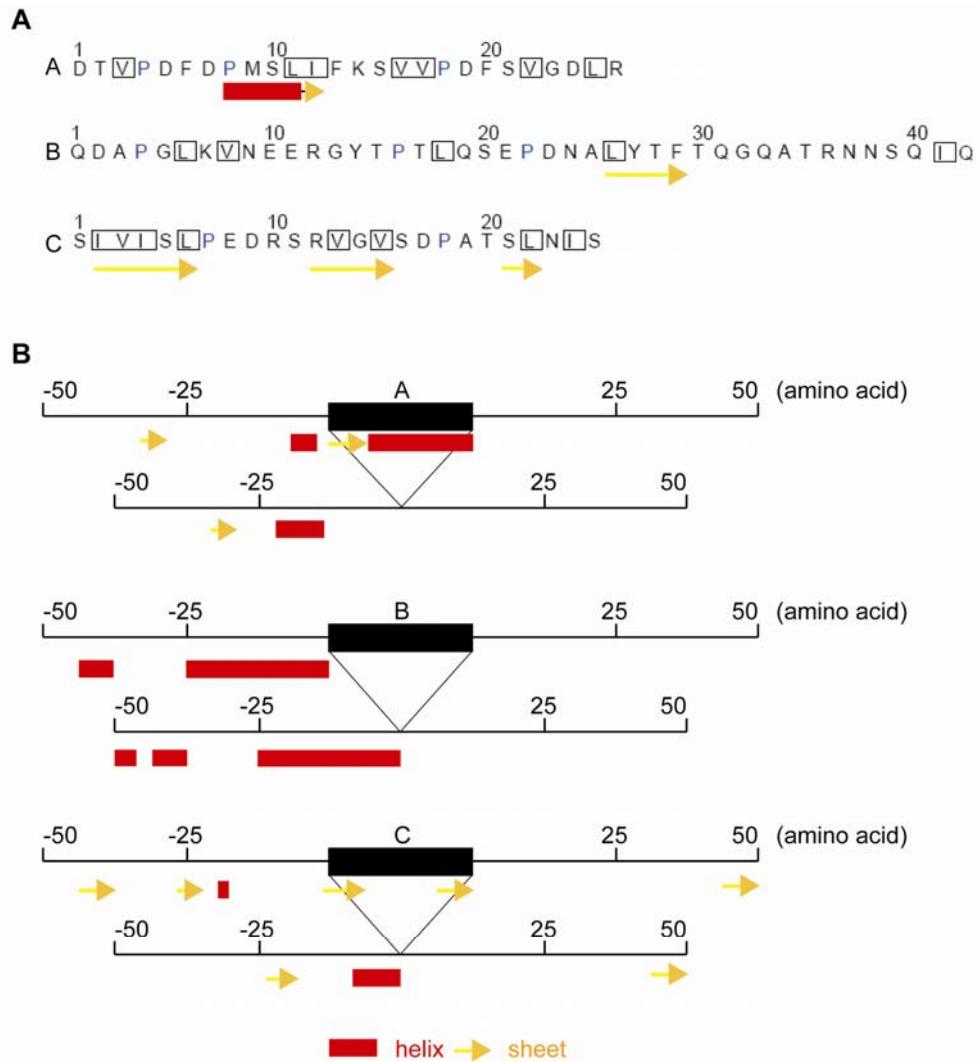


Figure 6. Jpred secondary structure prediction of delta-catenin splicing variants.

A. As isolated entities, splicing insert A encodes a potential interior helical structure, while inserts B or C contain one or more beta-sheets. B. A similar prediction approach was used as in A, except that included was 50 endogenous amino acids residing to either side of the A, B or C insert. In this sequence context, splicing variant A is favored to form helix, while the presence of B is predicted to produce few secondary structural effects. Sequence element C is predicted to contain two short sheet structures while nearby peptides favor a helical motif in its absence.

encode for beta-sheet structures. When the 50 amino acids of either side (upstream and downstream) were included in the analysis, splice variant A is predicted to form alpha-helix spanning about 20 amino acids. In conjunction with delta-catenin's Armadillo-domain, these secondary structures may contribute to its higher-order topology and protein interactions.

### **Delta-catenin temporal expression in *Xenopus* embryos**

To assess delta-catenin's temporal expression pattern, I performed semi-quantitative RT-PCR with total RNA extracted from *Xenopus* embryos at select stages. Delta-catenin transcripts are deposited maternally in oocytes (stage 0), and expressed throughout early embryonic development. Variants of A (a and a'), B (b and b'), and C (c and c') were detected. Expression of short forms of B (b') and C (c') were increased during and following neurulation, suggesting their possible distinct functions later in development (Figure 7).

To establish the profile of delta-catenin protein, I raised a polyclonal antibody against its amino-terminal residues 83-521. The purified antibody reacted with a delta-catenin isoform from embryo extracts migrating at approximately 100 kDa (Figure 8). Using immune-depletion and cadherin co-immuno-precipitation strategies, this reactivity was indicated to be authentic delta-catenin. I further tested commercial delta-catenin antibodies directed against the carboxyl-terminal amino acids 1229-1247 of mouse delta-catenin

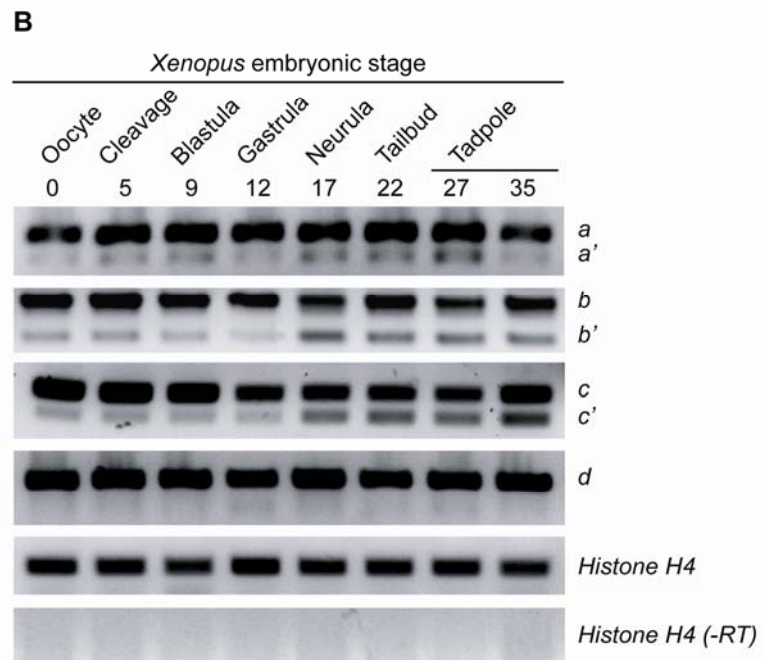
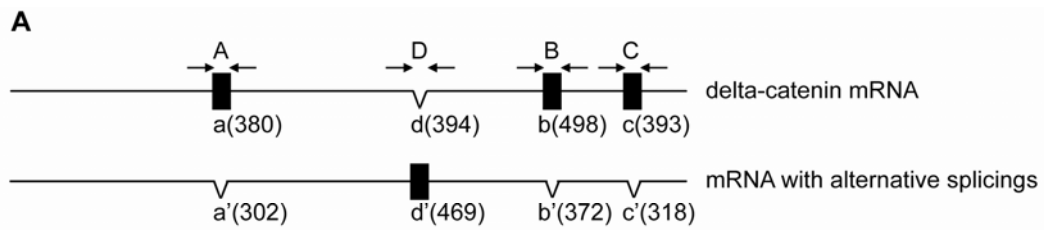


Figure 7. Characterization of delta-catenin alternative pre-mRNA splicing.

A. Schematic diagram of delta-catenin alternative splicing events, and the PCR oligos used to resolve them in panel (B). The nucleotide lengths of PCR products are indicated in parentheses. B. RT-PCR analyses indicate delta-catenin transcripts are deposited maternally and expressed throughout early embryonic stages. Both long (a, b, c) and short (a', b', c') variants were detected, with b' and c' having increased expression following neurulation.



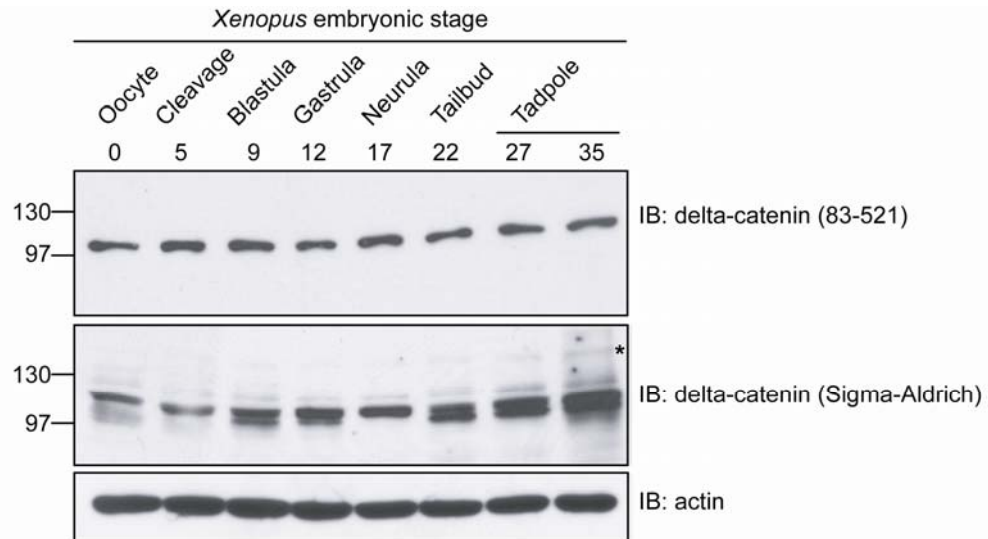


Figure 8. Endogenous delta-catenin protein expression in *Xenopus* embryos.

Immuno-blotting confirmed delta-catenin expression throughout *Xenopus* embryogenesis: antibodies directed against *Xenopus* amino-terminal residues 83-521 recognized a delta-catenin isoform migrating at approximately 100 kDa; antibodies directed against *Xenopus* amino acids carboxyl-terminal residues 1297-1314 (Sigma-Aldrich) reacts mainly with a 100 kDa doublet, with reactivity additionally appearing at 130 (marked with an asterisk) and 160 kDa (not shown).

(corresponds to amino acids 1297-1314 of the *Xenopus* ortholog, Sigma-Aldrich or Abcam). These antibodies mainly detected a doublet that migrates at approximately 100 kDa, with additional bands appearing at 130 kDa and 160 kDa depending on the experimental samples/ stages probed (Figure 8). Thus consistent with its temporal profile of mRNA transcripts, delta-catenin protein was apparent during *Xenopus* embryogenesis, suggesting that it may have functions during amphibian development.

### ***Xenopus* delta-catenin spatial characterization**

To examine the spatial profile of delta-catenin at the transcript level, I performed whole mount in-situ RNA hybridization. Delta-catenin anti-sense RNA probe was labeled with digoxigenin and detected transcripts enriched in the ectoderm of blastula and gastrula embryos (Figure 9, panel A, B, C and D). During neurulation (Panel E), the anterior region and dorsal neural tube displayed delta-catenin signals, with embryos at tadpole stages showing more distinctive staining in tissues of neural ectodermal and neural crest, including brain, eye and ear vesicles, branchial arches, spinal cord and somites (derived from mesoderm) (panel F, G and H). Panel I, J, K and L are section views of embryos from corresponding stages. Embryos hybridized in parallel using sense probe served as negative controls, wherein no significant signals were detected (panel M, N and O). The broad expression of *Xenopus* delta-catenin relative to the near brain-exclusive pattern of mammalian delta-catenins prompted me to

verify my findings using other approaches. Here I applied semi-quantitative RT-PCR and tested select tissues of adult *Xenopus*, which reproducibly showed the presence of delta-catenin transcripts (splicing variants c and c') in brain, nerve, muscle (mesoderm) and skin (surface ectoderm) (Figure 10A).

Following the same strategy, I explored the spatial profile of delta-catenin proteins using immuno-blotting analysis. Intriguingly, the amino-terminal antibody (against *Xenopus* amino acids 83-521) reacted with three isoforms (160, 130 and 100 kDa) from adult *Xenopus* tissues. The 130 and 100 kDa isoforms were present in all tissue extracts, while the 160 kDa band appeared to be brain-specific. In contrast, the delta-catenin carboxyl-terminal antibody (against *Xenopus* amino acids 1297-1314) detected only the two higher bands in brain using regular film exposures. When exposed longer, the 100 kDa band in brain and the 130 kDa band in muscle and liver were also seen (Figure 10B). The differing patterns seen upon use of amino- versus carboxyl-directed delta-catenin antibodies presumably result from distinct immune-reactivities. Differing post-translational modifications of delta-catenin isoforms may affect antibody recognition. Further complexity may come from the alternative splicing events of delta-catenin's amino- and carboxyl-terminal (and Armadillo) domains, with the amino-region likely to have additional alternative translations. Regardless of the underlying basis, my results indicate that delta-catenin is expressed in most adult *Xenopus* tissues at the transcript and protein levels, and that in developing animals it is most evident in tissues/ organs of neural derivation.

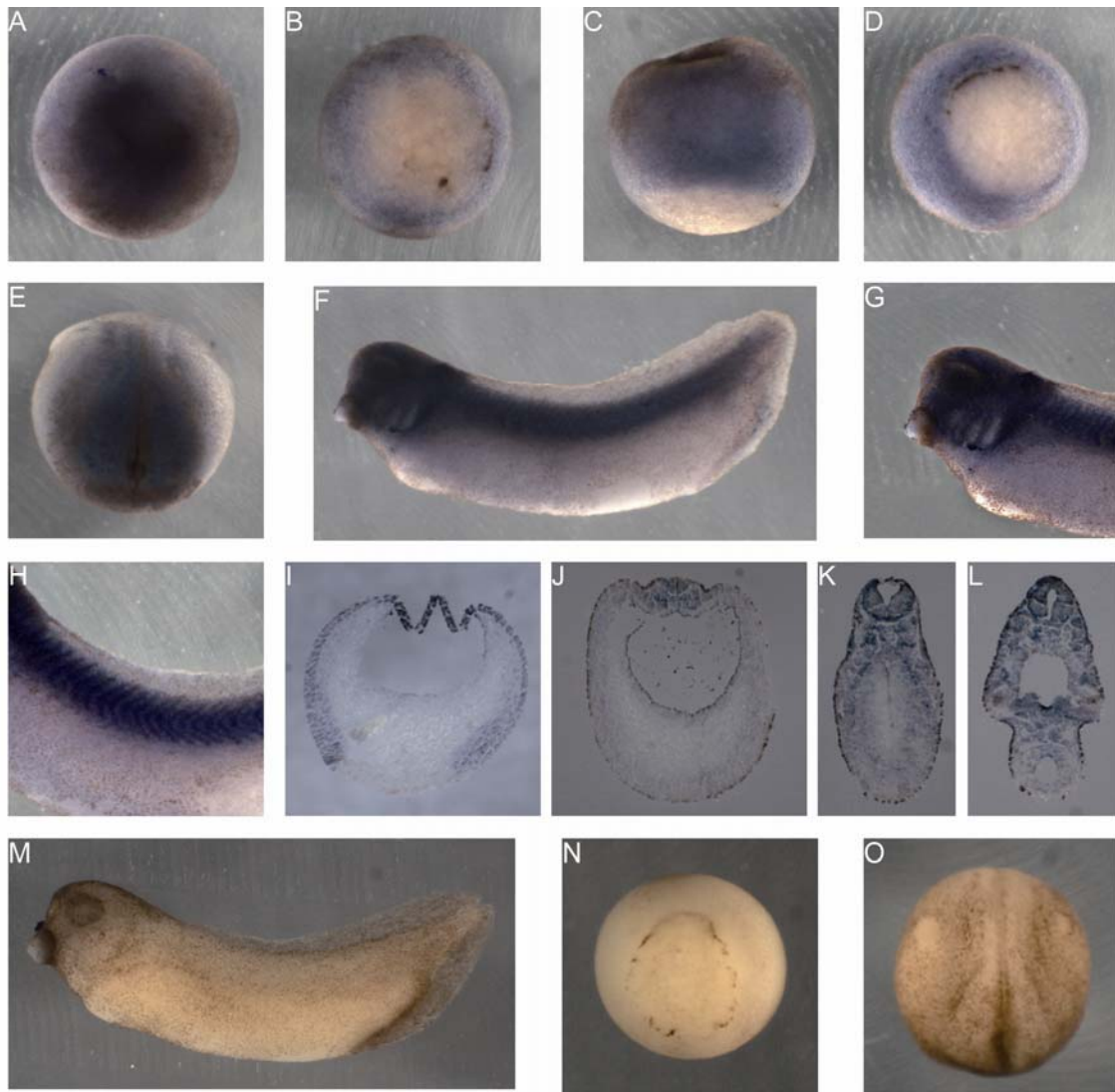


Figure 9. Whole mount in-situ RNA hybridization of delta-catenin.

Delta-catenin mRNA localizes in the ectoderm regions of blastula (A, B & C) and gastrula (D) embryos. At neurulation (E), the anterior and dorsal neural regions displayed the most apparent signals. Embryos at tadpole stages (F) showed a more distinctive staining pattern in tissues of neural derivation such as brain, eye vesicles, ear vesicles, branchial arches (G) and spinal cord as well as somites (H). Panels I, J, K & L are cross-sections of paraffin fixed embryos from corresponding stages. Sense probe hybridizations were processed in parallel as negative controls (M, N & O).

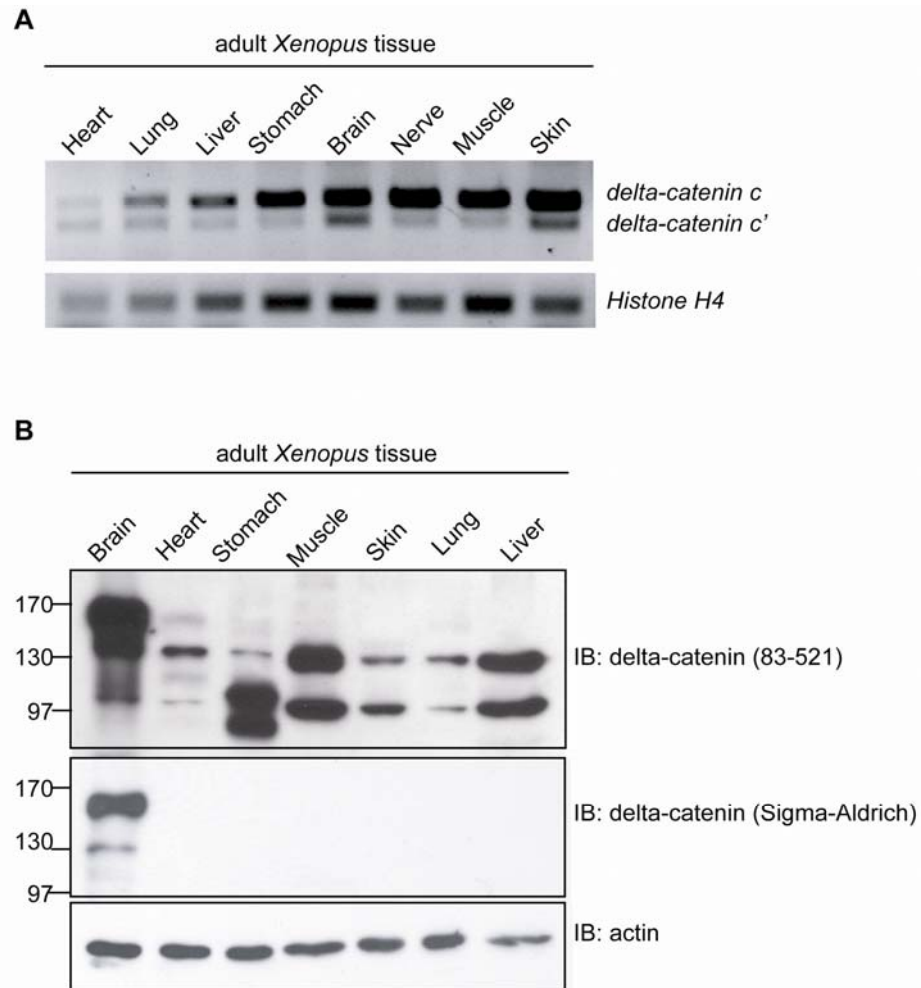


Figure 10. Delta-catenin expression profile in adult *Xenopus* tissues.

A. RT-PCR analyses detected delta-catenin transcripts in all adult *Xenopus* tissues examined. Histone H4 was applied as the internal control. B. Immuno-blotting using an amino-terminal antibody (83-521) detected three delta-catenin isoforms migrating at approximately 160, 130 and 100 kDa. The 130 and 100 kDa isoforms were ubiquitously present while the 160 kDa appeared to be brain-specific. An antibody directed against delta-catenin's carboxyl-terminus (Sigma-Aldrich) reacted with the 160 kDa and 130 kDa isoforms in brain.

## **Delta-catenin sub-cellular localization in *Xenopus* embryos**

Earlier work on p120-catenin has indicated diverse functions in differing sub-cellular compartments (Anastasiadis, 2007; McCrea and Gu, 2010; Reynolds, 2007). This includes binding to the juxta-membrane region of cadherins at cell contacts, interactions with small GTPases in the cytoplasm, and regulation of gene transcription in the nucleus. To validate the association of endogenous delta-catenin with classical cadherins, I performed co-immunoprecipitations from gastrula (stage 12) embryo lysates. Immuno-precipitates of delta-catenin antibody included C-cadherin, which is the principal cadherin isotype at early cleavage stages (Figure 11A). Given delta-catenin's wider expression in *Xenopus* tissues, I wished to test its interaction with E-cadherin (epithelial enriched), and N-cadherin which is concentrated in neural tissues (Figure 11B and 11C). As assessed from neurula (stage 15)/ tailbud (stage 22) stage embryo extracts, both cadherins associate with delta-catenin, further suggesting that *Xenopus* delta-catenin is present within cadherin complexes existing within cleaving blastomeres of the blastula stage, epithelial layers and neural tissues at neurula stages.

To determine delta-catenin's sub-cellular localization, I applied the established method of membrane fractionation in early stage embryos (Fagotto and Gumbiner, 1994). Extracts of gastrulating embryos were separated into membrane and non-plasma membrane crude fractions, and subjected to

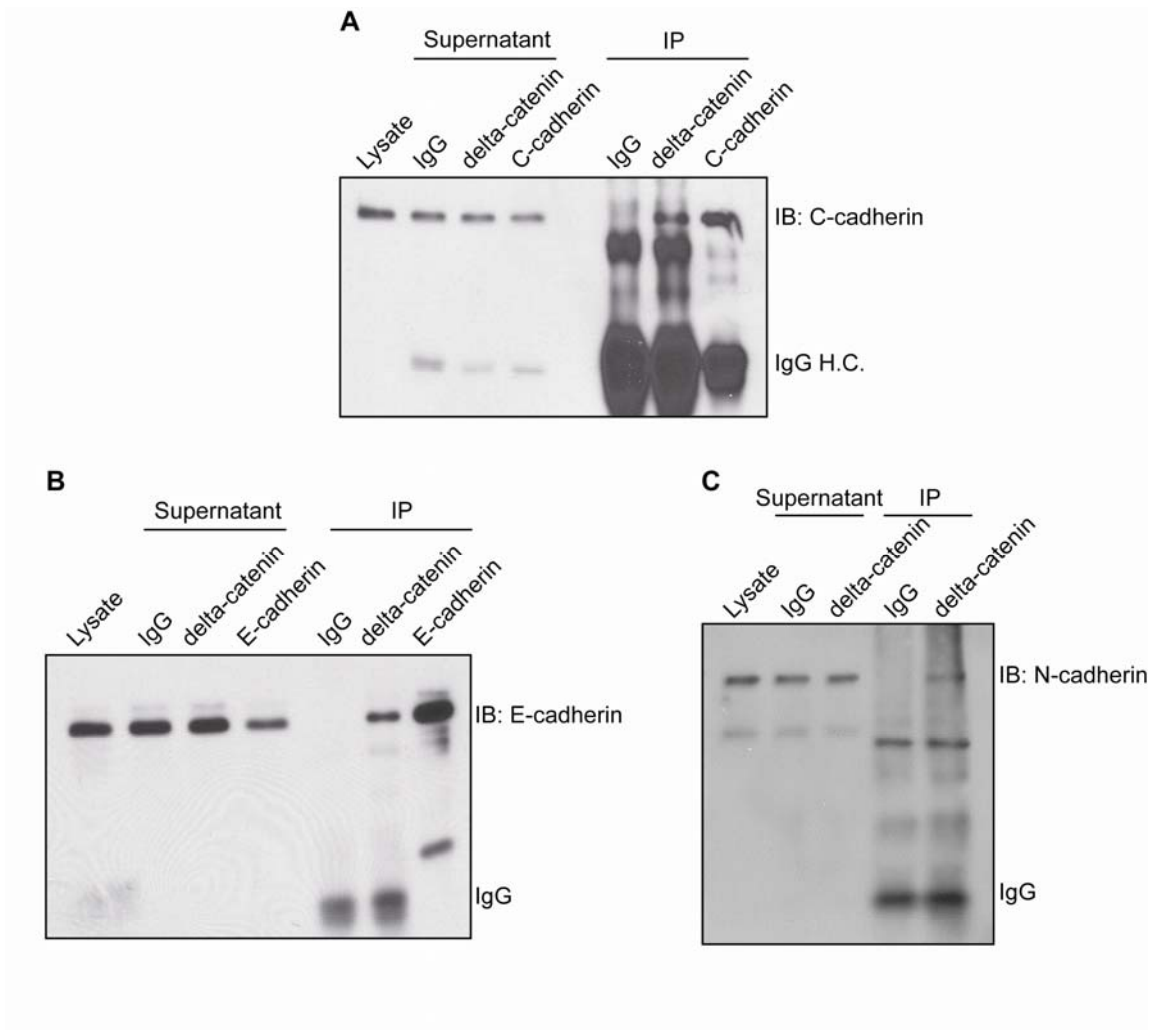


Figure 11. Delta-catenin associates with classical cadherins.

Endogenous delta-catenin complexes were immuno-precipitated using a carboxyl-directed antibody (Sigma-Aldrich), and immuno-blotted using antibodies direct against cadherins. Positive co-immuno-precipitation results suggest an association of delta-catenin with C-cadherin in gastrulating embryos (A), and with E-cadherin (B) and N-cadherin (C) in neurulation stage embryos. Immunoglobulin bands are included to reflect the specific versus negative control antibody input.

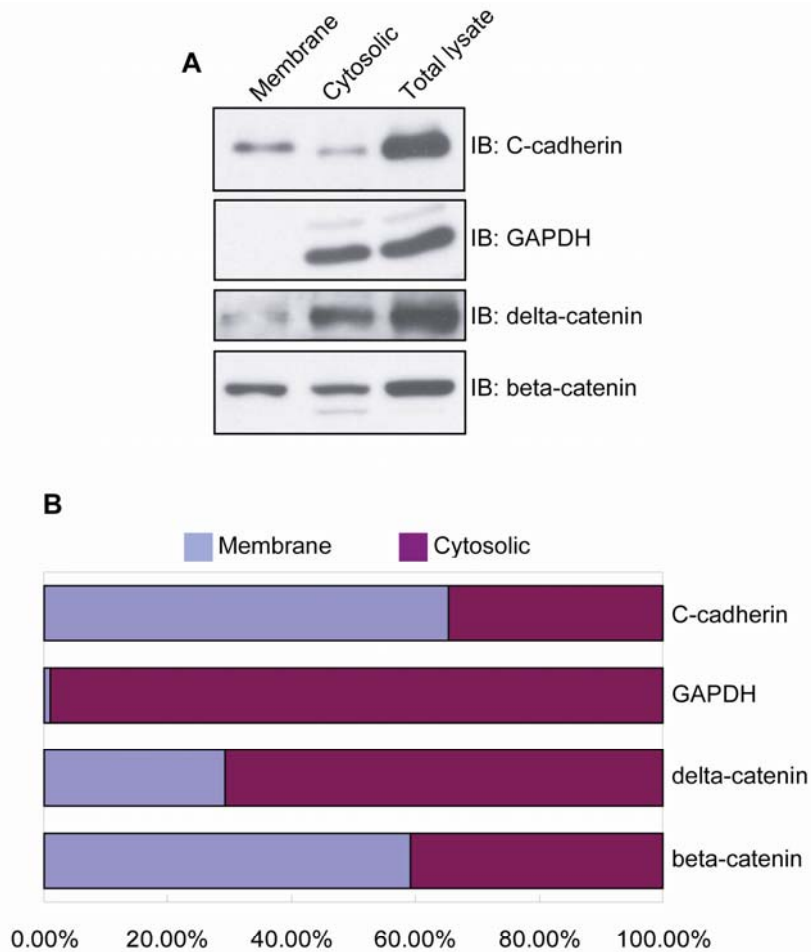


Figure 12. Membrane-cytosolic fractionation.

Crude membrane fractionations of gastrula embryos followed by immuno-blot analyses (A) indicate the predominant localization (~70%, quantified in B) of endogenous delta-catenin within the cytosolic pool. As expected, GAPDH was almost exclusively evident in the cytosolic fraction. C-cadherin predominantly resided within the plasma membrane pool (65%), with the remaining fraction likely to reflect associations with non-sedimenting vesicular stores, endoplasmic reticulum or Golgi.



immuno-blotting analysis with antibodies directed against select proteins (Figure 12). Endogenous delta-catenin was apparently predominantly localized within the non-membrane pool including cytosolic and nuclear components. Compared to beta-catenin (approximately 40%), a larger proportion (about 70%) of delta-catenin did not associate with the membrane fraction (bound to cadherins). My results are thus consistent with the possibility that delta-catenin regulates cytosolic and/ or nuclear processes, in addition to membrane/ cadherin dependent events during *Xenopus* embryogenesis.

### **Delta-catenin anti-sense morpholinos**

Given that the characterization of delta-catenin suggested its potential requirement during amphibian embryogenesis, I began to address its developmental roles. For this purpose, I employed an anti-sense morpholino oligo strategy to disrupt protein expression (loss-of-function approach). As *Xenopus* delta-catenin is putatively translated from multiple distinct initiation sites (see also Figure 4), I avoided use of the traditional morpholinos directed to block translation initiation. Instead, I employed the splicing type of morpholinos that interfere with pre-RNA splicing, with the predictable outcome of disrupting the protein coding frame and causing pre-mature termination (Draper et al., 2001; Nutt et al., 2001). I chose to target exon 6 of delta-catenin since its frame shift would generate the smallest possible protein products. I first acquired the sequence of intron 5 and exon 6 from tadpole stage genomic DNA by PCR

amplification and direct DNA sequencing. Delta-catenin morpholino-6 (MO-6) was indicated to perturb splicing between intron 5 and exon 6. Delta-catenin-MO-6 was injected into single-cell embryos and I used RT-PCR to assay its efficacy at later stages (Figure 13A). When harvested at blastula stages, injected embryos produced a smaller PCR product consistent with the expected alteration of RNA splicing (skipping of exon 6), which was confirmed by DNA sequencing. Next I used oligos matching more downstream sequences (d, see also Figure 7), finding no sign of alterations in delta-catenin DNA transcription or mRNA stability. Following the same strategy, I chose intron 8- exon 9 junction and designed another splice junction morpholino (delta-catenin MO-9), which was predicted to disrupt protein products originating from all translational start sites (Figure 13B). Delta-catenin MO-9 activated cryptic splicing sites and caused exon 9 skipping as well as additional partial skipping of exon 8 (') and 10(''). When evaluated at the protein level through immuno-blotting, both morpholino 6 and 9 reproducibly reduced delta-catenin intensities, with no obvious effects on a nonspecific cross-reacting band (labeled with asterisks), or upon actin (Figure 14).

### **Delta-catenin depletion results in developmental phenotypes in gastrulation, neural crest migration and kidney tubulogenesis**

To evaluate the effects of delta-catenin depletion, I injected the above morpholinos into early stage cleaving embryos. Those embryos underwent

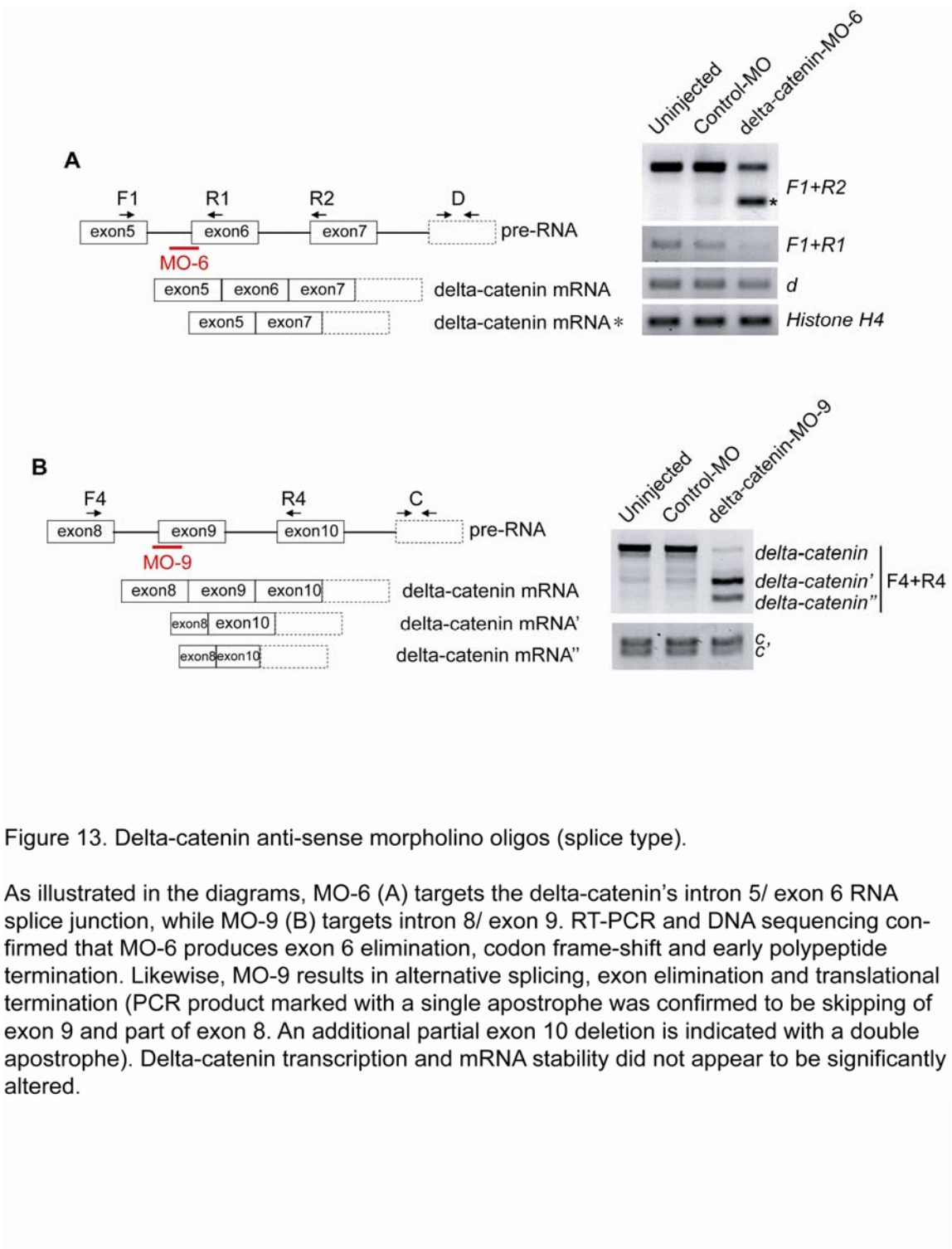


Figure 13. Delta-catenin anti-sense morpholino oligos (splice type).

As illustrated in the diagrams, MO-6 (A) targets the delta-catenin's intron 5/ exon 6 RNA splice junction, while MO-9 (B) targets intron 8/ exon 9. RT-PCR and DNA sequencing confirmed that MO-6 produces exon 6 elimination, codon frame-shift and early polypeptide termination. Likewise, MO-9 results in alternative splicing, exon elimination and translational termination (PCR product marked with a single apostrophe was confirmed to be skipping of exon 9 and part of exon 8. An additional partial exon 10 deletion is indicated with a double apostrophe). Delta-catenin transcription and mRNA stability did not appear to be significantly altered.

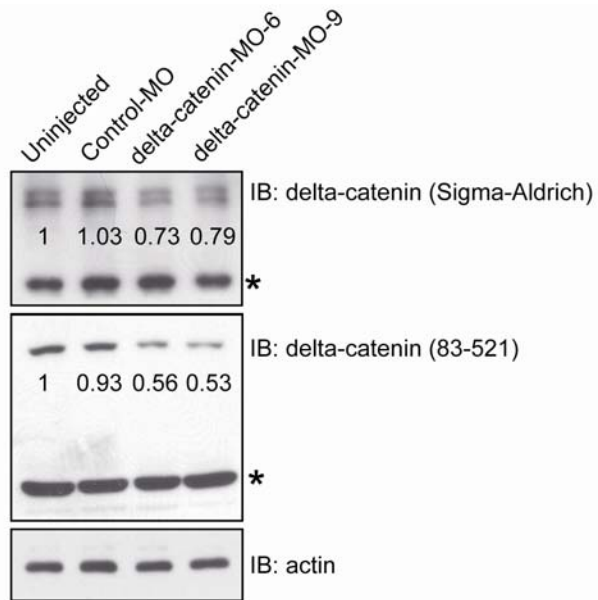


Figure 14. Immuno-blotting evaluation of delta-catenin knock-down.

Immuno-blotting of gastrula stage embryo extracts confirmed the reduction of delta-catenin proteins following morpholino injections. Non-specific reacting bands (labeled with asterisks) and actin provided loading controls.

cleavage and blastula stages with no noticeable phenotypes. However at gastrulation, injected embryos displayed significant delays in blastopore closure, and endodermal protrusions in certain experimental contexts (Figure 15). Based upon external observation, many embryos seemed to recover and complete gastrulation. However, most MO-9 injected embryos were developmentally arrested and died during later tailbud/ tadpole stages. I then employed biochemical assays to assess the effects of delta-catenin depletion on cell proliferation (antibody staining of phospho-histone H3, Millipore) or apoptosis (antibody staining of active caspase-3, BD Pharmingen), but my results were not conclusive. It remained possible that delta-catenin knock-down produces effects upon cell death that are below my detection methods when tested at early developmental stages (gastrulation), but is ongoing and ultimately results in more significant tissue necrosis at later stages (tailbud/ tadpole). Such effects may also come from as yet unexamined processes, for example, the largely uncharacterized functions of delta-catenin in the nucleus. It is noteworthy that many surviving tadpoles from MO-6 injections showed abnormalities including reduced anterior-posterior axes and gut malformations, which may have resulted from underlying earlier gastrulation defects.

Since delta-catenin knock-down affected blastopore closure, a morphogenetic process dependent on the proper orientation of cell intercalation processes (Keller, 2005; Keller et al., 2003; Solnica-Krezel, 2006), I investigated whether convergence-extension movements could be affected. I thus excised

dorsal mesodermal explants that are capable of recapitulating *ex vivo* the morphogenesis observed *in vivo* (explants assay). Note that delta-catenin depleted explants did not generate significant defects in elongation when compared with the controls (Figure 16A). Among other possibilities, reduction of delta-catenin functions may affect directed cell re-arrangements of more ventral or medial tissues (not examined in my study), or alternatively, the coordination of cell/ tissue movements. Next I followed an established method and scored delta-catenin knock-down embryos for their convergence-extension *in vivo* (Kim et al., 2004) (Figure 16B). In this assay, I injected delta-catenin MO-6 and an Alexa 488 fluorescent tracer into equatorial regions of four-cell stage embryos. At approximately *Xenopus* stage 11 (mid-gastrula stage), the aspect ratios (measured as ratios of length- to- width) of fluorescence intensity within dorsal zones/ DMZ were assessed. Again no significant differences were observed. Thus, my results indicate that while delta-catenin is crucial for normal gastrulation and later developmental events, its depletion may not significantly perturb convergent extension movements in the dorsal mesodermal compartment.

Given earlier studies that p120-catenin depletion in presumptive neural ectoderm results in eye and craniofacial defects (Ciesiolka et al., 2004), I sought to examine such potential effects following delta-catenin morpholinos (6 and 9) through targeted injections. Delta-catenin knock-down in the dorsal-animal blastomeres of eight-cell stage embryos likewise perturbed eye and craniofacial

development as evident in later tadpoles (Figure 17). As exogenously expressed delta-catenin partially rescued such phenotypes, the specificity of these loss-of-function effects was indicated. Next, I used Alcian blue staining to more clearly evaluate craniofacial abnormalities. As shown in Figure 18A, depletion of delta-catenin caused under-development of both the ceratohyal and ceratobranchial cartilages, cell lineages that originate from neural crest. It is thus conceivable that delta-catenin may play a role in this cell population. Indeed, whole mount in-situ RNA hybridization employing neural crest markers (Slug, etc.) illustrated that delta-catenin depletion impaired neural crest migration when examined at neurulation stage 18 (Figure 18B).

Following the same strategy, I injected delta-catenin morpholinos into ventral-vegetal blastomeres of early stage embryos, and employed 3G8 whole mount antibody staining to evaluate pronephric kidney tubulogenesis of tadpoles. 3G8 is a well-established antibody that recognizes pronephric tubules and nephrostomes (Lyons et al., 2009; Vize et al., 1995). It appeared that delta-catenin depletion resulted in impaired tubulogenesis and was associated with the edematous status (collection of fluids) of superficial tissues (Figure 19).

### **Delta-catenin depletions are rescued with delta- or p120-catenin**

To test the specificity of my obtained phenotypes and to examine delta-catenin's functional relationship with select catenins, I employed a rescue

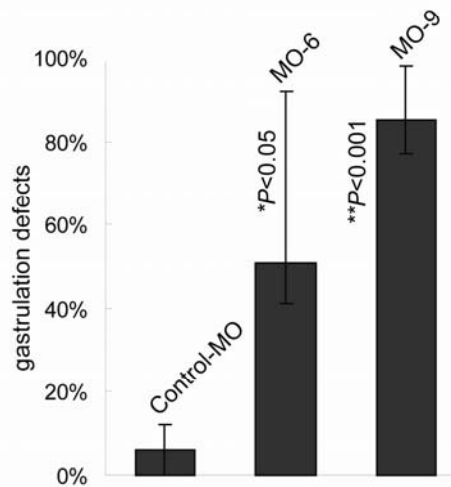
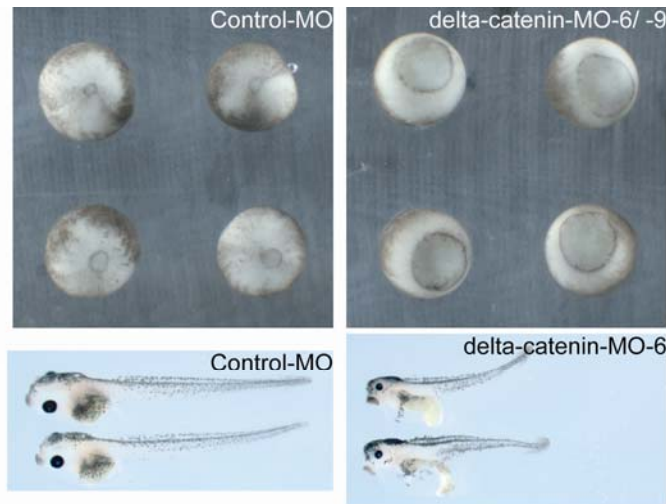


Figure 15. Gastrulation phenotypes of *Xenopus* embryos upon delta-catenin depletion.

Delta-catenin knock-down results in developmental phenotypes including significant delays in blastopore closures/ gastrulation defects. While most embryos outwardly appeared to recover from these effects and complete blastopore closure, the majority of MO-9 injected embryos were developmentally arrested during early tailbud/ tadpole stages and subsequently died. For surviving embryos, abnormalities were again outwardly evident, particularly at tadpole stages, including shortened anterior-posterior axes, smaller craniofacial skeletons and eyes, malformed gut and edema.



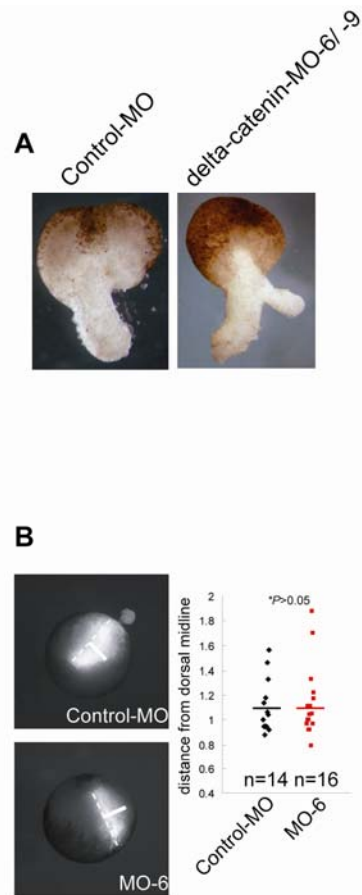


Figure 16. delta-catenin depletion does not affect dorsal convergent-extension.

A. Delta-catenin depletion does not significantly alter convergent-extension in Keller explants. All sets of explants underwent convergent-extension with no consistent differences observed. Spurs such as the one seen on the right side of the delta-catenin depleted embryos appear occasionally for all conditions. B. Delta-catenin knock-down does not detectably alter in vivo convergent-extension of the dorsal marginal region marked with a fluorescent lineage tracer, and evaluated using fluorescent length-to-width ratios taken at mid-gastrula stages. Compared with control morpholino injected embryos, no statistically significant difference in convergent-extension was observed in delta-catenin depletion embryos.

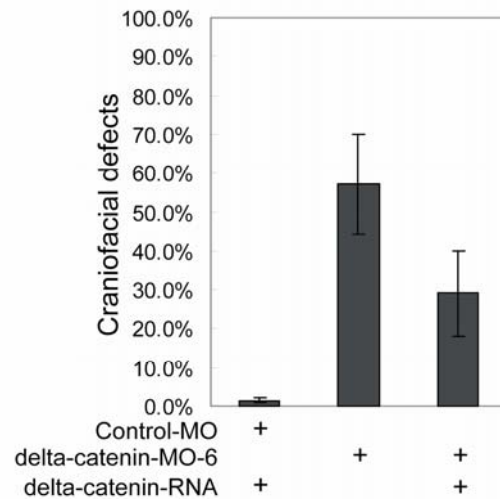
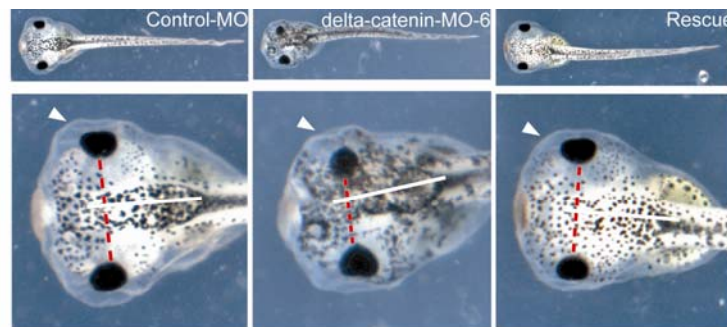


Figure 17. Delta-catenin depletion in presumptive neural ectoderm causes eye and craniofacial defects.

Delta-catenin or control morpholino was injected into one dorsal-animal blastomere of 8-cell stage embryos. Exterior observation of delta-catenin-depleted tadpoles showed reduced craniofacial structures as well as eyes, relative to control embryos, or the uninjected side of experimental embryos. Reproducible rescues were achieved when delta-catenin RNA was co-injected with the MO-6. Arrowheads point to the injected sides, while solid lines indicate the embryo midlines (upper panels). Experiments were repeated and results quantified in the lower panel.

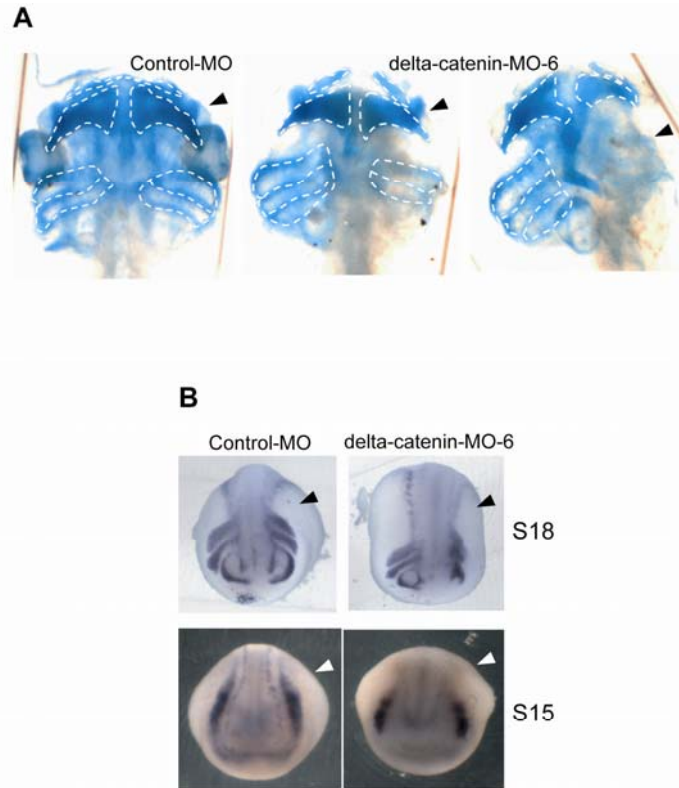


Figure 18. Delta-catenin depletion perturbs neural crest migration.

A. After morpholino injections at 4-cell stage, tadpoles were fixed and stained with Alcian blue dye. Impaired craniofacial cartilage formation (outlined using Photoshop CS3) was repeatedly observed with the delta-catenin depleted embryos. B. Whole mount RNA in-situ hybridization of Slug in neurulation stage embryos indicated the perturbation of neural crest migration (upper panel) upon delta-catenin knock-down. Arrowheads point to the injected sides.

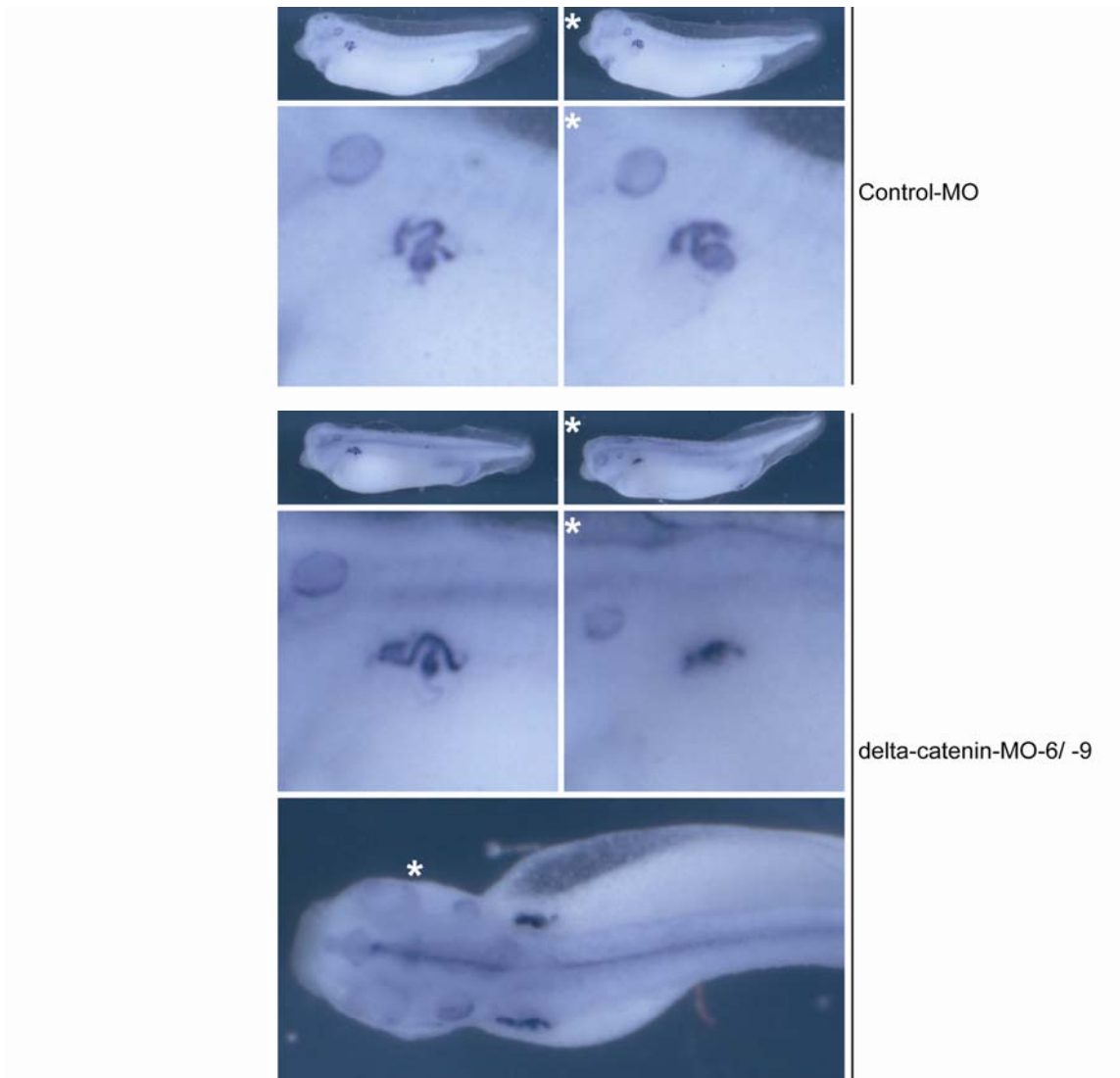


Figure 19. Delta-catenin depletion impairs pronephric kidney tubulogenesis.

Delta-catenin or control morpholinos were injected into one ventral-vegetal blastomere of 8-cell stage embryos. At tadpole stages, embryos were fixed and stained for pronephric kidney tubules using the 3G8 antibody. Delta-catenin depleted embryos displayed reduced tubulogenesis. Reductions in 3G8 staining were correlated with superficial tissue edema. Asterisks mark the injected sides.

strategy by scoring for blastopore closure (completion of gastrulation). A full-length delta-catenin RNA (resistant to splice junction morpholinos) effectively rescued phenotypes and supported the specificity of knock-down. As I mentioned earlier that p120 sub-family proteins share certain attributes, I further examined whether p120-catenin could rescue delta-catenin depletion. Indeed, p120-catenin repeatedly displayed significant rescuing activity (Figure 20B), while as expected the more distantly related beta-catenin did not (Figure 21B). Moreover, when morpholinos of delta- and p120-catenin were injected at sub-phenotypic (titrated) doses, combined depletion of delta- and p120-catenin produced more pronounced effects than either alone (Figure 20A). Thus these results were consistent with the literature and my findings in that delta- and p120-catenin might share some roles during *Xenopus* gastrulation, although it is important to note that endogenous level of either catenin is not sufficient to compensate for/ rescue depletion of the other.

To begin to identify regions of delta-catenin required to rescue delta-catenin depletion, I tested the rescuing capacity of a delta-catenin RNA beginning at the most downstream putative translation start site (Methionine434) finding that it displayed rescuing activity comparable to the full-length construct (Figure 21A). Likewise, a delta-catenin mutant missing the carboxyl-terminal PDZ binding motif (delta-catenin  $\Delta$ PDZ) successfully rescued blastopore closure defects (Figure 21B). These results suggest that the observed gastrulation delay phenotypes more likely resulted from the loss of Armadillo- and/ or carboxyl-

terminal regions, rather than delta-catenin's amino-terminal 433 amino acid residues or its PDZ motif (four amino acids). Consistent with this speculation, delta-catenin's amino-terminal region containing amino acids 1- 500 (NT construct) displayed little rescuing ability (Figure 21B). The Armadillo-domain of delta-catenin in isolation (delta-catenin ARM) also failed to generate statistically significant rescue effects, suggesting that the Armadillo-domain is necessary but not sufficient. In Figure 21C, various delta-catenin constructs are illustrated along with their capacity to rescue blastopore closure.

As was the case for depletion, over-expression of delta-catenin perturbed gastrulation (causing delays in blastopore closure) in a dose-dependent manner (Figure 22). Thus, similar to other p120-catenin sub-family members, it appears that delta-catenin levels must be kept within a defined range to execute normal embryogenesis.

### **Delta-catenin depletion impairs cadherin-dependent adhesive functions**

To explore mechanisms underlying delta-catenin's depletion phenotypes, I examined cadherin levels and cell adhesive functions using biochemical approaches. Immuno-blotting repeatedly detected reductions in C (cleavage)-, E (epithelial)- and N (neural)-cadherin levels following delta-catenin morpholino injections. In comparison, other catenins including p120- and beta-catenin, or the loading control actin, were not significantly changed (Figure 23A). Next I

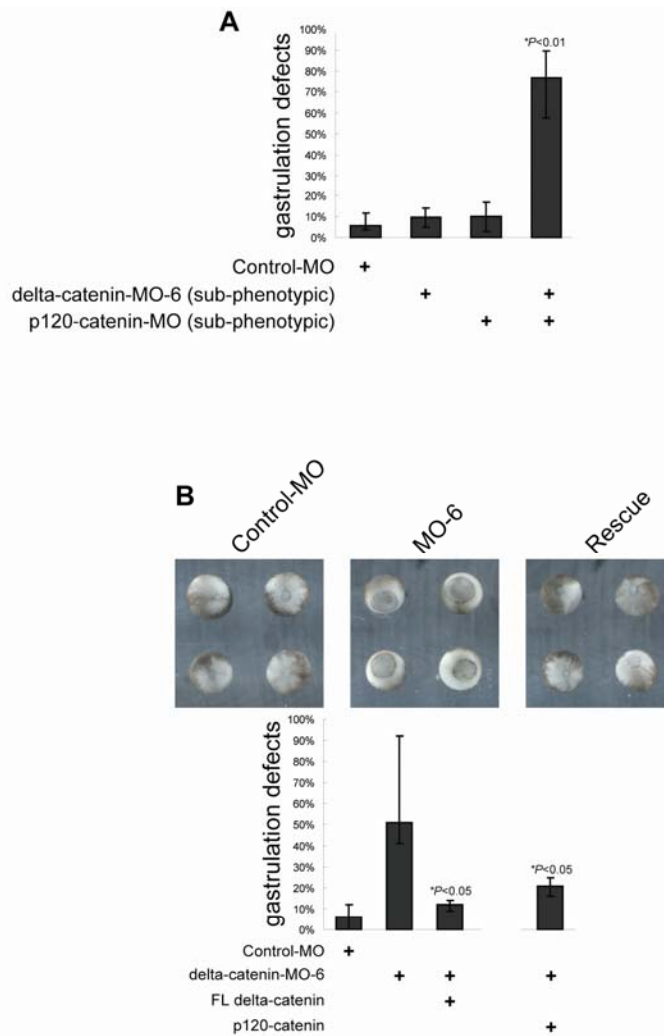


Figure 20. Synergism between delta- and p120-catenin depletions in *Xenopus*.

A. Co-injection of delta-catenin and p120-catenin morpholino, each at sub-phenotypic doses, produces enhanced phenotypic effects. B. Full-length delta-catenin rescued blastopore closure defects, confirming the specificity of knock-down phenotypes. P120-catenin also reproducibly displayed significant rescuing activity.

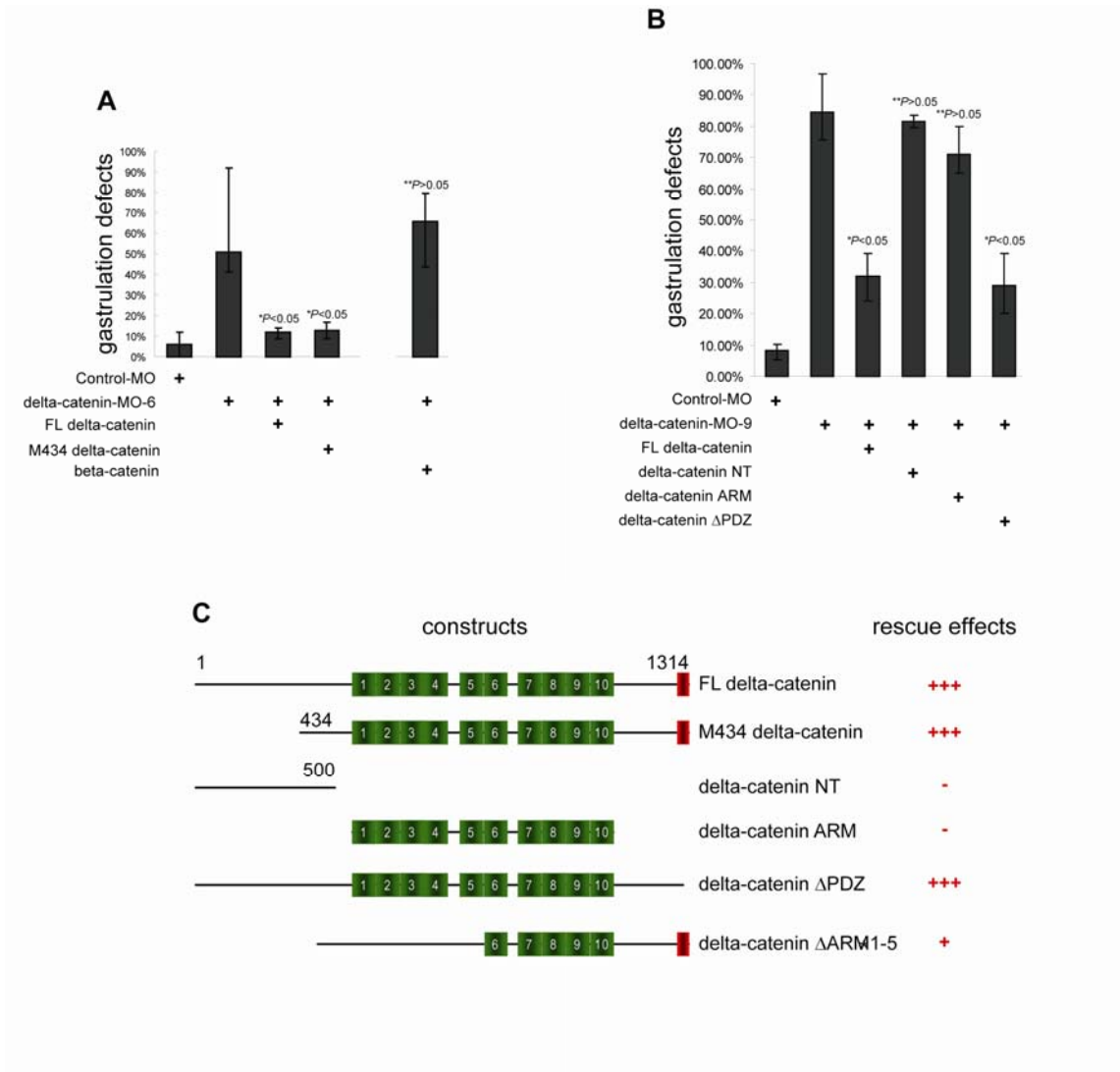


Figure 21. Delta-catenin depletion-rescue experiments.

A. M434 rescued blastopore closure defects following delta-catenin depletion, while the more distantly-related beta-catenin did not have such capability. B. PDZ-binding motif of delta-catenin is dispensable for its rescuing activity in blastopore closure. In contrast, delta-catenin's amino-terminus or Armadillo-domain in isolation failed to rescue depletion. C. Schematic presentation of various delta-catenin constructs with a summary of their rescuing effects.



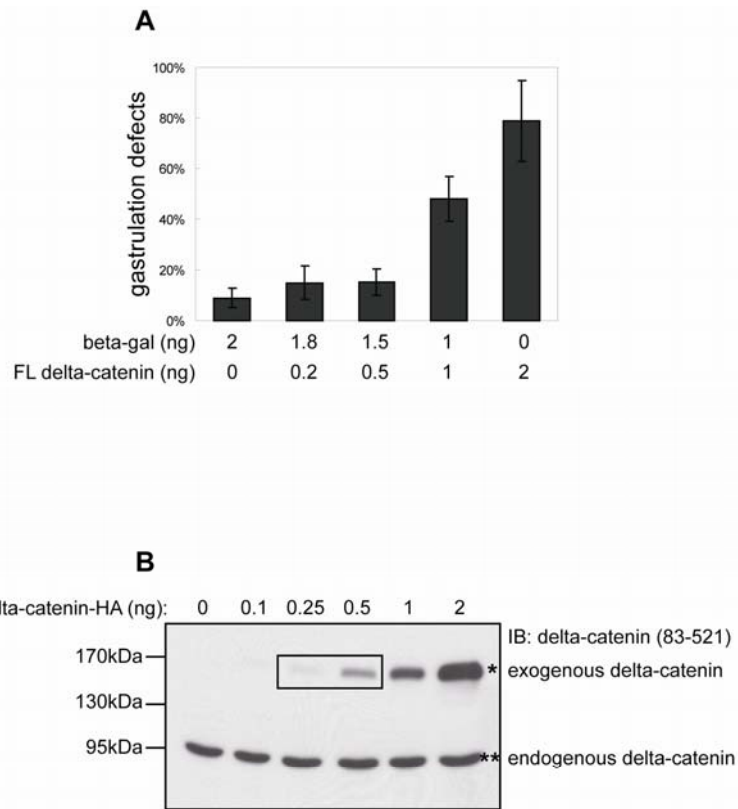


Figure 22. Over-expression of delta-catenin produces delays in blastopore closure.

A. Over-expression of delta-catenin produces delays in blastopore closure in a dose-dependent manner. B. As reflected in an immuno-blot, we evaluated rescuing levels of exogenous full-length delta-catenin relative to the endogenous delta-catenin (rectangle indicates doses used for rescue analysis).

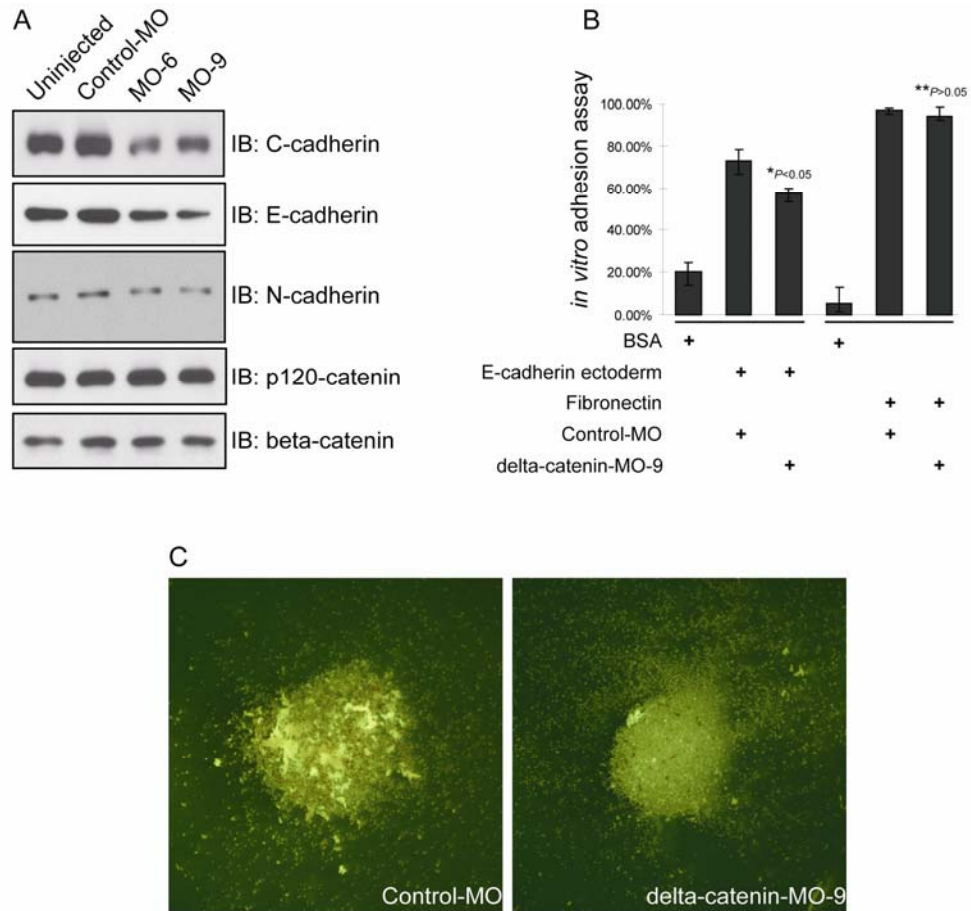


Figure 23. Delta-catenin depletion leads to reduced cadherin functions.

A. In immuno-blotting, delta-catenin depletion reproducibly leads to reduced C-, E- & N-cadherin levels, while depletion did not significantly alter p120- and beta-catenin levels. B. An *in vitro* assay indicated cadherin-mediated adhesion to be decreased in naive ectoderm cells depleted of delta-catenin. In contrast, a similar assay that employing tethered fibronectin, did not resolve changes in cell attachment (presumably integrin mediated). C. Calcium dependent adhesive functions were decreased in delta-catenin depleted naive ectoderm cells. Following calcium removal from the ectoderm explants, note the larger cell aggregates remaining in the control-MO injection.

accessed cadherin-dependent cell adhesion in *Xenopus* embryos using animal cap dissociation and re-aggregation assays. In embryos injected with delta-catenin MO-9, cell adhesion was reduced when measured using either of these methods (Figure 23C). To quantify such effects, I applied an in vitro adhesion experiment. Here I coated glass coverslips with the purified ectoderm of mouse E-cadherin (recombinant peptide, Sigma-Aldrich), or with the extracellular matrix component fibronectin (Sigma-Aldrich, negative control), and incubated the coverslips with dissociated ectodermal cells from control versus delta-catenin depleted embryos. The percentage of cells remaining after buffer washing was calculated as a rough measurement of adhesive strength. While I noticed some reductions in cadherin heteromeric interactions (presumably reduced interaction of endogenous C- with exogenous E-cadherin) in the condition of delta-catenin depletion, changes were not seen upon fibronectin association (endogenous integrin with exogenous fibronectin) (Figure 23B).

Next I asked whether such reductions in cadherin-mediated adhesion might contribute to the developmental defects resulting from delta-catenin knock-down. I addressed this through depletion-rescue assays, testing whether ectopically-expressed cadherins could rescue delta-catenin depletion. As expected, C-cadherin (major isotype in early *Xenopus* stages) displayed a significant capacity to rescue blastopore closure defects (Figure 24). I further wished to address the relevance of the delta-catenin: cadherin interaction by evaluating the capacity of a mutant C-cadherin to perform rescues. As

mentioned earlier, p120-catenin sub-family catenins bind to the juxta-membrane regions of cadherins. A triple-point (AAA) mutation of E-cadherin in this region was reported to abolish the interaction with p120-catenin in mammalian cell lines (Maeda et al., 2006). Yet in *Xenopus* embryos, unpublished results from McCrea Laboratory indicated that the corresponding C-cadherin AAA mutant retained some association with ARVCF-catenin (another member of the p120-catenin sub-family). Thus, the cadherin AAA mutant may not be an ideal reagent to address this question. Instead, I constructed a delta-catenin deletion mutant ( $\Delta$ ARM1-5) which is missing Armadillo repeats 1-5. Evaluated by co-immunoprecipitation tests from *Xenopus* extracts,  $\Delta$ ARM1-5 failed to interact with endogenous C-cadherin (Figure 25A). However,  $\Delta$ ARM1-5 largely preserved the capability to modulate Rho and Rac functions, which were measured through RhoA and Rac1 pull-down assays in HeLa cells. Here in common with full-length delta-catenin,  $\Delta$ ARM1-5 inhibits RhoA while activating Rac1 (Figure 25B and 25C). Supporting the above biochemical assays,  $\Delta$ ARM1-5 transfection in neuro-2a neuroblastoma cells resulted in the formation of neurite-like structures as seen for the full-length protein. Such effects are generally expected to result from Rho and Rac modulation (Figure 26). It is important to note that  $\Delta$ ARM1-5 showed only weak rescue effects compared to the full-length construct (Figure 24). Thus, my results are consistent with the significance of the delta-catenin: cadherin association in *Xenopus* gastrulation. In this regard, delta-catenin protein knock-down via antisense morpholino oligos appears to lessen cadherin levels and impair cell adhesion, leading to the defects of embryogenesis.

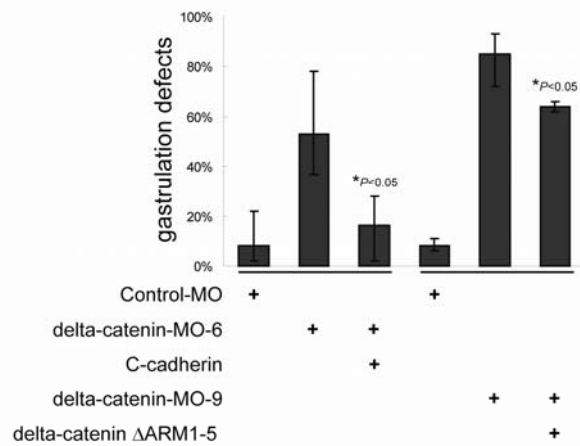


Figure 24. C-cadherin effectively rescues delta-catenin depletion in *Xenopus* embryos.

A titrated dose of exogenous C-cadherin significantly rescues blastopore closure defects induced by depletion of endogenous delta-catenin. In contrast, a delta-catenin mutant construct lacking Armadillo repeats 1-5, and failing to co-immuno-precipitate with C-cadherin showed minimal rescuing effects.

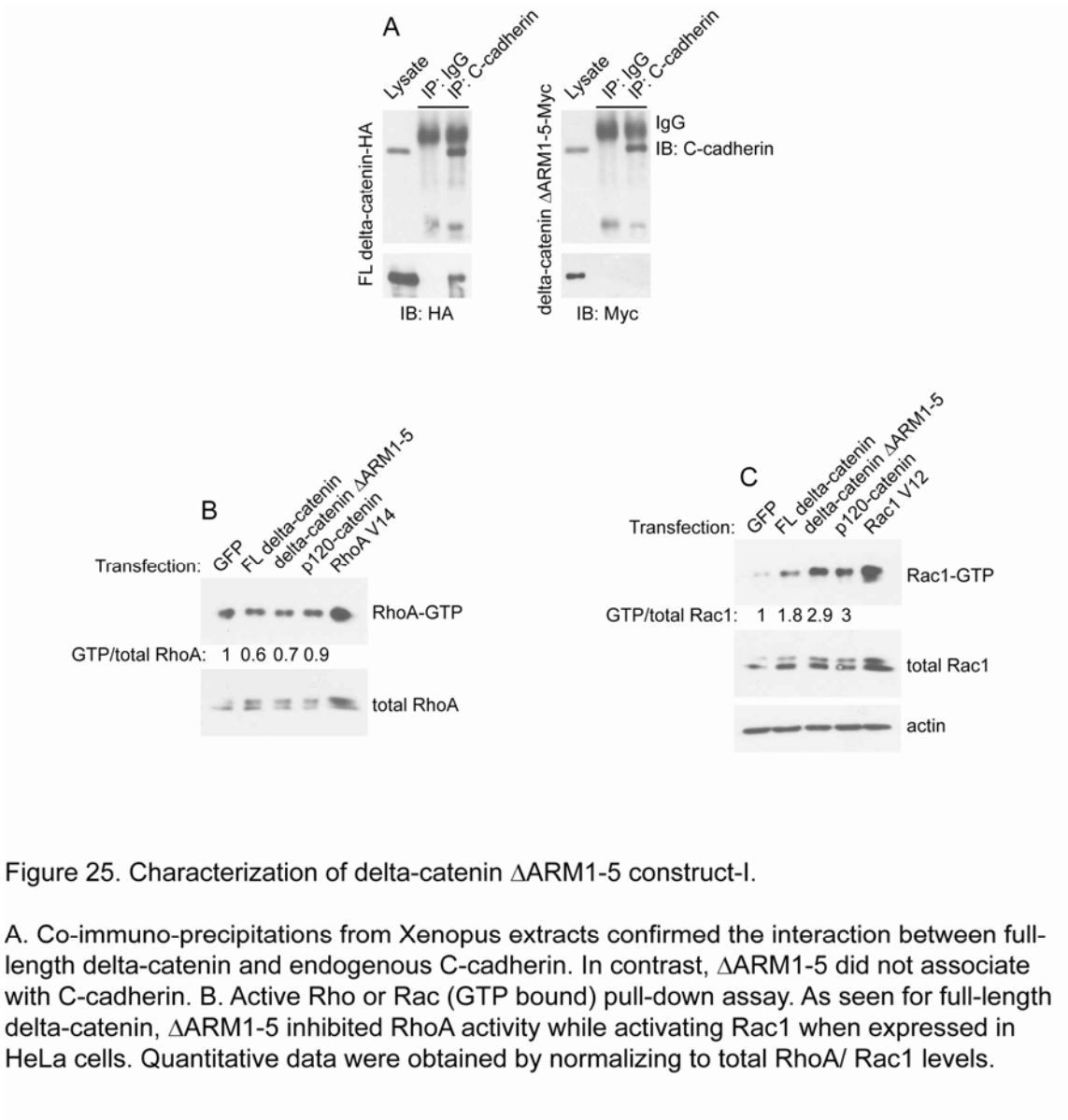


Figure 25. Characterization of delta-catenin  $\Delta$ ARM1-5 construct-I.

A. Co-immuno-precipitations from *Xenopus* extracts confirmed the interaction between full-length delta-catenin and endogenous C-cadherin. In contrast,  $\Delta$ ARM1-5 did not associate with C-cadherin. B. Active Rho or Rac (GTP bound) pull-down assay. As seen for full-length delta-catenin,  $\Delta$ ARM1-5 inhibited RhoA activity while activating Rac1 when expressed in HeLa cells. Quantitative data were obtained by normalizing to total RhoA/ Rac1 levels.

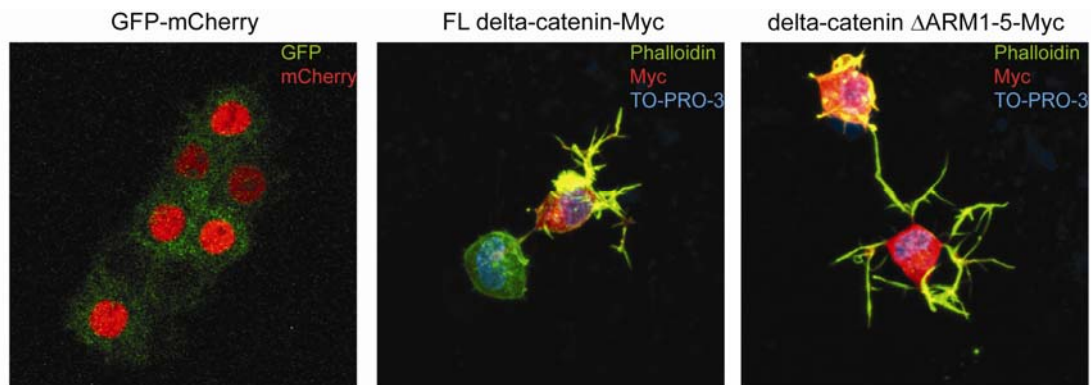


Figure 26. Characterization of delta-catenin  $\Delta$ ARM1-5 construct-II.

In common with wild-type delta-catenin, expression of  $\Delta$ ARM1-5 enhanced neurite-like process formation in Neuro-2a cells. The round to multi-polar morphology of control Neuro-2a cells was visualized by transfecting a construct that simultaneously labels nuclear (mCherry) and membranous structures (GFP).

## Depletion of delta-catenin perturbs Rho and Rac activities

Rho family small G proteins are important regulators of actin dynamics, and based on earlier work, likely interact with delta-catenin in mediating some of its downstream effects (Abu-Elneel et al., 2008; DeBusk et al., 2010; Kim et al., 2008a; Martinez et al., 2003). To examine whether Rho responds to delta-catenin depletion in *Xenopus* embryos, I measured active RhoA (GTP-bound) levels using total RhoA protein as the control. Remarkably, I observed a significant Rho activation in *Xenopus* extracts following delta-catenin depletion (Figure 27A). To test whether such changes might be relevant to the observed developmental defects upon delta-catenin depletion, I again employed a rescue strategy wherein dominant-negative RhoA (RhoA N19, titrated) was co-injected with delta-catenin MO-6. I repeatedly observed a significant rescue using this form of RhoA, whereas as a negative control, no rescue was achieved from constitutively-active RhoA (RhoA V14) (Figure 27C). Given multiple reports regarding Rac1 activation by p120 sub-family members including delta-catenin (Ciesiolka et al., 2004; Elia et al., 2006; Fang et al., 2004; Grosheva et al., 2001; Hou et al., 2006; Wildenberg et al., 2006), I then tested Rac activation using a similar pull-down assay. As expected, I resolved modest inhibition of Rac1 in *Xenopus* extracts (Figure 27B). Pointing to the functional relevance, a dominant-active form of Rac1 (Rac1 V12) significantly rescued gastrulation defects following delta-catenin depletion, whereas a dominant-active Cdc42 did not (Cdc42 V12, used as a negative control) (Figure 27C). Thus, my results are in



line with other studies of cell lines and animals and supported models that delta-catenin depletion in *Xenopus* activates RhoA functions, while repressing Rac1.

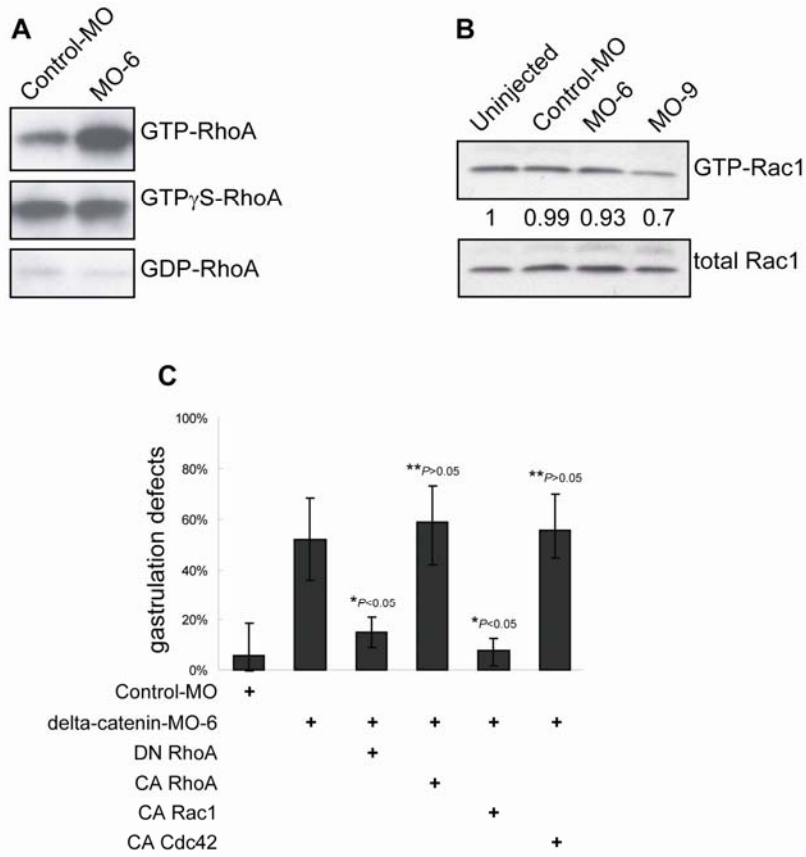


Figure 27. Delta-catenin depletion results in activation of RhoA and inhibition of Rac1.

A. Rhotekin pull-down assays reveal strong activation of RhoA following delta-catenin depletion. B. Delta-catenin depletion modestly reduces active Rac1 levels as measured by PBD (PAK binding domain) affinity pull-down experiments. C. Consistent with our biochemical evidence, a titrated dose of dominant-negative (DN) RhoA, but not constitutively-active (CA) RhoA, significantly rescues delta-catenin knock-down phenotypes. Likewise, constitutively-active Rac1, but not constitutively-active Cdc42, rescues blastopore closure defects in delta-catenin-depleted embryos.

## Part II: Exploring the roles of delta-catenin in the nucleus

**Summary:** Delta-catenin is an Armadillo protein of p120-catenin sub-family capable of modulating cadherin stability, small GTPase activity and nuclear transcription. In part II of my dissertation work, I identified delta-catenin as a substrate of the caspase-3 protease, which plays essential roles in apoptotic as well as non-apoptotic processes. Delta-catenin's interaction with caspase-3 was confirmed using cleavage assays conducted in vitro, in *Xenopus* apoptotic extracts and in cell line chemically induced contexts. The cleavage site, a highly conserved caspase consensus motif (DELD) within Armadillo-repeat 6 of delta-catenin, was identified through peptide sequencing. Cleavage thus generates an amino- (1-816) and carboxyl-terminal (817-1314) fragment each containing about half of the central Armadillo-domain. I found that cleavage of delta-catenin both abolishes its association with cadherins, and impairs its ability to modulate small GTPases. Interestingly, the carboxyl-terminal fragment 817-1314 possesses a conserved putative nuclear localization signal that may facilitate delta-catenin's nuclear targeting in defined contexts. To probe for novel nuclear roles of delta-catenin, I performed yeast two-hybrid screening of a mouse brain cDNA library, resolving and then validating delta-catenin's interaction with an uncharacterized KRAB family zinc finger protein ZIFCAT. My results indicate that ZIFCAT is nuclear, and suggest that it may associate with DNA as a transcriptional repressor. I further determined that other p120 sub-family catenins are similarly cleaved by caspase-3, and likewise bind ZIFCAT.

My findings potentially reveal a simple yet novel signaling pathway based upon caspase-3 cleavage of p120-catenin sub-family members, facilitating the coordinate modulation of cadherins, small GTPases and nuclear functions.

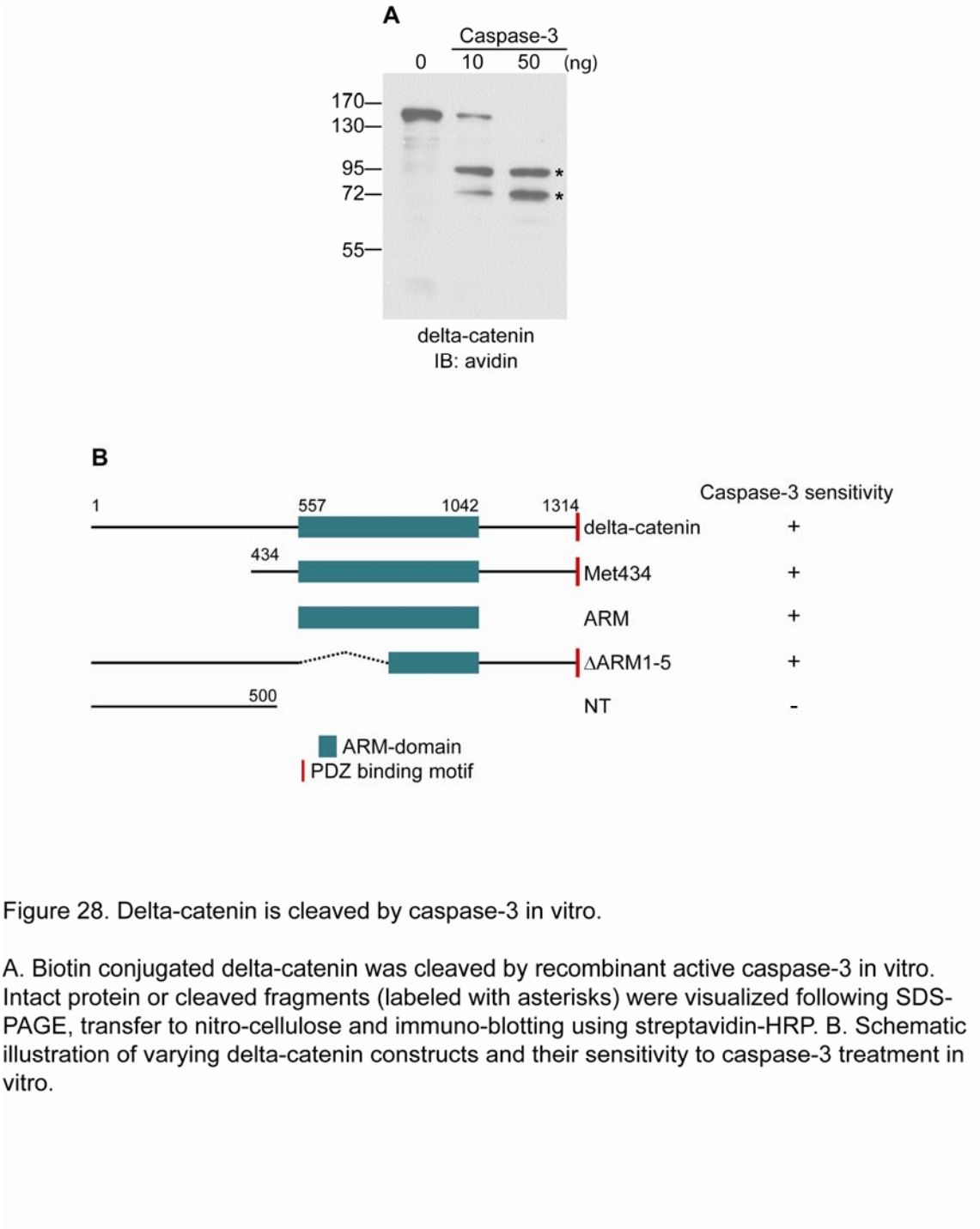
### **Delta-catenin is a novel caspase-3 substrate**

Yeast two-hybrid screening of a human embryonic stem cell cDNA expression library pointed to delta-catenin as a potential substrate of constitutively-active caspase-3 (mcas3rev), which was employed as bait (Dejosez et al., 2008; Fujita et al., 2008). Mcasp3rev spontaneously folds into its active conformation and binds target proteins but no longer cleaves them owing to a C163S substitution.

To begin to test this interaction's validity, I employed a classic *in vitro* assay wherein delta-catenin was mixed with recombinant active caspase-3. Delta-catenin had been biotin-labeled on lysine residues, ensuring that all major fragments could be visualized through streptavidin-HRP immuno-blotting (Promega Transcend Non-Radioactive Translation Detection System). Remarkably, I observed significant cleavage at a low caspase-3 dose (10ng), with complete cleavage occurring at higher doses (50ng) (Figure 28A). To map the region necessary for caspase-3 binding and cleavage, I collected additional delta-catenin constructs and tested them using the same assay. Figure 28B summarizes their responses to caspase-3 *in vitro*. The Armadillo-domain of

delta-catenin, and more specifically repeats 6-10, appeared to be the region of caspase-3 recognition.

Next, I used an established *in vivo*-derived assay of caspase function (Kornbluth and Evans, 2001). Apoptotic extracts harvested from *Xenopus* eggs were incubated with the bacterially expressed entire Armadillo-domain of delta-catenin, which became markedly cleaved and apparently further metabolized (Figure 29A). Notably, addition of DEVD-CHO (Calbiochem), a specific inhibitor for caspase-3 and 7, completely abolished this cleavage in apoptotic *Xenopus* extracts. To examine endogenous delta-catenin cleavage in mammalian cells, I screened six glioblastoma stem cell lines, finding one (GSC11) that expressed delta-catenin at significant levels. Four independent antibodies confirmed delta-catenin migrating on SDS-PAGE as a ~150 kDa doublet (calculated molecular weight 133 kDa). Delta-catenin was cleaved following the incubation of GSC11 cells with Puromycin, a protein synthesis inhibitor and established apoptotic inducer (Figure 29B). Such *in vivo* cleavage was likewise observed for Met434 delta-catenin, expressed exogenously in 293T cells (see also Figure 38). These findings together suggest that caspase-3 may be the predominant enzyme responsible for initial delta-catenin cleavage during apoptotic or potentially non-apoptotic events.



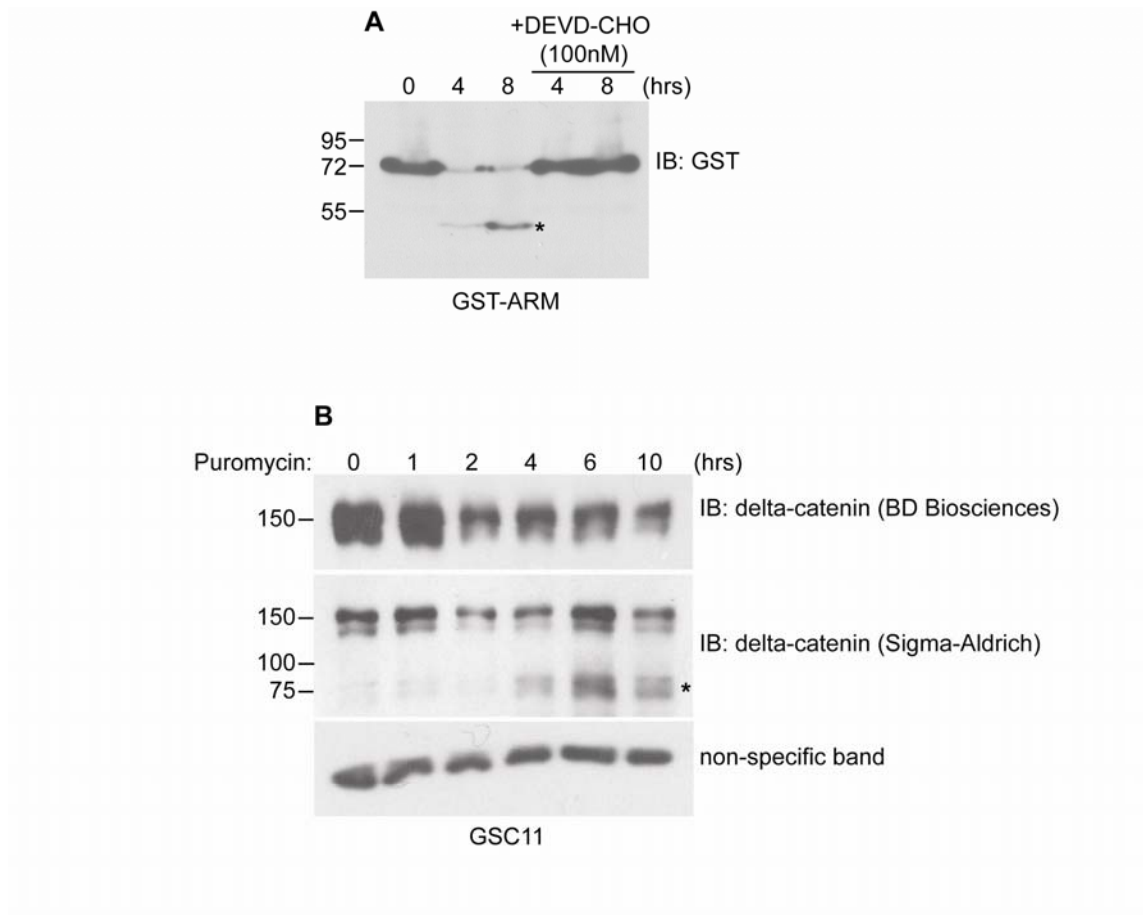


Figure 29. Delta-catenin is cleaved in apoptotic extracts.

A. Recombinant Armadillo-domain of delta-catenin (GST fusion) was incubated in *Xenopus* egg extracts for the indicated times in the absence versus presence of DEVD-CHO, a specific inhibitor of caspase-3 and -7. Cleavage of delta-catenin (labeled with asterisk) was detected by immuno-blotting, using antibodies directed against GST. B. Extracts from GSC11 cells treated with Puromycin were tested for endogenous delta-catenin cleavage. An antibody recognizing delta-catenin's amino-terminal region (BD Biosciences) reproducibly showed a Puromycin dependent loss of full-length delta-catenin as expected, while a carboxyl-directed antibody (Sigma-Aldrich) resolved the appearance of a delta-catenin fragment migrating at a size consistent with caspase-3 generation of 817-1314 (labeled with asterisk). A non-specific band was included as the loading control.

### **Caspase-3 cleaves delta-catenin at DELD816 consensus motif**

To identify the tetra-peptide motif for caspase-3 targeting, I performed *in vitro* cleavage as noted above, using the Armadillo-domain of delta-catenin purified from *E. coli*. Cleavage was confirmed by coomassie blue staining (Figure 30A). A separate gel with equal loading was blotted onto a PVDF membrane, the peptide band was excised, and the first 10 amino-terminal residues were sequenced (Genomics and Proteomics Core Laboratory, Baylor College of Medicine). Figure 30B illustrates the 'GLLCADNNGK' sequencing result, which in turn pointed to the upstream tetra-peptide motif 'DELD816', a typical caspase-3 consensus site. Residue 'D816' likely represents position 'P1', the key amino acid for caspase-3 binding, after which peptide bond cleavage occurs. Upstream amino acids 'D', 'E' and 'L' would then respectively represent the 'P4' 'P3' 'P2' residues, each contributing to caspase-3 recognition and association (Solary et al., 1998). It is notable that this caspase-3 site of delta-catenin is highly conserved across species (Figure 30B).

To verify the significance of D816, I carried out site-directed mutagenesis, converting native D (aspartate) to E (glutamate), an amino acid that resembles aspartate in the chemical nature yet is resistant to caspase cleavage. Remarkably, the D816E mutant completely blocked caspase-3 cleavage *in vitro* compared to the wild-type delta-catenin (an asterisk in Figure 31 marks the cleavage product of wild-type delta-catenin). Intriguingly, the p120- and ARVCF-



catenins also contain conserved predicted caspase-3 consensus sites within their Armadillo-domains. These additional catenins are likewise sensitive to caspase-3 in vitro, suggesting that caspase-3 regulation of p120-catenin sub-family members may be a general phenomenon (Figure 32).

Collectively, my in vitro and in vivo data strongly suggest that delta-catenin is a novel substrate of caspase-3 and is cleaved after the DELD816 motif.

### **Cleavage of delta-catenin abolishes cadherin binding**

To probe for potential physiological relevance, I sub-cloned the two delta-catenin fragments formed as a result of caspase-3 cleavage, and examined their ability to bind cadherin in vitro and in live cells. Hereafter I designate '1-816' to refer to the amino-terminal fragment (Xenopus delta-catenin amino acids 1-816), and '817-1314' to refer to the carboxyl-terminal fragment (Xenopus delta-catenin amino acids 817-1314). As expected, and employed as a positive control, full-length delta-catenin bound C-cadherin when translated and tested in vitro. In contrast, neither 1-816 nor 817-1314 displayed comparable immuno-blot signals, suggesting that both these fragments had greatly reduced capacities to bind cadherin (Figure 33A).

Next, I in vitro transcribed these cDNA constructs into capped mRNAs

and injected them into one-cell stage *Xenopus* embryos, a classic approach used to test interactions with endogenous (or exogenous) proteins *in vivo*. Repeatedly, I observed a positive association between full-length delta-catenin with endogenous C-cadherin, a major cadherin mediating blastomere adhesion during early embryonic cleavage stages. Neither 1-816 nor 817-1314 produced a specific signal when compared to the IgG negative control pull-downs (Figure 33B). These results suggest that caspase-3 cleavage of delta-catenin (and likely of p120- and ARVCF-catenins), prevents its association with cadherins. Given the recognized protective effects of bound p120-catenin sub-family members on cadherin stability, this may contribute to the known reduction of cadherin function following caspase activation.

### **Cleaved delta-catenin fragments are impaired in Rho and Rac modulation**

Rho and Rac are Ras-family small G proteins that critically mediate actin dynamics and tissue morphogenesis (Hall, 1998; Heasman and Ridley, 2008). A prominent function of p120-catenin sub-family catenins, including delta-catenin, is their direct or indirect association and modulation of small GTPases, affecting their GTP- (active) versus GDP-bound (inactive) states (Anastasiadis, 2007; Keil et al., 2007). To test if the impact of delta-catenin upon Rho and Rac is affected upon caspase cleavage, I compared full-length versus 1-816 or 817-1314 (cleaved) delta-catenin, evaluating Rho or Rac activity using RBD or PBD pull-down assays, respectively. Consistent with other reports (Abu-Elneel et al., 2008;

DeBusk et al., 2010; Gu et al., 2009; Martinez et al., 2003), expression of full-length delta-catenin in HeLa cells inhibited RhoA while partially activating Rac1 (Figure 34A and 34B). Both 1-816 and 817-1314, in contrast, failed to alter RhoA activity. With respect to Rac1, 1-816 as anticipated lacked stimulatory or other effects, while unexpectedly, 817-1314 reproducibly displayed inhibitory, possibly dominant negative effects (Figure 34B). These results suggest that caspase-3 cleavage of delta-catenin reduces or alters delta-catenin's modulation of small GTPases, likely coincident and possibly in coordination with effects upon cadherin functions.

### **An NLS within delta-catenin's Armadillo-repeat 6 enhances 817-1314 nuclear localization**

The 817-1314 fragment resulting from caspase-3 cleavage contains an 'WGKKKKKKKSQ' sequence element previously demonstrated to possess nuclear localization activity (Lu et al., 1999) (see also Figure 4 and Figure 30B). To test if this putative NLS might contribute to 817-1314's nuclear entry, epitope-tagged delta-catenin constructs were transiently expressed in various cell types, and this was followed by confocal immuno-fluorescence visualization. As shown in Figure 35 using 293T cells, full-length delta-catenin appeared concentrated near cell-cell borders, with residual staining in the cytoplasm. Lacking the ability to bind cadherin, 1-816 was instead more diffusely localized in the cytosol. Likewise in contrast to full-length, but also differing from 1-816, prominent

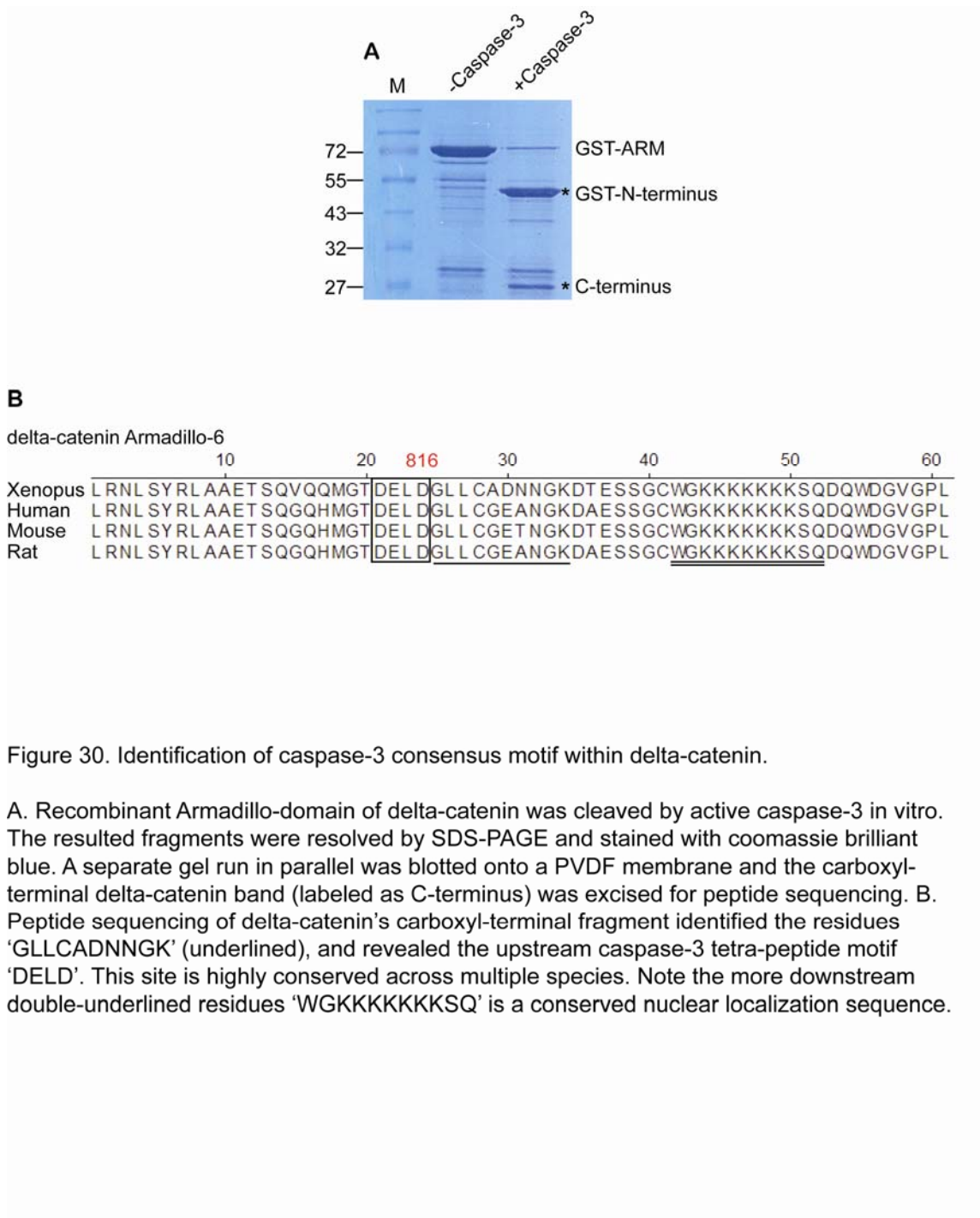


Figure 30. Identification of caspase-3 consensus motif within delta-catenin.

A. Recombinant Armadillo-domain of delta-catenin was cleaved by active caspase-3 in vitro. The resulted fragments were resolved by SDS-PAGE and stained with coomassie brilliant blue. A separate gel run in parallel was blotted onto a PVDF membrane and the carboxyl-terminal delta-catenin band (labeled as C-terminus) was excised for peptide sequencing. B. Peptide sequencing of delta-catenin's carboxyl-terminal fragment identified the residues 'GLLCADNNGK' (underlined), and revealed the upstream caspase-3 tetra-peptide motif 'DELD'. This site is highly conserved across multiple species. Note the more downstream double-underlined residues 'WGKKKKKKKSQ' is a conserved nuclear localization sequence.

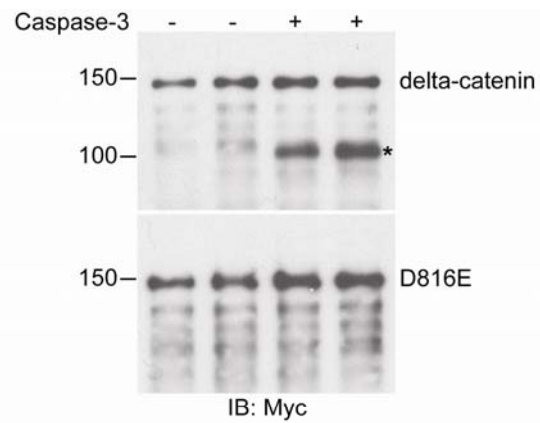


Figure 31. Caspase cleavage site verified via site-directed mutagenesis.

Mutation of the critical residue D (aspartate) 816 to E (glutamate) abolished delta-catenin susceptibility to active caspase-3 in vitro when compared side-by-side with the wild-type protein. An asterisk labels the partial cleavage product of wild-type delta-catenin.

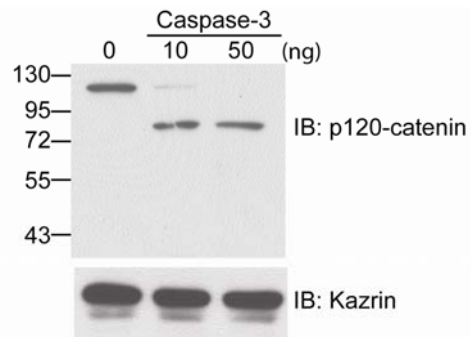


Figure 32. P120-catenin is cleaved by caspase-3 in vitro.

Myc-tagged p120-catenin is likewise an in vitro caspase-3 substrate as indicated upon immuno-blotting. Kazrin in contrast was resistant to caspase treatment when processed in parallel.

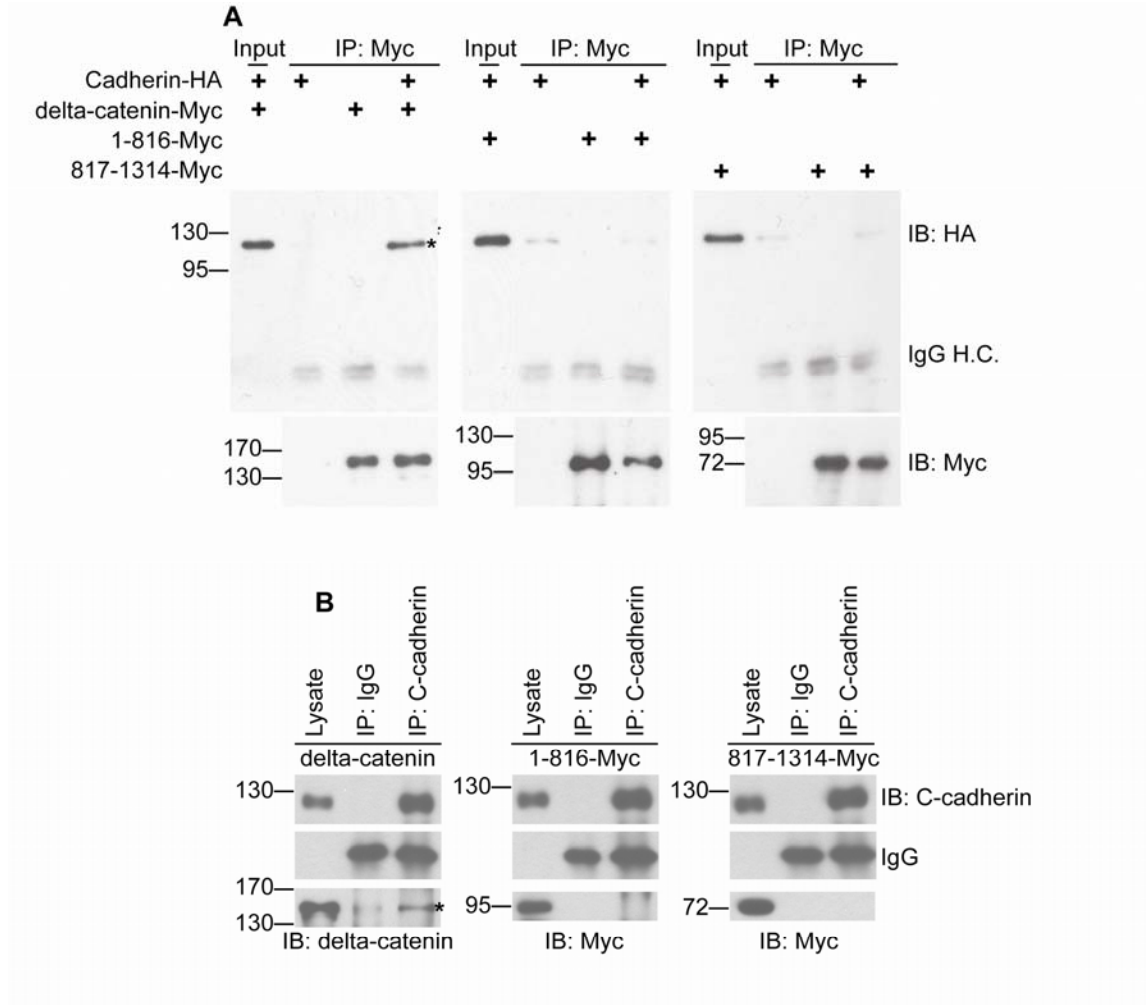


Figure 33. Cleaved delta-catenin fragments fail to associate with cadherins.

A. Selected constructs were translated in vitro and then incubated together using established conditions. Antibody against the Myc-epitope was added followed by Protein A/ G beads, allowing immuno-precipitation of Myc-tagged delta-catenin proteins with (or without) associated C-cadherin. Immuno-blotting using HA antibody indicated C-cadherin associated with full-length delta-catenin, but not the cleaved fragments 1-816 or 817-1314. IgG heavy chains were used as a loading reference. B. Delta-catenin cDNA constructs were transcribed in vitro as capped mRNAs and then injected into *Xenopus* embryos for expression. Immuno-precipitates of endogenous C-cadherin from stage 12 gastrulating embryo extracts were resolved by SDS-PAGE and blotted for delta-catenin. Full-length delta-catenin displayed a positive association (labeled with asterisk), in contrast to the cleaved fragments 1-816 or 817-1314, or the IgG controls.

localization to nuclei was observed for 817-1314, with additional cytosolic presence. Results from MDA-MB-435 melanoma cells (Figure 36), MDA-MB-231 breast cancer cells and Neuro-2a neuroblastoma cells were consistent with observations from 293T cells.

To test if the nuclear localization of 817-1314 required the NLS, I removed an amino-terminal region of 28 amino acid residues that included the 'WGKKKKKKKSQ' element. When compared with 817-1314, removal of the NLS placed a much greater proportion of the resulting construct in the cytoplasm (Figure 35 and Figure 36). Next, I employed biochemical fractionation to better quantify their intracellular distribution. Shown in Figure 37, a prominent portion of 817-1314 localized to the nuclear fraction (57% of 100%), as distinguished from full-length delta-catenin (18%), 1-816 (15%) or 817-1314 $\Delta$ NLS (11%). Similar results were obtained for 817-1314 in 293T cells subject to Puromycin-induced cell death (Figure 38). Thus, the resolved caspase-3 cleavage of delta-catenin generates a fragment (817-1314) that becomes enriched in the nucleus, leaving open the possibility that 817-1314 has nuclear roles.

### **Delta-catenin had no detectable effect upon chemical-induced apoptosis**

Considering that caspase-3 is best known as an 'executioner' caspase in the apoptotic cascade, one could imagine that delta-catenin may exert effects within cell death programs. Indeed, in independent work, exogenous delta-



catenin expression resulted in limited cell death in NIH 3T3 cells (Kim et al., 2000). Conversely, however, delta-catenin has been reported to have pro-survival activities in prostate adenocarcinoma cells (Zeng et al., 2009), and elicited feedback suppression of Pax6-induced apoptosis in HeLa cells (Lu et al.).

In the present study I employed a cell death ELISA method (Roche), but did not observe significant increases or decreases in chromatin breakage upon delta-catenin expression (Figure 39). Likewise, neither full-length delta-catenin, nor the D816E, 1-816 or 817-1314 constructs, protected HeLa cells from Staurosporine- or Puromycin-induced apoptosis (Figure 40). Thus, pro-survival or apoptotic effects may be context dependent, or their detection may require a more sensitive assay to reach a definitive conclusion regarding delta-catenin's role in apoptosis.

### **ZIFCAT is a novel KRAB zinc finger protein associating with delta-catenin and ARVCF**

The localization of 817-1314 encouraged me to test for potential functions of delta-catenin in the nucleus. Using *Xenopus* delta-catenin as bait, I performed a second yeast two-hybrid screen, this time employing an adult mouse brain cDNA library (Hybrigenics, Inc.). Since full-length delta-catenin exhibited auto-activation, I chose a delta-catenin construct deleted of its amino-terminus (intact

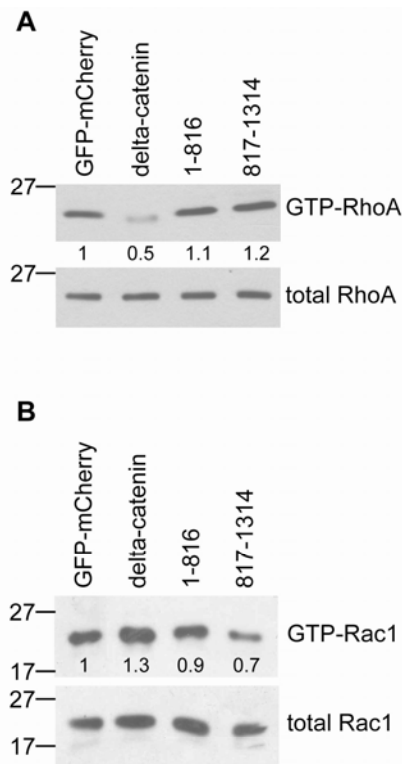


Figure 34. Cleaved delta-catenin fragments exhibit impaired small GTPase regulation.

A. Rho activation was measured in extracts of HeLa cells transiently expressing selected delta-catenin constructs. Transfections were optimized to achieve maximal efficiency and monitored by GFP-mCherry expression. Full-length delta-catenin reduced the cellular level of active RhoA while neither 1-816 nor 817-1314 displayed a significant impact relative to the control transfection. Numeric values represent the quantitations of GTP-RhoA (active) relative to total RhoA. B. Rac activation assays were conducted in a similar manner as in (C), except that PBD agarose beads were used to pull-down GTP-Rac (active), and Rac1 antibody was used for immuno-blotting. In HeLa cells, full-length delta-catenin modestly but reproducibly increased the cellular levels of GTP-Rac1. 1-816 did not produce effects consistently different from the control. 817-1314 reproducibly showed a partial inhibition of Rac1 (N>3 independent experiments). Numeric values represent the quantitations of GTP-Rac1 (active) relative to total Rac1.

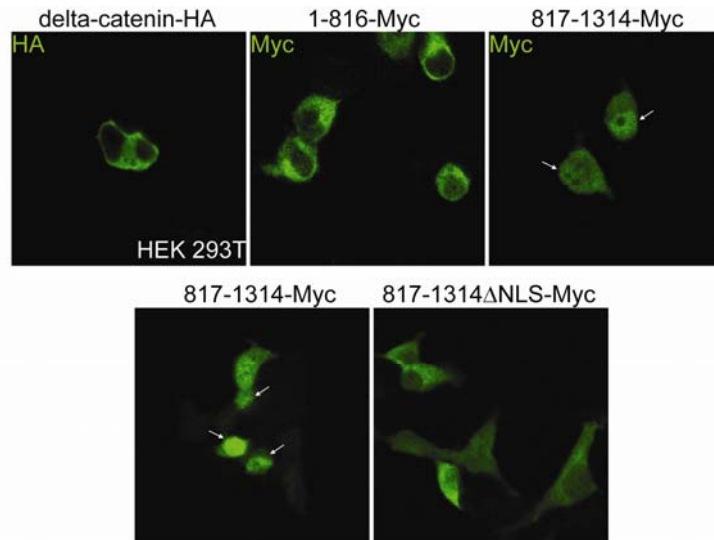


Figure 35. The NLS within Armadillo-repeat 6 enhances 817-1314 localization to 293T cell nuclei.

Confocal immuno-fluorescence localizations of various delta-catenin constructs. Full-length delta-catenin predominantly localizes to cell-cell borders and the cytoplasm in 293T cells, visualized via HA-epitope staining. 1-816 is largely distributed within the cell cytosol, with lesser intensity at cell-cell borders. 817-1314, in contrast, displays a significant nuclear staining (marked with arrows), with additional cytosolic localization. Deletion of the NLS in 817-1314 reduced the presence of 817-1314 in the nucleus of 293T cells.

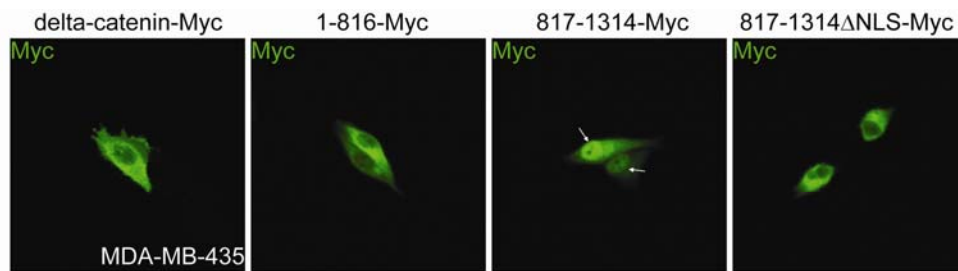


Figure 36. Sub-cellular localizations of delta-catenin constructs in MDA-MB-435 melanoma cells.

Immuno-fluorescence results were consistent with those from HEK 293T cells.

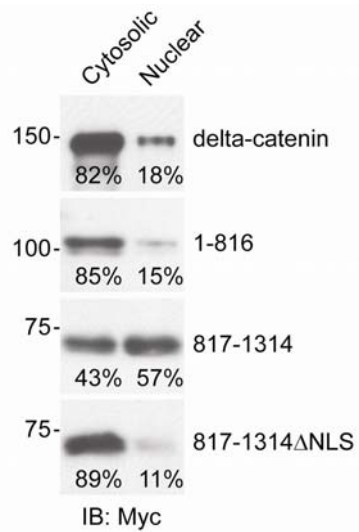


Figure 37. Cytosolic-nuclear fractionation.

Fractionation of 293T cells followed by immuno-blotting indicates that delta-catenin and 1-816 largely distribute to the cytosolic fraction, whereas 817-1314 exhibits a larger nuclear presence. Deletion of the NLS from 817-1314 efficiently redistributed the resulting construct to the cytosol.

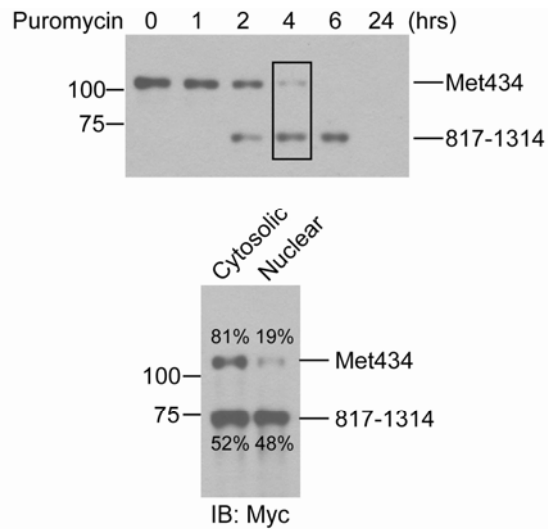


Figure 38. The NLS within Armadillo-repeat 6 enhances 817-1314 localization to nuclei.

293T cells transfected with the Met434 delta-catenin construct were treated with Puromycin. Whole-cell extracts (obtained 4 hours after treatment) were separated by cytosolic-nuclear fractionation and subject to Myc immuno-blotting. Given that the Myc-epitope was present at delta-catenin's carboxyl-terminus, the nuclear enrichment of 817-1314 was confirmed relative to Met434 (lower panel).

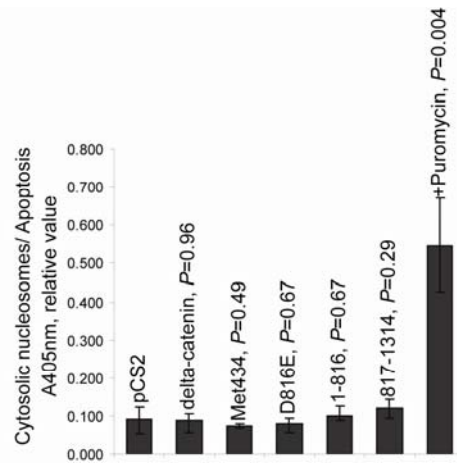


Figure 39. Cell death detection ELISA-I.

HeLa cells transiently expressing the noted cDNA constructs were lysed followed by ELISA-based detection of free nucleosomes as a measure of apoptosis. The expression of delta-catenin or of delta-catenin mutants did not induce obvious chromatin breakages in untreated HeLa cells, using Puromycin treatment as a positive control.

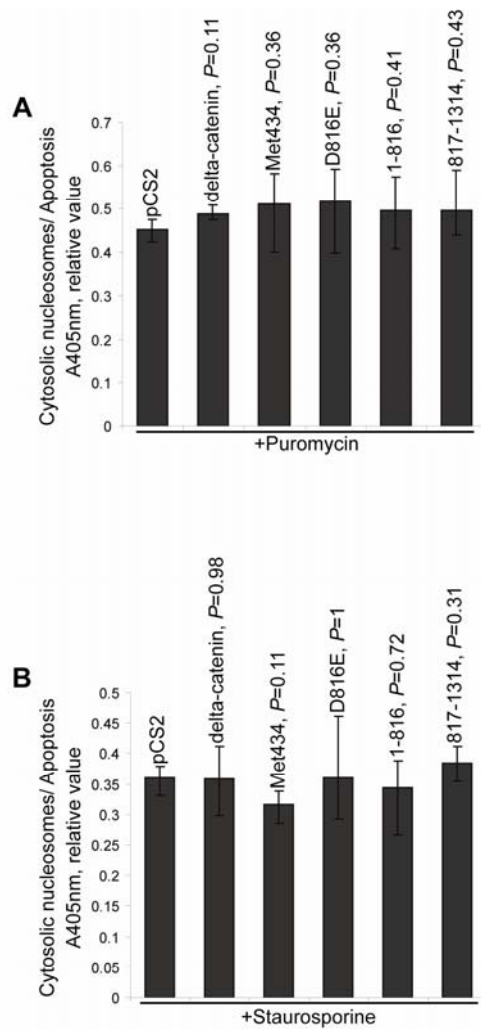


Figure 40. Cell death detection ELISA-II.

The expression of delta-catenin constructs did not exert any obvious protective effect from Puromycin (A)- or Staurosporine (B)-induced apoptosis, or in promoting apoptosis.



Armadillo and carboxyl-terminal domains). A total of 159 clones were obtained representing 27 distinct potential interactions, including known associations with cadherins and Erbin (internal positive controls) (Figure 41). My screen was not saturating given that additional known interactions were not resolved. Intriguingly, the best-rated interaction (Hybrigenics, Inc.) included 11 independent clones encoding a novel KRAB (Kruppel Associated Box) zinc finger protein (2610008E11Rik).

KRAB zinc finger proteins feature a carboxyl-terminal zinc finger region that binds DNA, and an amino-terminal KRAB motif associating with transcriptional cofactors (Looman et al., 2002). To be memorable as well as easily vocalized, I termed the resolved novel protein ZIFCAT (ZInc Finger protein associating with CATenins). Figure 42 displays the phylogenetic tree of ZIFCAT across select species. As deduced from the 11 yeast two-hybrid ZIFCAT clones obtained, the minimal interacting sequence with delta-catenin included zinc finger repeats 6-8 (Figure 43). Intriguingly, ZIFCAT was once again resolved in a parallel yeast two-hybrid screen aimed to identify novel ARVCF-catenin interactions (Hybrigenics, Inc.). Based simply on the yeast two-hybrid clones resolved, the minimal ZIFCAT interacting sequence associating with ARVCF likewise appears to include a similar (perhaps larger) zinc finger region. Thus, ZIFCAT was suggested to employ its zinc finger domain to bind delta- and ARVCF-catenin, the same region that might be anticipated to bind DNA.

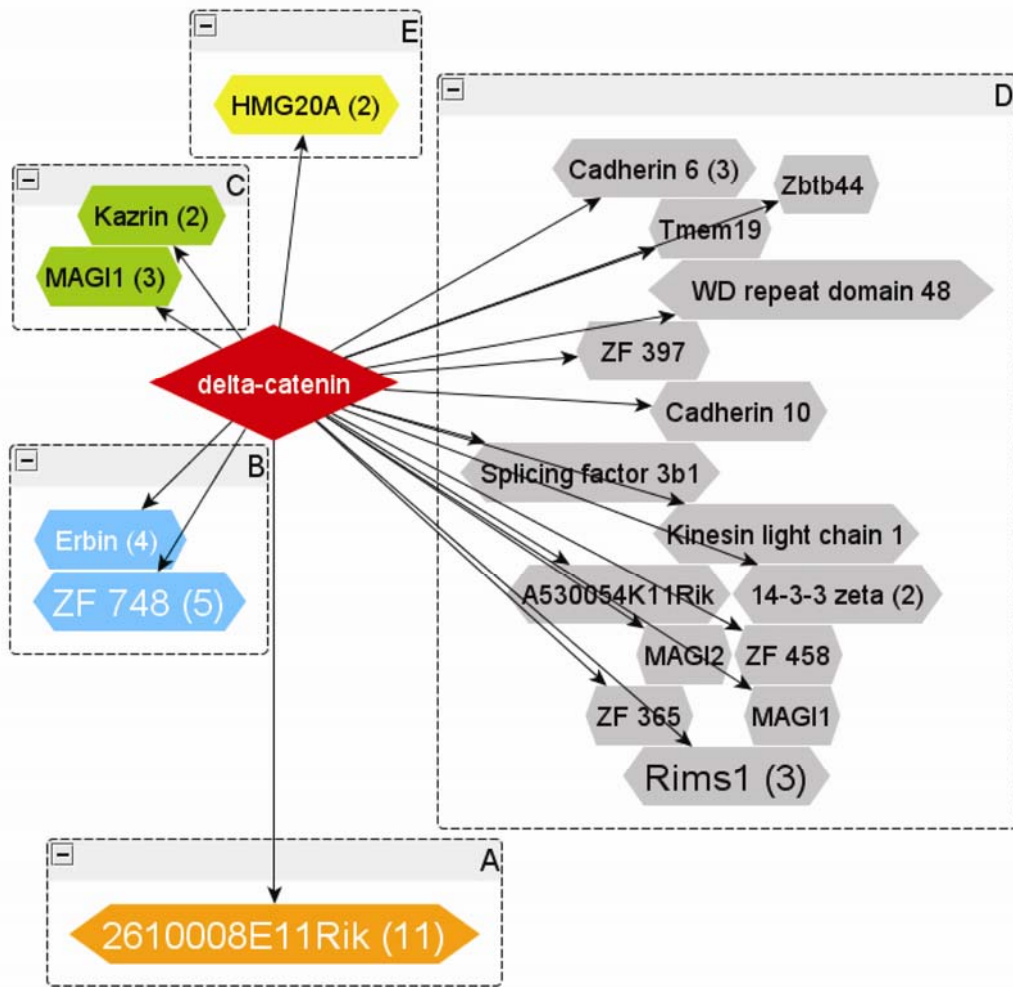


Figure 41. Diagram of delta-catenin protein interactions identified through yeast two-hybrid screening.

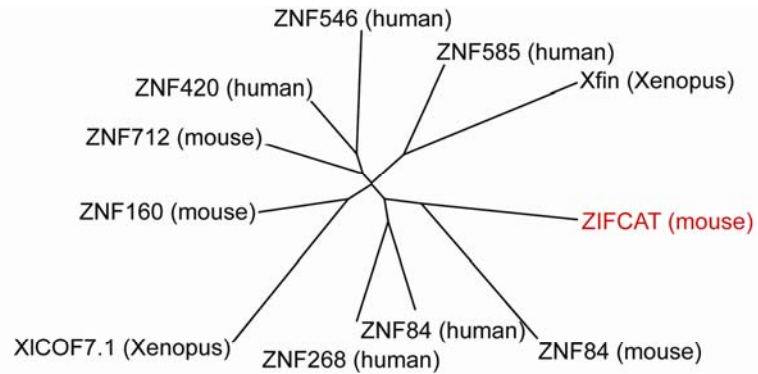


Figure 42. Phylogenetic tree of ZIFCAT and related proteins.

Following Clustal V sequence alignment of ZIFCAT with similar proteins across selected species, a phylogenetic tree representation was generated of their inter-relatedness. The length of the lines reflects the relative amino acid sequence divergence, as determined following the application of MegAlign in the DNASTAR package and the TreeView software.

MSAEPVMESVSVFEDIAVFFTWEEWODLDIAOKLLYRDVMLENYSSLVSLG	50
CCVIKPELILMLEREFGPWRVADTSVWNLPGYCMTRPELNFKLSHGFEPW	100
NGSEASLWSLPDVHKVSVLGNQETHLWQAEVTGGITSYEQMVEAELQIQE	150
KIHREAKIHEYKDCMETFY PNSQHTRNQTSQSYENPFGWEEFRKAFYYQS	200
TLTQHQRFHIGEKLY <sup>1</sup> DSPOCWEIFPWKSOLSVHETFHAGERR <sup>2</sup> ECCECRK	250
SFHRKANLIRHORRTHSREKP <sup>3</sup> ECIECGKTFYCKSDVTRHORRTHSREKP	300
<u>YECVECSKTFYCKSYLIRHQSRTHSREKP<sup>4</sup>ECTECTKTFYCKSDLTRHOT</u>	350
<u>THSGEKPF<sup>5</sup>ECNECSKTFYKSDLANHOKTHTDDNP<sup>6</sup>YECKECRKTECSKSS</u>	400
<u>LNOHHRITHTGEKPY<sup>7</sup>ECNECKKSENSKSNL<sup>8</sup>TEHORRTHTREKPY<sup>9</sup>ECNECWK</u>	450
<u>SFYCRSELTNHORTHHTVERY<sup>10</sup>YECKECRKNFYCKSNLNOHORTHHTGEKPY<sup>11</sup>E</u>	500
<u>CKDCNKAFYCKSNLNOHORTHHTGEKPY<sup>12</sup>ACKDCSKAFYCKSSLVKHOKIHS</u>	550
<u>GEKPY<sup>13</sup>ECCECRKTFFOKSDLTRHORTHHTGEKPY<sup>14</sup>ECKDCSKTFYCKSNLNO</u>	600
<u>HORTHHTHEKPY<sup>15</sup>ECKECRETFYKSELTEHORTHHTDEKPYVMFNIDCQLDK</u>	650
IWDHLGDRPVGMPVKDYLD	

Figure 43. Primary sequence analysis of novel KRAB zinc finger protein ZIFCAT.

Underlined in black is the amino-terminal KRAB domain, and in red are 15 C2H2 type zinc finger repeats occupying approximately two-thirds of ZIFCAT including its carboxyl-terminal region. The shaded residues comprise the minimal region deduced from yeast two-hybrid screening to associate with delta-catenin.

To test the resolved yeast two-hybrid interactions, I performed in vitro binding assays as described earlier. Full-length delta-catenin bound to ZIFCAT in vitro. 817-1314, which is generated by caspase-3 cleavage and displays nuclear localization, also bound ZIFCAT (Figure 44A). I failed, in contrast, to observe a positive association of ZIFCAT with either 1-816, with the isolated Armadillo-domain of delta-catenin, or with delta-catenin's amino-terminal domain. I then confirmed the in vitro interaction between ARVCF and ZIFCAT following a similar strategy, but using ARVCF fused to maltose binding protein/ MBP and purified from *E. coli*. Lacking antibodies against endogenous ZIFCAT, I next sought to resolve an interaction in vivo with full-length delta-catenin. This proved challenging, for while ZIFCAT is predominantly nuclear (see also Figure 46A), the majority of full-length delta-catenin or ARVCF remains at cell-cell contacts in complex with cadherins, or cadherin-free within the cytoplasm, where it acts upon small GTPases. Given that my evidence pointed to a potential nuclear role of 817-1314, I co-transfected 817-1314 with ZIFCAT. As anticipated, co-immunoprecipitation from 293T nuclear fractions clearly confirmed the association of 817-1314 with ZIFCAT (Figure 44B). I further wished to test for an in vivo association of ARVCF-catenin with ZIFCAT. Not knowing the precise caspase-3 cleavage site(s) within ARVCF, or its validated endogenous NLS, I employed a different strategy, fusing an amino-terminal ectopic NLS to full-length ARVCF. This notably increased ARVCF's presence in the nucleus, and allowed us to resolve an association with ZIFCAT (Figure 45). My results together indicate that two distinct p120-catenin sub-family members, delta- and ARVCF-catenin, each

associate with ZIFCAT. Under physiologic circumstances involving caspase-3, I conjecture that a resulting fragment (such as 817-1314) is more likely to enter the nucleus and associate with ZIFCAT than the corresponding full-length catenin.

### **ZIFCAT associates with chromosomal DNA, and may act as a transcriptional repressor**

To gain further insight of ZIFCAT, I examined its sub-cellular localization. As expected, HA-tagged ZIFCAT localized strongly to the nuclei of HeLa or 293T cells (Figure 46A). I next tested if ZIFCAT associates with genomic DNA in vitro, using an established assay (Hosking et al., 2007). Here, full-length ZIFCAT, or a ZIFCAT construct lacking the amino-terminal 169 residues including the KRAB domain (ZIFCAT-ZF), was co-incubated with cellulose-conjugated genomic DNA purified from calf thymus (Sigma-Aldrich). Both constructs associated with the genomic DNA, while in contrast, this association was largely lost when the carboxyl-terminus 497 residues including the zinc finger region of ZIFCAT was removed (ZIFCAT $\Delta$ ZF) (Figure 46B). My data are thus consistent with the possibility that ZIFCAT associates directly or indirectly with DNA through its zinc finger repeats, and speculatively, exerts gene regulatory functions via KRAB domain co-factors such as KAP1 (KRAB associated protein 1) (Urrutia, 2003).

As an initial test of whether ZIFCAT might modulate gene transcription, I

utilized the Gal4-UAS-luciferase system, wherein constructs of ZIFCAT were fused to the DNA binding domain/ DBD of Gal4, and their activity tested by co-transfection in HeLa or 293T cells, followed by luciferase assay. In this artificial setting, Gal4DBD mediates an interaction with the UAS sequence element present on the reporter construct, thereby bringing ZIFCAT into close proximity with the promoter governing luciferase activity. Repression was reproducibly observed with Gal4DBD-ZIFCAT, or the Gal4DBD-ZIFCAT $\Delta$ ZF mutant lacking the carboxyl-terminus 497 residues including the zinc finger region (Figure 47). Such effects were not observed for Gal4DBD alone, or for HA-tagged ZIFCAT (negative controls). My results suggest a model where ZIFCAT gene activity may depend upon the zinc finger region for DNA association, and the amino-terminal region (likely the KRAB domain) for recruitment of transcriptional co-factors/ co-repressors.

Finally, to probe for a functional interplay between ZIFCAT and delta-catenin (or ARVCF-catenin) in the context of this Gal4-UAS-luciferase system, I co-expressed delta-catenin (or ARVCF-catenin) with Gal4DBD-ZIFCAT. As seen in Figure 48, no significant changes followed such co-expression. This was perhaps to be expected, since my data had already indicated that delta- as well as ARVCF-catenin bind the zinc finger region of ZIFCAT, whereas the Gal4DBD-ZIFCAT construct no longer requires this domain for DNA association (imparted instead by the Gal4DBD fusion). In vivo, I speculate that nuclear delta- or ARVCF-catenin, or more likely caspase-3 fragments such as 817-1314,

displaces ZIFCAT from its presently unknown consensus binding sites in promoter/ enhancer DNA, relieving ZIFCAT mediated gene repression.



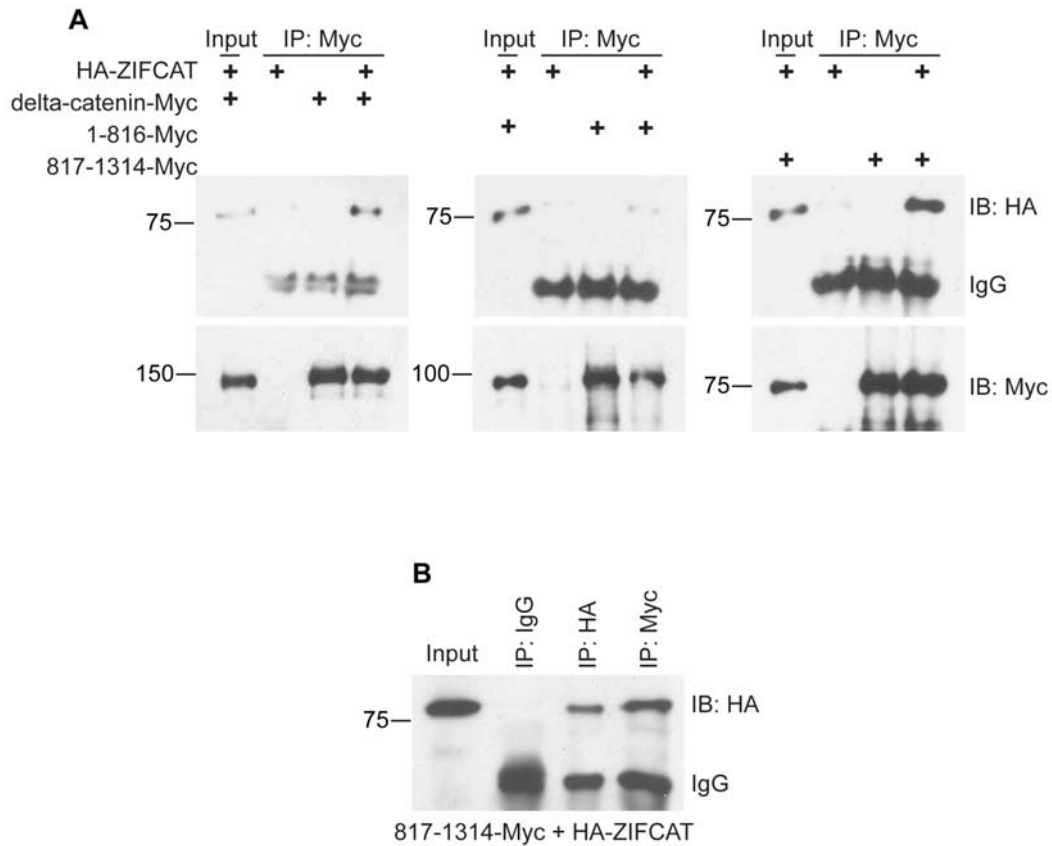


Figure 44. ZIFCAT associates with delta-catenin.

A. 817-1314, found to result from caspase-3 cleavage, is sufficient to bind ZIFCAT in vitro. Selected constructs were translated in vitro and incubated together. Myc-antibody followed by Protein A/ G beads was used to immunoprecipitate delta-catenin proteins. Immunoblotting with HA antibody indicated that ZIFCAT associates in vitro with full-length delta-catenin (left panel), or 817-1314 (right panel), but not with 1-816 (middle panel) relative to control precipitations. B. 817-1314 associates with ZIFCAT in 293T cells. Myc-tagged 817-1314 and HA-tagged ZIFCAT were co-transfected into 293T cells. Myc antibody was employed to precipitate 817-1314, with HA immunoblotting confirming 817-1314's association with ZIFCAT.

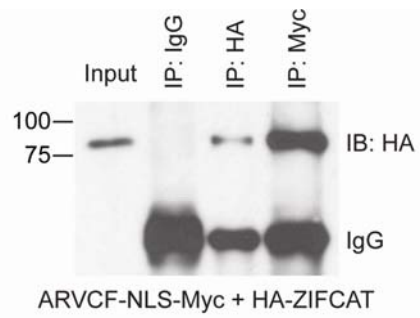


Figure 45. ZIFCAT associates with ARVCF-catenin.

ARVCF likewise associated with ZIFCAT in vivo. Experimental conditions were as for delta-catenin, except that NLS-Myc-tagged ARVCF was employed for co-transfection with ZIFCAT.

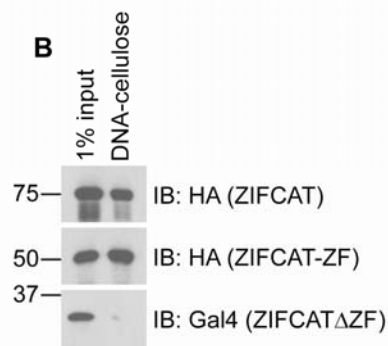
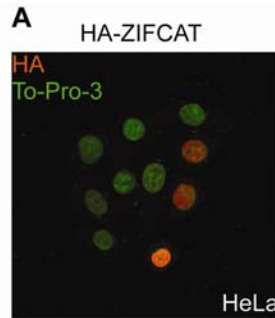


Figure 46. ZIFCAT is a DNA-associating nuclear protein.

A. HA immuno-fluorescence (orange) of ZIFCAT in HeLa cells, displaying a strong overlap with the To-Pro-3 nuclear counter-stain in green. B. ZIFCAT associates with DNA through its zinc finger region. Selected constructs were translated in vitro and incubated with cellulose-conjugated calf thymus genomic DNA. After extensive washing, bound proteins were eluted and immuno-blotted with the indicated antibodies. Full-length ZIFCAT, as well as region of ZIFCAT containing its zinc fingers (ZIFCAT-ZF) displayed positive DNA association, while the ZIFCAT mutant containing the KRAB but not zinc finger domain (ZIFCAT $\Delta$ ZF) lacked this interaction.

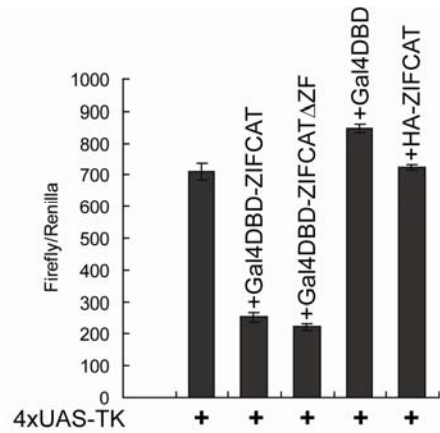


Figure 47. The amino-terminal region of ZIFCAT represses UAS-luciferase activity.

Selected constructs were fused to the Gal4 DNA Binding Domain, which promotes DNA association with UAS sequence elements residing within a standard TK-luciferase reporter construct. Full-length ZIFCAT, and the mutant lacking the zinc finger region (ZIFCAT $\Delta$ ZF), repressed the expression of TK-luciferase. Serving as negative controls, Gal4DBD or HA-tagged ZIFCAT (not recruited to the reporter's promoter) did not achieve significant inhibitory effects. Luciferase assays were repeated three times or more in HeLa or 293T cells, with one representative experiment being shown.

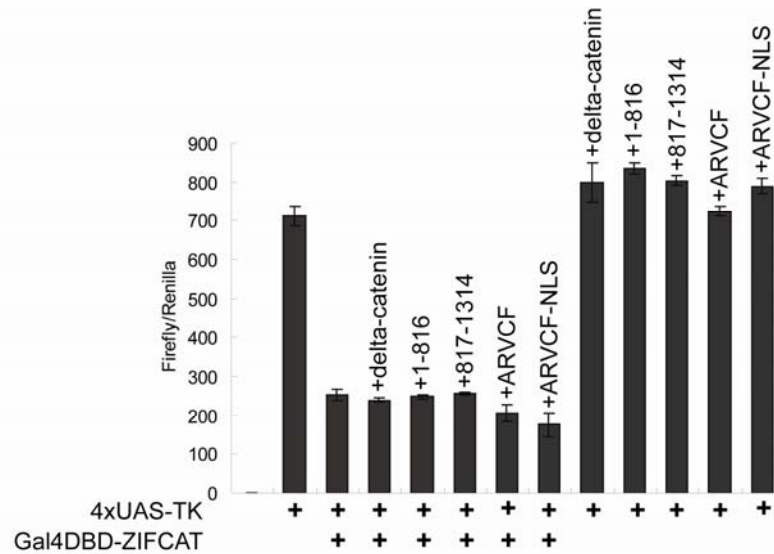


Figure 48. Neither delta-, nor ARVCF-catenin, have a notable impact upon the transcriptional repression conferred by Gal4DBD-ZIFCAT.

Delta- and ARVCF-catenin constructs were co-transfected with the TK-luciferase reporter in the presence or absence of Gal4DBD-ZIFCAT. Relative to the repressed state conferred by Gal4DBD-ZIFCAT expression alone (lane 2), no significant relief or repression was observed (lanes 3-7). Luciferase assays were reproduced three times or more using Renilla as the internal control, with one representative experiment being shown.

## **CHAPTER III**

## **DISCUSSION**

## **Part I: Developmental characterization of *Xenopus* delta-catenin**

Delta-catenin is a member of the p120 sub-family of Armadillo proteins able to modulate various activities, including those involving the cadherin complex, the actin cytoskeleton and intracellular signaling. As for the beta-catenin sub-family, altered expression of p120 sub-family catenins have been correlated with human pathologies including cancer progression and genetic disorders (McCrea and Park, 2007; Reynolds and Roczniak-Ferguson, 2004; van Hengel and van Roy, 2007; van Roy and McCrea, 2005).

In Part I of my dissertation, I examined delta-catenin in *Xenopus laevis* (African clawed frog), using knock-down as opposed to genetic approaches. My isolation and characterization of delta-catenin in *Xenopus* resolved three alternative RNA splicing events not previously reported. The shorter b' and c' variants have increased expression in later stages, while the A variants (a and a') were more uniformly present across development. When I translated these spliced elements into peptide sequences, I could not identify (BLAST in PubMed) similar sequences in the human or mouse genome database, suggesting that these splicing variants may be amphibian specific.

Compared to the neural restricted pattern of mouse delta-catenin transcripts (Ho et al., 2000), I found that delta-catenin mRNA and protein are readily detected across all *Xenopus* embryonic stages and in adulthood, and

likely contribute to development and/ or tissue maintenance. While RNA in-situ analysis of whole mount embryos indicated enrichment of delta-catenin mRNA in the neural ectoderm and its derivatives, differences existed in adult frog tissues. The 160 kDa delta-catenin isoform migrated at a position consistent with that calculated from the cloned delta-catenin cDNA. Given that this isoform displayed a brain-specific pattern, it may provide distinctive functions in neural tissues. The other two isoforms (130 and 100 kDa), may originate from alternative protein translation and/ or splicing, possibly in combination with post-translational modifications (enzymatic cleavage, phosphorylation, etc.). Such modifications and their underlying functional significance will require future investigation. In contrast to adult tissues, I had initial difficulty detecting the longer 160 and 130 kDa isoforms in embryo extracts. Nonetheless, I ultimately confirmed their presence using immuno-precipitation followed by immuno-blotting approaches and a number of delta-catenin antibodies. Interestingly, antibodies directed against delta-catenin's most amino-terminal region failed to recognize the shortest (100 kDa) isoform, indicating that it may arise from a downstream translational initiation (such as Methionine434), or from proteolytic cleavages at amino-terminus.

To determine delta-catenin's in vivo functions, I designed anti-sense morpholino oligos to perturb normal splicing of pre-RNA, causing frame-shifts and pre-mature termination of protein translation. With two distinct morpholinos (MO-6 and MO-9), this approach produced consistent outcomes. The



phenotypic effects were indicated to be specific based upon a number of rescue experiments. Delta-catenin MO-9, directed against the intron 8-exon 9 junction, displayed greatest efficacy. In common with MO-6, it perturbed blastopore closure during gastrulation, which is a delicate process of mesoderm involution in response to multiple signaling events and mechanical forces (such as convergent extension morphogenesis) (Keller, 2005; Wallingford et al., 2002). I applied two assays including Keller open face explants and fluorescent tracer analysis within dorsal tissues, but failed to identify an apparent reduction of convergence-extension movements. It is possible that the assays I employed largely measure intercalation of superficial cells, but not deeper cell movements where delta-catenin may act. Indeed, in bisected embryos, exposed dorsal head mesoderm displayed lessened association with the blastocoel roof, with such defects perhaps contributing to aberrant tissue movements during blastopore closure. Alternatively, delta-catenin knock-down may affect convergent extension of more lateral or ventral tissues, or the coordination between these processes. Further, given the complexity of gastrulation, disruption of other morphogenetic events may produce similar effects to those observed in my experiments.

To explore biochemical mechanisms by which loss of delta-catenin leads to perturbed gastrulation, I generated a delta-catenin  $\Delta$ ARM1-5 construct that when expressed fails to interact with endogenous C-cadherin yet retains the capacity to modulate small GTPase activities. Given that  $\Delta$ ARM1-5 exhibited little rescuing effects compared to full-length delta-catenin, the gastrulation

phenotypes may have arisen in significant part from reduced cadherin-based adhesion and/ or downstream signaling. As exogenously expressed Rho or Rac could rescue delta-catenin knock-down, they are likely to be involved. Indeed, Rho family GTPases have well-documented roles in coordinated cell movements including gastrulation (Anastasiadis, 2007; Ridley, 2001a; Ridley, 2001b). In migrating cells, Rho is localized predominantly to stress fibers and focal adhesion complexes, which are dissipated upon cell motility. Rac promotes actin polymerization at the cell periphery and provides the driving force for protrusive activities (lamellipodia), while Cdc42 has been indicated to define the migratory polarity by directing localization of Rac-dependent protrusions. Gastrulation involves several distinct types of cell movements, including presumptive head mesoderm migration, epiboly, endoderm rotation, and convergent extension (Keller, 2005; Keller et al., 2003). In the best-studied convergent extension process, cells polarize and elongate along the medio-lateral axis and intercalate towards the midline leading to the extension of the anterior-posterior axis. Work in *Xenopus* and Zebrafish has established the roles of non-canonical Wnt signaling and Rho family GTPases (Habas et al., 2003; Habas et al., 2001; Heisenberg et al., 2000; Liu et al., 2008). Wnt-11, the prototypal non-canonical ligand, complexes with Frizzled 7 membrane receptor and activates Dishevelled, Daam1 and subsequent downstream RhoA and Rho-associated kinase. Rac1 activation in contrast does not require Daam1 and results in the activation of JNK (JUN N-terminal kinase). Thus parallel Rho and Rac activations are essential to complete convergent extension in gastrulation. Other studies have

further indicated that small GTPases reside downstream and functionally interact with cadherins (Charrasse et al., 2007; Charrasse et al., 2002; Fukuyama et al., 2006; Goodwin et al., 2003; Johnson et al., 2004; Lampugnani et al., 2002; Morishita et al., 2001; Nelson and Chen, 2003; Semina et al., 2009; Yap and Kovacs, 2003). Thus, their re-introduction in the context of rescue experiments may restore needed downstream signals, possibly in part compensating for the reduction in cadherin functions (Braga and Yap, 2005). Regardless of the mechanism, the gross effects I observe following delta-catenin depletion support its essential role in *Xenopus* embryogenesis.

The requirement for delta-catenin in amphibian development, however, did not agree with the milder effects seen upon its knock-out in mice. In mammals, delta-catenin is largely restricted to the central nervous system, with a whole-body knock-out producing learning deficits and altered synaptic function (Israely et al., 2004; Matter et al., 2009). Also observed was a reduction in N-cadherin levels, and small G proteins may have been consequently affected, leading to altered synaptic junctions as well as neuronal morphology (Bamji, 2005; Kosik et al., 2005). Given that delta-catenin was reported to associate with the transcriptional repressor Kaiso (Rodova et al., 2004), it may further regulate gene programs essential for neuronal functions.

One possible explanation of the phenotypic differences is that the formal targeting strategy employed for mouse knock-out might have generated an

amino-terminal fragment retaining partial activity (not a complete null). Indeed, this truncated delta-catenin fragment migrated at approximately 50 kDa and was detected through immuno-blotting of mouse brain extracts (Israely et al., 2004). In *Xenopus*, morpholino 9 of delta-catenin is likewise predicted to generate an amino-terminal fragment of similar size. However, this fragment was not seen in immuno-blots probed with delta-catenin antibodies that readily recognize similar protein fragments if artificially expressed in vitro. Thus, such a fragment could be targeted for rapid degradation in *Xenopus* embryos.

An alternative possibility is that during evolution, other catenins in mammals assumed the roles that are maintained by delta-catenin in amphibians. In this case, this transition would have occurred while delta-catenin remained the primordial member of the p120-catenin sub-family, showing the highest similarity to the single family member in *Drosophila* (p120-catenin) and in *C. elegans* (JAC-1) (Carnahan et al., 2010). Interestingly, the invertebrate p120-catenin appears to be dispensable when disrupted in laboratory contexts (Myster et al., 2003; Pettitt et al., 2003), although one study has differed and indicated it to be essential (Magie et al., 2002).

A final possibility comes from differences in the experimental approaches by which loss-of-function was achieved in mice versus *Xenopus*. Although the morpholinos I used were effective and specific as noted earlier, knock-down in *Xenopus* embryos are generally partial, as I observed for delta-catenin. However,

it is expected that an acute knock-down might have a more profound impact than the corresponding constitutive knock-out carried out at an earlier developmental stage, as the latter may provide a more suitable environment for functional compensation to arise. Thus, although the phenotypic outcomes I observed may be different from those reported in the knock-out mouse, my results clearly point to a requirement for delta-catenin in embryonic development.

In summary, my study is the first to uncover an essential role for delta-catenin in amphibian development, as well as supplying in vivo evidence of delta-catenin's functional interplay with cadherins and small GTPases. Perturbation of other delta-catenin interactions may further be contributory to the phenotypes, including delta-catenin's putative yet largely uncharacterized roles in nuclear gene regulation.

## **Part II: Exploring the roles of delta-catenin in the nucleus**

The means by which biological signals produce coordinate effects in varying cellular compartments is relevant to many developmental and pathological processes, often involving events that take place at the plasma membrane, cytoplasm and in the nucleus. Canonical Wnt signaling, for example, generally occurs upon Wnt-ligand binding to cell surface receptors (e.g. Frizzled, Lrp5/ 6), facilitating Dishevelled mediated inhibition of beta-catenin's destruction complex (composed of Axin, GSK-3beta and APC, etc.). This results in beta-catenin's cytoplasmic and ultimately nuclear accumulation, and thus activation of canonical Wnt/ beta-catenin target genes (Logan and Nusse, 2004). The membrane-spanning Notch receptors, on the other hand, are protease-cleaved upon the binding of ligands such as Delta or Jagged, such that the intracellular portion of Notch is liberated to enter the nucleus, associate with the CSL transcription factor complex (CBF1/ Su(H)/ Lag-1), and modulate specific gene targets (Artavanis-Tsakonas et al., 1999). Both the Wnt and Notch pathways participate in multiple developmental/ cellular processes, and when abnormally regulated, contribute to many human disorders including cancer.

Apoptosis or programmed cell death is a physiologically controlled process of cell suicide. Activated caspases cleave specific cellular substrates, with dying cells presenting characteristic molecular and morphological features (Kumar, 2007; Lockshin and Zakeri, 2007). Caspase deployment and apoptotic

death programs are critical during embryonic development including *Xenopus* metamorphosis (Coen et al., 2007; Du Pasquier et al., 2006; Tseng et al., 2007). It has been long appreciated that caspases have many roles apart from apoptosis, such as in immune defense, proliferation, fate determination, terminal differentiation, cell migration and neuro-degeneration (Appleby and Modak, 1977; Arama et al., 2003; Arama et al., 2007; Bassnett and Mataic, 1997; Carlile et al., 2004; Gabet et al., 2010; Ishizaki et al., 1998; Kolbus et al., 2002; Lee et al., 2001; Muro et al., 2006; Zermati et al., 2001). The mechanisms by which caspases exert these non-apoptotic functions are still under active investigation, yet likely relate to their temporally, spatially or quantitatively controlled enzymatic activations (Feinstein-Rotkopf and Arama, 2009; Kuranaga and Miura, 2007).

In Part II of my study, I presented data that delta-catenin is a novel substrate of caspase-3. Delta-catenin interacts with caspase-3 as resolved from yeast two-hybrid screening, and is cleaved by caspase-3 in vitro and in apoptotic cell extracts. This response may be conserved across the p120 sub-family of catenin proteins, since p120-catenin also showed sensitivity to caspase-3 in vitro.

Considering the best known role of caspase-3 as an 'executioner' in the apoptotic pathway, one could imagine that delta-catenin may be involved in cell death programs. In earlier work, exogenous delta-catenin expression resulted in limited cell death in NIH 3T3 cells (Kim et al., 2000). Conversely, however, delta-catenin has been reported to have pro-survival activities in prostate

adenocarcinoma cells (Zeng et al., 2009), and elicited feedback suppression of Pax6-induced apoptosis in HeLa cells (Zhang et al., 2010a). In the present study I employed a cell death ELISA assay, but did not observe significant increase or decrease in chromatin breakage upon delta-catenin expression. Likewise, delta-catenin did not protect HeLa cells from Staurosporine- or Puromycin-induced apoptosis. As mentioned earlier, these pro-survival/ -apoptotic effects may be context dependent. Although *Xenopus* and murine delta-catenin are highly homologous (~90% identity), sequence divergences do exist, as might alternative splicing events. Further, I employed Staurosporine and Puromycin as potent general cell death inducers, whereas Pax6 expression would likely have more defined apoptotic roles. Ultimately, more sensitive gain/ loss of function assays in additional systems may be required to reach a definitive conclusion regarding delta-catenin's role in apoptosis.

The caspase-3 cleavage of delta-catenin potentially abolishes its binding to cadherins since the resulting fragments failed to co-immuno-precipitate with C-cadherin when expressed *in vitro* or *in vivo*. In GSC11 cells, where an antibody directed against delta-catenin's carboxyl-terminal region reproducibly detected the presence of 817-1314 (especially upon apoptosis induction), I failed to observe 1-816, employing amino-terminal directed antibodies from three different sources. Thus, 1-816 appears to be rapidly metabolically degraded following its generation. In that classic cadherins and some catenins are targeted during apoptotic events (Brancolini et al., 1997; Cirillo et al., 2008;



Dusek et al., 2006; Herren et al., 1998; Hunter et al., 2001; Kessler and Muller, 2009; Ling et al., 2001; Senthivinayagam et al., 2009; Steinhusen et al., 2000; Steinhusen et al., 2001; Weiske and Huber, 2005), delta-catenin's cleavage in this context may assist in orchestrating the disassembly of adherens junctions, where cadherins are known to be endocytosed following the disassociation of p120-catenin sub-family members. Additionally, as noted earlier, since caspases further participate in non-apoptotic processes, such modulation of cadherin levels and functions may instead have other physiologic outcomes, such as transitions to less adhesive and more motile cell phenotypes.

Another recognized role of p120 sub-family catenins is their modulation of small GTPases (Anastasiadis, 2007; Keil et al., 2007; Yanagisawa et al., 2008). In my experimental setting, delta-catenin lost the ability to inhibit RhoA following its cleavage, with neither 1-816 nor 817-1314 exhibiting inhibitory activity. Regarding Rac1, while 1-816 and 817-1314 displayed no stimulatory activity in contrast to that of full-length delta-catenin, 817-1314 exhibited partial inhibitory effects. Rho and Rac contribute to a myriad of cellular processes, prominently including cytoskeletal organization and function (Heasman and Ridley, 2008). It is thus conceivable that caspase-3 cleavage of delta-catenin, likely in concert with that of other p120 sub-family members, is relevant to cell morphological changes in both apoptotic and non-apoptotic settings.

Caspase-3 cleaves Armadillo-repeat 6 of delta-catenin. Since delta-

catenin's NLS resides only 18 amino acids downstream of this cleavage site, it may become more exposed, and possibly account for the observed stronger nuclear localization of 817-1314 relative to full-length delta-catenin. Interestingly, an earlier report indicated delta-catenin's localization to the nuclear compartment of C2C12 myoblasts following treatment with the nuclear export inhibitor Leptomycin B (Rodova et al., 2004). Other potential means of modulating delta-catenin's nuclear entry exist. As I and others have indicated, signaling pools of p120-catenin sub-family members, including delta-catenin, appear to be subject to canonical Wnt signals or the pathway's destruction complex (Bareiss et al., ; Hong et al., ; Oh et al., 2009; Park et al., 2006). For p120 itself (and possibly delta-catenin), this has an impact upon its nuclear presence/ activity in a manner analogous to the key signal transducer beta-catenin. Intriguingly, the Wnt11 ligand was recently reported to activate caspases in cardiomyocytes, resulting in suppression of beta-catenin signaling and cardiac differentiation (Abdul-Ghani and Megeney, 2008). Thus, differing Wnt ligands or contexts may conceivably have distinctive effects on p120-catenin sub-family members, wherein certain Wnts (or contexts) lead to catenin stabilization with consequent effects, while other Wnt ligands or contexts may employ caspases to generate catenin fragments capable of executing nuclear or other roles.

My current study indicates that 817-1314, corresponding to a caspase-3 cleavage product, is efficiently enriched in the nucleus. I also found that delta-catenin (and 817-1314) binds to a novel zinc finger protein, ZIFCAT, present in

the nuclear compartment. KRAB family zinc finger proteins such as ZIFCAT make up a family of several hundred members, with the functions of most still to be determined. Yet, based on published studies, these proteins share features including the presence of multiple zinc finger repeats within their carboxyl-termini that directly bind DNA, and in my particular case with ZIFCAT, also delta-catenin. The amino-terminal KRAB domain in turn recruits cofactors such as KAP1, to modulate gene transcription (Looman et al., 2002; Urrutia, 2003).

Intriguingly, I further resolved the binding of ZIFCAT to ARVCF-catenin. My *in vitro* and *in vivo* binding assays authenticated ZIFCAT's interaction with delta-catenin and ARVCF. I have not yet tested whether this interaction extends to p120-catenin, or less likely beta-catenin, which belongs to a related but more distant catenin sub-family. If ZIFCAT is later found to bind p120 itself, it would be the third gene regulatory protein (after Kaiso and Glis2) to bind p120 (Daniel, 2007; Hosking et al., 2007).

My initial characterization of ZIFCAT indicates that it is enriched in nuclei, binds to genomic DNA *in vitro* and represses UAS-luciferase expression when fused to Gal4DBD. Neither delta-catenin nor ARVCF had an impact upon ZIFCAT (Gal4-UAS) mediated reporter repression, likely because I showed that delta-catenin binds the zinc finger region of ZIFCAT, which bears little relevance in the artificial context employed (DNA binding being mediated via the Gal4DBD). *In vivo*, it is conceivable that delta-catenin (and/ or ARVCF, etc.) may interfere

with ZIFCAT binding to DNA, resulting in gene de-repression (activation).

The recent intriguing work by (Abdul-Ghani et al., 2011) reported the Wnt11 activation of caspase activity leading to beta-catenin cleavage and the differentiation of cardiomyocytes. The cross-talk between components of the canonical Wnt pathway and apoptotic cascade has been long appreciated. For example, beta-catenin and APC are targeted by caspases, respectively leading to suppression or activation of Wnt signaling (Qian et al., 2007; Senthivinayagam et al., 2009; Steinhusen et al., 2000; Webb et al., 1999). Conversely, GSK3beta and APC were indicated to augment caspase activation and promote apoptosis (Chen et al., 2003; Yun et al., 2009). Wnt11 is generally recognized as a ligand for the non-canonical Wnt/ PCP (Planar Cell Polarity) pathway, leading to Rho/ Rac activation and directional mitotic divisions or cell movements (Heisenberg et al., 2000; Tada et al., 2002), although one study in *Xenopus* has indicated its role as a canonical Wnt transducer (Tao et al., 2005). In cardiomyocytes, caspase activations did not elicit significant cell death, rather they suppressed beta-catenin signaling which otherwise must be maintained to keep cells in a progenitor state.

The exact mechanism regarding caspase-3/ 8 activation by Wnt11 is currently being pursued, with certain existing evidence pointing to the involvement of Frizzled receptors. Frizzled are membrane proteins belonging to the family of G protein coupled receptors (GPCRs). They can activate

heterotrimeric G proteins and initiate a multitude of intracellular signaling pathways, such as PKC activation (Salazar et al., 2007; Schulte and Bryja, 2007). The activation of certain GPCRs results in intracellular changes including the activation of caspase-3 (Adams et al., 2000; Revankar et al., 2004). Additionally, Frizzled receptors may engage caspase activity by directly associating with membrane components of the classic death receptor pathway (Fernando and Megeney, 2007; Senthivinayagam et al., 2009). Alternatively, given the wide variety of cytoskeletal or signaling events that are modulated by small GTPases, which reside downstream of the non-canonical Wnt pathway initiated through Wnt11, their involvement can also be envisaged. As one might expect, there were multiple reports regarding that dysregulation of Rho/ Rac resulting in caspase activations and cell damage (He and Baldwin, 2008; He et al., 2008; Iguchi et al., 2009; Le et al., 2005). Regardless of the underlining mechanism, this study (Abdul-Ghani et al., 2011) was the first to identify an essential role of Wnts in activating caspases in a non-apoptotic setting.

Given that in my studies delta-catenin and other p120 sub-family members are targeted by caspase-3, and are regulated by Wnt signals as reported in independent publications (Hong et al., 2010; Oh et al., 2009; Park et al., 2006), it would be interesting to examine the functional significance of p120 sub-family catenins in contexts independent of cell death. Once cleaved by caspase-3, I speculate that a delta-catenin fragment such as 817-1314 couples with ZIFCAT to alter transcriptional profiles, leading to events such as

differentiation of embryonic progenitors, where the caspase/ delta-catenin interaction was identified (Dejosez et al., 2008; Fujita et al., 2008). Or, that similarly, a partial p120-catenin product from caspase cleavage has greater activity de-repressing Kaiso at certain well-defined gene promoters.

Another essential future work is to identify the DNA element(s) that ZIFCAT binds, so as to allow the testing of such models in vivo and in vitro. For example, one could employ genome-wide Chromatin Immuno-Precipitation (ChIP-seq) coupled with Solexa massively parallel DNA sequencing to identify the endogenous gene targets of ZIFCAT. Additionally, ChIP-seqs can also be performed for the p120 sub-family catenins. Given the limited distributions of delta-catenin across mammalian tissues, C2C12 myoblasts might serve as model wherein delta-catenin is expressed and apparently localized to the nuclear compartment (Rodova et al., 2004). Alternatively, CWR22Rv-1 prostate adenocarcinoma cells could be of advantages given its high delta-catenin mis-expression (Lu et al., 2005; Zeng et al., 2009). Although their direct binding to DNA is not suggested by the current models (Daniel, 2007; van Roy and McCrea, 2005), delta-catenin and other p120 sub-family members might indirectly complex with chromatin through transcription and other nuclear cofactors. One could thus identify shared gene targets and the micro-environments wherein functions of one catenin might be shared by that of another. Alternatively, it would be informative to discover a unique set of candidate genes that are modulated by one single such member. A comparison between gene profiles of

delta-catenin and ZIFCAT will also be crucial to reach an understanding of the nuclear activities of delta-catenin (and/ or ARVCF, etc.) in conjunction with ZIFCAT (or that with other transcription factors such as Kaiso).

Collectively, my work may have revealed a novel signaling cascade triggered by caspase-3 cleavage of p120-catenin sub-family members, facilitating the coordinate modulation of cadherin, small GTPases and nuclear functions.

## **CHAPTER IV**

### **MATERIALS AND METHODS**



## **DNA cloning**

5' RACE was employed to obtain delta-catenin 5' UTR (Untranslated Regions) of *Xenopus laevis*, according to the manufacturer's protocol (5' 3' RACE kit, Roche). Delta-catenin cDNA was acquired by high fidelity PCR, and a cDNA pool reverse transcribed from adult *Xenopus* brain RNA. To generate expression constructs for the subsequent making of in vitro transcribed RNAs or for transfections in mammalian cell lines, PCR approaches were used to put restriction enzyme sites into both 5' and 3' ends of parental inserts. PCR products were then directionally sub-cloned into various vectors, fusing epitope-tags to their amino- or carboxyl-termini followed by DNA sequence confirmation. Mutagenesis of delta-catenin D816 to E816 was performed using the manufacturer's protocol (Quickchange site-directed mutagenesis kit, Stratagene).

## **Antibodies and chemicals**

Antibodies direct against *Xenopus* delta-catenin were generated against its recombinant amino-terminal domain (amino acids 83-521, tagged with histidines), and affinity-purified from rabbit serum. Additional antibodies reacting with various regions of delta-catenin were obtained commercially from BD Biosciences, Abcam, Millipore or Sigma-Aldrich. C-cadherin, p120- and beta-catenin antibodies were developed in earlier studies. Other antibodies are listed as follows: actin, Sigma-Aldrich; GAPDH, Santa Cruz Biotechnology; E-cadherin,

BD Transduction Laboratories; N-cadherin, Calbiochem; RhoA, Santa Cruz Biotechnology; Rac1, Millipore or BD Pharmingen; Myc- or HA-epitope, Developmental Studies Hybridoma Bank or Sigma-Aldrich; GST, Developmental Studies Hybridoma Bank; Alexa-Fluor conjugated secondary antibodies, Invitrogen.

Chemicals used in this study are as have listed: mouse E-cadherin extracellular domain and fibronectin, Sigma-Aldrich; apoptosis inducer Puromycin and Staurosporine, Calbiochem; recombinant active caspase-3, BD Pharmingen; cellulose-conjugated calf thymus genomic DNA, Sigma-Aldrich; and Alcian blue dye, Sigma-Aldrich.

### **Cell culture, transfection and luciferase assays**

Cell lines (293T, HeLa, Neuro-2a, MDA-MB-435, etc.) were cultured following standard mammalian protocols and maintained in complete medium (DMEM, 10% FBS and antibiotic additives). Glioblastoma stem cells were grown in suspension to form neurospheres, or as monolayers on laminin-coated surfaces while being maintained in neurobasal medium (DMEM/ F12, B27, with 10ng/ ml each of EGF and bFGF).

Transient protein expression was achieved by transfecting plated cells with selected DNA constructs according to the manufacturer's instructions

(Lipofectamine 2000, Invitrogen or FuGene 6, Roche Applied Science) and cultured for a minimum of 24 hours prior to following procedures. Luciferase assays were performed according to the Promega Dual-Luciferase Reporter Assay protocol, employing Renilla as a transfection control.

### **Yeast two-hybrid screening**

Yeast two-hybrid screening using *Xenopus* delta-catenin deleted of its amino-terminus (intact Armadillo and carboxyl-terminal domains) as bait was performed by Hybrigenics, Inc. as a collaboration, employing an adult mouse brain cDNA library.

### **PCR oligos and morpholinos**

RNA extraction, reverse transcription and PCR followed standard procedures. PCR oligos used to characterize delta-catenin alternative splicing are as follows: A: 5'-GAT CGG GTG TAT CAG AAG CCA C-3', 5'-CCT TCT GGT GGG ATA GCT GGT-3'; B: 5'-GTA GTA AAG GCA GCG TCT CAG-3', 5'-AGG GGT ACC ATA GGA ATT CC-3'; C: 5'-GAA CAC ACG TCT AGG AAA G-3', 5'-AAG TTC ACT ATA GGG ACG AGC AG-3'; D: 5'-CAG ATC CAC CAA AAG GAA TA-3', 5'-ATG GCA GTA ACA GTG TCA TC-3'; Histone H4: 5'-CGG GAT AAC ATT CAG GGT A-3', 5'-TCC ATG GCG GTA ACT GTC-3'. DNA oligos employed to determine delta-catenin morpholino efficiencies were as

follows: F1: 5'-ATG GCC AAA AAG ACA TAG AGG ATG-3'; R1: 5'-TTG ATG AAT ACT GGA AAG ACC-3'; R2: 5'-CCT CAC AAT CAC ATG CTG CCT CCC AGT C-3'; F4: 5'-GTC CCT GAT TTT TAA GAG TG-3'; R4: 5'-AAG GGA ACT GAT GCT GTA AC-3'.

Intron 5 and 8, and exon 6 and 9 sequences of *Xenopus* delta-catenin were obtained using a high fidelity PCR system and *Xenopus* tadpole genomic DNA. Delta-catenin splice junction type morpholinos (delta-catenin MO-6 5'-GTA CTT GTC CAC TTA CTT GAC TGT A-3' and delta-catenin MO-9 5'-GCT ACG ACA GGA AAG TAG GGA CAA A-3'), and a control morpholino (5'-CCT CTT ACC TCA GTT ACA ATT TAT A-3'), were acquired from Gene Tools. P120-catenin and Kaiso morpholino oligos were designed in earlier studies of McCrea Laboratory (Fang et al., 2004; Kim et al., 2004).

### **Co-immuno-precipitation and immuno-blotting**

Standard procedures were applied for immuno-precipitations from whole cell/ embryo extracts or from diluted nuclear fractions, followed by SDS-PAGE and immuno-blotting. Streptavidin-HRP was obtained from Promega and employed to detect biotin labeled proteins. Immuno-blot band densities following scanning were quantified using AlphaEaseFC 6 or ImageJ 1.38x software.

## **Caspase-3 cleavage and apoptotic assays**

Selected cDNA constructs were transcribed/ translated in vitro using the TnT high-yield wheat germ protein expression system. Transcend tRNA was added into certain experimental reactions to non-radioactively (Biotin) label lysine residues of translated proteins. Following translation, 5 ul of the reaction mix was incubated with recombinant caspase-3 at 37 degree for 1 hour. Apoptotic extracts were isolated from *Xenopus* eggs using published protocols (Deming and Kornbluth, 2006), and incubated with the Armadillo-domain of delta-catenin purified from *E. coli* (GST tagged), for the indicated periods at room temperature. Cleavage products were resolved by immuno-blotting using GST antibody.

For cell death induction of mammalian cells, Puromycin or Staurosporine was added to culture medium at the final concentrations of 0.5 and 20ng/ ul, respectively. Cytosolic nucleosomes resulting from DNA breakage were quantified using an ELISA-based cell death detection kit following the manufacturer's protocol (Roche Applied Science).

## **Manipulation of *Xenopus* embryos and microinjection**

Expression constructs were linearized by Not I restriction enzyme digestions and purified by phenol-chloroform extraction. Capped RNAs were

thus generated in vitro using these templates in conjunction with the mMESSAGE SP6 kit (Ambion). Intactness of RNA was verified through standard agarose gel electrophoresis. Induction of female *Xenopus laevis*, in vitro fertilization of eggs, and embryo injections were carried out according to standard methods (Sive et al., 2000). Typically, morpholinos or RNA constructs were injected into animal cells of early stage embryos. Embryos were kept in 0.1x MMR containing 50 ug/ ml gentamycin antibiotics at 18 degree until desired stages. The volume of injections was 20 nl at the single-cell stage, 10 nl/ cell at the two-cell stage or plus with the doses as follows: 80 ng for delta-catenin and control morpholinos; 20 ng for titrated (sub-phenotypic) dose of delta-catenin morpholinos; 40 ng for p120-catenin morpholino; 10 ng for titrated (sub-phenotypic) dose of p120-catenin morpholino; 250 pg for full-length delta-catenin, M434 delta-catenin,  $\Delta$ PDZ and  $\Delta$ ARM1-5 RNA constructs; 500pg for delta-catenin NT and Armadillo (ARM) constructs; 100 pg for p120-catenin and C-cadherin RNAs; 200 pg for beta-catenin RNA, 50 pg for RhoA N19 (dominant-negative) and RhoA V14 RNAs, 5 pg for Rac1 V12 and Cdc42 V12 RNAs. Embryonic phenotypes were scored using a standard binocular dissecting microscope from Zeiss.

For explants assay, delta-catenin or control morpholinos were injected into equatorial regions of dorsal blastomeres at the four-cell stage. Dorsal marginal zones were manually excised at the mid-gastrula stage and cultured in vitro as open-face Keller explants until control embryonic stage 15.

## **Cell dissociation, re-aggregation and in vitro adhesion assays**

For assay of cell dissociation and re-aggregation, naive ectoderm tissue fragments (animal caps) from mid-gastrula stage embryos were isolated and maintained in calcium free 0.6x MMR buffer (achieved through EGTA chelating) until the cells dissociated. Cells were then supplied with 1 mM of  $\text{Ca}^{2+}$  and  $\text{Mg}^{2+}$ . Dissociation and re-aggregation were timed to evaluate cell adhesive strength in control versus delta-catenin depletion conditions.

E-cadherin and integrin in vitro adhesion assays followed published procedures, with modifications. Lab-Tek Chamber Slides were first coated with either mouse E-cadherin extracellular domain or fibronectin, and blocked with 1% BSA. Disassociated blastomeres (triplicates of two animal caps per condition) were allowed to attach for one hour at 16 degree. Chambers were then inverted (to allow cells to separate from the glass slides by gravity) and washed for the indicated times on a rotary shaker. The aggregation state of cells before or after washing was recorded by digital photography and Adobe Photoshop CS3.

## **Immuno-fluorescence and antibody staining**

Immuno-fluorescence antibody staining of mammalian cells on coverslips was performed using standard methods, employing 4% para-formaldehyde (Electron Microscopy Sciences) as fixative. Similar procedures were followed

when staining actin filaments with phalloidin conjugated with Alexa Fluor488 (Molecular Probes). For *Xenopus* immuno-fluorescence, late blastula stage embryos were fixed in MEMFA, blocked in 20% goat serum and incubated with the indicated antibodies. Following the final wash, ectoderm tissues were manually isolated as animal caps and mounted on glass slides. All confocal images were acquired using an Olympus IX-70 inverted microscope equipped with the Olympus Fluoview FV500 software.

### **In vitro DNA association assay**

ZIFCAT's association with genomic DNA in vitro was tested by established methods (Hosking et al., 2007). In brief, ZIFCAT expression constructs were translated using the TnT system, and mixed for 1 hour at 4° C in an optimized buffer with cellulose-conjugated calf thymus genomic DNA. After extensive washing of the cellulose-DNA-protein complex, associated proteins were eluted, resolved on SDS-PAGE and detected by immuno-blotting.

### **Rho and Rac activation assays**

Rho activation was measured according to the manufacture's instructions (Upstate Rho Activation Assay Kit). In summary, embryo extracts were prepared using the provided buffer (Mg<sup>2+</sup> Lysis/ Wash Buffer), incubated with agarose-coated Rhotekin RBD (Rhotekin Binding Domain) at 4 degree, pelleted by



centrifugation, gently washed and followed by immuno-blot detection of RhoA. Active Rac1 levels were determined using similar methods, except that the Rac-GTP binding domain of Pak was used for the pull-downs, and total Rac1 was employed as the normalization control. When measuring Rho and Rac activities in mammalian cells, extra preparative steps involved: 24 hours post-transfection, complete medium was withdrawn and substituted with DMEM containing 0.1% FBS, and cells starved for 16 hours to minimize non-specific serum effects. For Rho assays, cells were further treated with lysophosphatidic acid/ LPA for 5 minutes to enhance basal Rho levels.

### **Fractionation methods**

Membrane-cytosolic fractionation of *Xenopus* embryos was carried out according to published methods (Fagotto and Gumbiner, 1994). Nuclear-cytosolic fractionation of 293T or HeLa cells also followed published protocols (Schreiber et al., 1989).

### **Alcian blue staining**

For craniofacial cartilage staining, *Xenopus* embryos were fixed with 95% ethanol and incubated in Alcian blue solution. Following staining, embryos were washed extensively and treated with KOH. The skin was surgically removed in certain experiments to expose the interior structures prior to photography.

## **Whole mount RNA in-situ hybridization**

Procedures of in-situ RNA hybridization of whole mount embryos were conducted as reported (Sive et al., 2000). Digoxigenin-labeled sense and anti-sense RNA probes were made from linearized DNA templates (DIG RNA Labeling Kit, Roche). In the final color reaction steps, NBT/ BCIP (Roche) served as the substrate for alkaline phosphatase reactions. To better visualize internal in situ signals, embryos were embedded in paraffin and sectioned into 10mm slices using a Leica computerized rotary microtome.

## **Biostatistics**

The statistical significance of various experiments was evaluated using SigmaPlot with error bars representing standard deviations. P values from t-tests that were less than 0.05 were deemed significant, while more than 0.05 were considered insignificant.

## **CHAPTER V**

### **Bibliography**

**Abdul-Ghani, M., Dufort, D., Stiles, R., De Repentigny, Y., Kothary, R. and Megeney, L. A.** (2011). Wnt11 promotes cardiomyocyte development by caspase-mediated suppression of canonical Wnt signals. *Mol Cell Biol* **31**, 163-78.

**Abdul-Ghani, M. and Megeney, L. A.** (2008). Rehabilitation of a contract killer: caspase-3 directs stem cell differentiation. *Cell Stem Cell* **2**, 515-6.

**Abu-Elneel, K., Ochiishi, T., Medina, M., Remedi, M., Gastaldi, L., Caceres, A. and Kosik, K. S.** (2008). A delta-catenin signaling pathway leading to dendritic protrusions. *J Biol Chem* **283**, 32781-91.

**Adams, J. W., Pagel, A. L., Means, C. K., Oksenberg, D., Armstrong, R. C. and Brown, J. H.** (2000). Cardiomyocyte apoptosis induced by Galphaq signaling is mediated by permeability transition pore formation and activation of the mitochondrial death pathway. *Circ Res* **87**, 1180-7.

**Anastasiadis, P. Z.** (2007). p120-ctn: A nexus for contextual signaling via Rho GTPases. *Biochim Biophys Acta* **1773**, 34-46.

**Anastasiadis, P. Z., Moon, S. Y., Thoreson, M. A., Mariner, D. J., Crawford, H. C., Zheng, Y. and Reynolds, A. B.** (2000). Inhibition of RhoA by p120 catenin. *Nat Cell Biol* **2**, 637-44.

**Anastasiadis, P. Z. and Reynolds, A. B.** (2001). Regulation of Rho GTPases by p120-catenin. *Curr Opin Cell Biol* **13**, 604-10.

**Appleby, D. W. and Modak, S. P.** (1977). DNA degradation in terminally differentiating lens fiber cells from chick embryos. *Proc Natl Acad Sci U S A* **74**, 5579-83.

**Arama, E., Agapite, J. and Steller, H.** (2003). Caspase activity and a specific cytochrome C are required for sperm differentiation in *Drosophila*. *Dev Cell* **4**, 687-97.

**Arama, E., Bader, M., Rieckhof, G. E. and Steller, H.** (2007). A ubiquitin ligase complex regulates caspase activation during sperm differentiation in *Drosophila*. *PLoS Biol* **5**, e251.

**Arikkath, J., Israely, I., Tao, Y., Mei, L., Liu, X. and Reichardt, L. F.** (2008). Erbin controls dendritic morphogenesis by regulating localization of delta-catenin. *J Neurosci* **28**, 7047-56.

**Artavanis-Tsakonas, S., Rand, M. D. and Lake, R. J.** (1999). Notch signaling: cell fate control and signal integration in development. *Science* **284**, 770-6.

**Bamji, S. X.** (2005). Cadherins: actin with the cytoskeleton to form synapses. *Neuron* **47**, 175-8.

**Bareiss, S., Kim, K. and Lu, Q.** Delta-catenin/NPRAP: A new member of the glycogen synthase kinase-3beta signaling complex that promotes beta-catenin turnover in neurons. *J Neurosci Res* **88**, 2350-63.

**Bassnett, S. and Mataic, D.** (1997). Chromatin degradation in differentiating fiber cells of the eye lens. *J Cell Biol* **137**, 37-49.

**Braga, V. M. and Yap, A. S.** (2005). The challenges of abundance: epithelial junctions and small GTPase signalling. *Curr Opin Cell Biol* **17**, 466-74.

**Brancolini, C., Lazarevic, D., Rodriguez, J. and Schneider, C.** (1997). Dismantling cell-cell contacts during apoptosis is coupled to a caspase-

dependent proteolytic cleavage of beta-catenin. *J Cell Biol* **139**, 759-71.

**Burger, M. J., Tebay, M. A., Keith, P. A., Samaratunga, H. M., Clements, J., Lavin, M. F. and Gardiner, R. A.** (2002). Expression analysis of delta-catenin and prostate-specific membrane antigen: their potential as diagnostic markers for prostate cancer. *Int J Cancer* **100**, 228-37.

**Bustelo, X. R., Sauzeau, V. and Berenjeno, I. M.** (2007). GTP-binding proteins of the Rho/Rac family: regulation, effectors and functions in vivo. *Bioessays* **29**, 356-70.

**Cadigan, K. M. and Peifer, M.** (2009). Wnt signaling from development to disease: Insights from Model Systems. *Cold Spring Harbor Perspectives in Biology* **In Press**.

**Carlile, G. W., Smith, D. H. and Wiedmann, M.** (2004). Caspase-3 has a nonapoptotic function in erythroid maturation. *Blood* **103**, 4310-6.

**Carnahan, R. H., Rokas, A., Gaucher, E. A. and Reynolds, A. B.** (2010). The molecular evolution of the p120-catenin subfamily and its functional associations. *PLoS One* **5**, e15747.

**Casagolda, D., Del Valle-Perez, B., Valls, G., Lugalde, E., Vinyoles, M., Casado-Vela, J., Solanas, G., Batlle, E., Reynolds, A. B., Casal, J. I. et al.** (2010). A p120-catenin-CK1epsilon complex regulates Wnt signaling. *J Cell Sci* **123**, 2621-31.

**Castano, J., Solanas, G., Casagolda, D., Raurell, I., Villagrasa, P., Bustelo, X. R., Garcia de Herreros, A. and Dunach, M.** (2007). Specific phosphorylation of p120-catenin regulatory domain differently modulates its

binding to RhoA. *Mol Cell Biol* **27**, 1745-57.

**Charrasse, S., Comunale, F., Fortier, M., Portales-Casamar, E., Debant, A. and Gauthier-Rouviere, C.** (2007). M-cadherin activates Rac1 GTPase through the Rho-GEF trio during myoblast fusion. *Mol Biol Cell* **18**, 1734-43.

**Charrasse, S., Meriane, M., Comunale, F., Blangy, A. and Gauthier-Rouviere, C.** (2002). N-cadherin-dependent cell-cell contact regulates Rho GTPases and beta-catenin localization in mouse C2C12 myoblasts. *J Cell Biol* **158**, 953-65.

**Chen, T., Yang, I., Irby, R., Shain, K. H., Wang, H. G., Quackenbush, J., Coppola, D., Cheng, J. Q. and Yeatman, T. J.** (2003). Regulation of caspase expression and apoptosis by adenomatous polyposis coli. *Cancer Res* **63**, 4368-74.

**Ciesiolka, M., Delvaeye, M., Van Imschoot, G., Verschuere, V., McCrea, P., van Roy, F. and Vleminckx, K.** (2004). p120 catenin is required for morphogenetic movements involved in the formation of the eyes and the craniofacial skeleton in *Xenopus*. *J Cell Sci* **117**, 4325-39.

**Cirillo, N., Lanza, M., De Rosa, A., Cammarota, M., La Gatta, A., Gombos, F. and Lanza, A.** (2008). The most widespread desmosomal cadherin, desmoglein 2, is a novel target of caspase 3-mediated apoptotic machinery. *J Cell Biochem* **103**, 598-606.

**Coen, L., Le Blay, K., Rowe, I. and Demeneix, B. A.** (2007). Caspase-9 regulates apoptosis/proliferation balance during metamorphic brain remodeling

in *Xenopus*. *Proc Natl Acad Sci U S A* **104**, 8502-7.

**Daniel, J. M.** (2007). Dancing in and out of the nucleus: p120(ctn) and the transcription factor Kaiso. *Biochim Biophys Acta* **1773**, 59-68.

**Davis, M. A., Ireton, R. C. and Reynolds, A. B.** (2003). A core function for p120-catenin in cadherin turnover. *J Cell Biol* **163**, 525-34.

**DeBusk, L. M., Boelte, K., Min, Y. and Lin, P. C.** (2010). Heterozygous deficiency of delta-catenin impairs pathological angiogenesis. *J Exp Med* **207**, 77-84.

**Deguchi, M., Iizuka, T., Hata, Y., Nishimura, W., Hirao, K., Yao, I., Kawabe, H. and Takai, Y.** (2000). PAPIN. A novel multiple PSD-95/Dlg-A/ZO-1 protein interacting with neural plakophilin-related armadillo repeat protein/delta-catenin and p0071. *J Biol Chem* **275**, 29875-80.

**Dejosez, M., Krumenacker, J. S., Zitur, L. J., Passeri, M., Chu, L. F., Songyang, Z., Thomson, J. A. and Zwaka, T. P.** (2008). Ronin is essential for embryogenesis and the pluripotency of mouse embryonic stem cells. *Cell* **133**, 1162-74.

**Deming, P. and Kornbluth, S.** (2006). Study of apoptosis in vitro using the *Xenopus* egg extract reconstitution system. *Methods Mol Biol* **322**, 379-93.

**Draper, B. W., Morcos, P. A. and Kimmel, C. B.** (2001). Inhibition of zebrafish fgf8 pre-mRNA splicing with morpholino oligos: a quantifiable method for gene knockdown. *Genesis* **30**, 154-6.

**Du Pasquier, D., Rincheval, V., Sinzelle, L., Chesneau, A., Ballagny, C., Sachs, L. M., Demeneix, B. and Mazabraud, A.** (2006). Developmental cell



death during *Xenopus* metamorphosis involves BID cleavage and caspase 2 and 8 activation. *Dev Dyn* **235**, 2083-94.

**Dusek, R. L., Getsios, S., Chen, F., Park, J. K., Amargo, E. V., Cryns, V. L. and Green, K. J.** (2006). The differentiation-dependent desmosomal cadherin desmoglein 1 is a novel caspase-3 target that regulates apoptosis in keratinocytes. *J Biol Chem* **281**, 3614-24.

**Elia, L. P., Yamamoto, M., Zang, K. and Reichardt, L. F.** (2006). p120 catenin regulates dendritic spine and synapse development through Rho-family GTPases and cadherins. *Neuron* **51**, 43-56.

**Fagotto, F. and Gumbiner, B. M.** (1994). Beta-catenin localization during *Xenopus* embryogenesis: accumulation at tissue and somite boundaries. *Development* **120**, 3667-79.

**Fang, X., Ji, H., Kim, S. W., Park, J. I., Vaught, T. G., Anastasiadis, P. Z., Ciesiolka, M. and McCrea, P. D.** (2004). Vertebrate development requires ARVCF and p120 catenins and their interplay with RhoA and Rac. *J Cell Biol* **165**, 87-98.

**Feinstein-Rotkopf, Y. and Arama, E.** (2009). Can't live without them, can live with them: roles of caspases during vital cellular processes. *Apoptosis* **14**, 980-95.

**Ferber, E. C., Kajita, M., Wadlow, A., Tobiansky, L., Niessen, C., Ariga, H., Daniel, J. and Fujita, Y.** (2008). A role for the cleaved cytoplasmic domain of E-cadherin in the nucleus. *J Biol Chem* **283**, 12691-700.

**Fernando, P. and Megeney, L. A.** (2007). Is caspase-dependent

apoptosis only cell differentiation taken to the extreme? *Faseb J* **21**, 8-17.

**Fujita, J., Crane, A. M., Souza, M. K., Dejosez, M., Kyba, M., Flavell, R. A., Thomson, J. A. and Zwaka, T. P.** (2008). Caspase activity mediates the differentiation of embryonic stem cells. *Cell Stem Cell* **2**, 595-601.

**Fujita, T., Okada, T., Hayashi, S., Jahangeer, S., Miwa, N. and Nakamura, S.** (2004). Delta-catenin/NPRAP (neural plakophilin-related armadillo repeat protein) interacts with and activates sphingosine kinase 1. *Biochem J* **382**, 717-23.

**Fukuyama, T., Ogita, H., Kawakatsu, T., Inagaki, M. and Takai, Y.** (2006). Activation of Rac by cadherin through the c-Src-Rap1-phosphatidylinositol 3-kinase-Vav2 pathway. *Oncogene* **25**, 8-19.

**Gabet, A. S., Coulon, S., Fricot, A., Vandekerckhove, J., Chang, Y., Ribeil, J. A., Lordier, L., Zermati, Y., Asnafi, V., Belaid, Z. et al.** (2010). Caspase-activated ROCK-1 allows erythroblast terminal maturation independently of cytokine-induced Rho signaling. *Cell Death Differ.*

**Goodwin, M., Kovacs, E. M., Thoreson, M. A., Reynolds, A. B. and Yap, A. S.** (2003). Minimal mutation of the cytoplasmic tail inhibits the ability of E-cadherin to activate Rac but not phosphatidylinositol 3-kinase: direct evidence of a role for cadherin-activated Rac signaling in adhesion and contact formation. *J Biol Chem* **278**, 20533-9.

**Groner, A. C., Meylan, S., Ciuffi, A., Zangger, N., Ambrosini, G., Denervaud, N., Bucher, P. and Trono, D.** (2010). KRAB-zinc finger proteins and KAP1 can mediate long-range transcriptional repression through

heterochromatin spreading. *PLoS Genet* **6**, e1000869.

**Grosheva, I., Shtutman, M., Elbaum, M. and Bershadsky, A. D.** (2001). p120 catenin affects cell motility via modulation of activity of Rho-family GTPases: a link between cell-cell contact formation and regulation of cell locomotion. *J Cell Sci* **114**, 695-707.

**Gu, D., Sater, A. K., Ji, H., Cho, K., Clark, M., Stratton, S. A., Barton, M. C., Lu, Q. and McCrea, P. D.** (2009). *Xenopus* delta-catenin is essential in early embryogenesis and is functionally linked to cadherins and small GTPases. *J Cell Sci* **122**, 4049-61.

**Gumbiner, B. M.** (2005). Regulation of cadherin-mediated adhesion in morphogenesis. *Nat Rev Mol Cell Biol* **6**, 622-34.

**Habas, R., Dawid, I. B. and He, X.** (2003). Coactivation of Rac and Rho by Wnt/Frizzled signaling is required for vertebrate gastrulation. *Genes Dev* **17**, 295-309.

**Habas, R., Kato, Y. and He, X.** (2001). Wnt/Frizzled activation of Rho regulates vertebrate gastrulation and requires a novel Formin homology protein Daam1. *Cell* **107**, 843-54.

**Hall, A.** (1998). Rho GTPases and the actin cytoskeleton. *Science* **279**, 509-14.

**Harris, T. J. and Tepass, U.** (2010). Adherens junctions: from molecules to morphogenesis. *Nat Rev Mol Cell Biol* **11**, 502-14.

**Hatzfeld, M.** (2005). The p120 family of cell adhesion molecules. *Eur J Cell Biol* **84**, 205-14.

**He, H. and Baldwin, G. S.** (2008). Rho GTPases and p21-activated kinase in the regulation of proliferation and apoptosis by gastrins. *Int J Biochem Cell Biol* **40**, 2018-22.

**He, H., Yim, M., Liu, K. H., Cody, S. C., Shulkes, A. and Baldwin, G. S.** (2008). Involvement of G proteins of the Rho family in the regulation of Bcl-2-like protein expression and caspase 3 activation by Gastrins. *Cell Signal* **20**, 83-93.

**Heasman, S. J. and Ridley, A. J.** (2008). Mammalian Rho GTPases: new insights into their functions from in vivo studies. *Nat Rev Mol Cell Biol* **9**, 690-701.

**Heisenberg, C. P., Tada, M., Rauch, G. J., Saude, L., Concha, M. L., Geisler, R., Stemple, D. L., Smith, J. C. and Wilson, S. W.** (2000). Silberblick/Wnt11 mediates convergent extension movements during zebrafish gastrulation. *Nature* **405**, 76-81.

**Herren, B., Levkau, B., Raines, E. W. and Ross, R.** (1998). Cleavage of beta-catenin and plakoglobin and shedding of VE-cadherin during endothelial apoptosis: evidence for a role for caspases and metalloproteinases. *Mol Biol Cell* **9**, 1589-601.

**Ho, C., Zhou, J., Medina, M., Goto, T., Jacobson, M., Bhide, P. G. and Kosik, K. S.** (2000). delta-catenin is a nervous system-specific adherens junction protein which undergoes dynamic relocalization during development. *J Comp Neurol* **420**, 261-76.

**Hong, J. Y., Park, J. I., Cho, K., Gu, D., Ji, H., Artandi, S. E. and McCrea, P. D.** Shared molecular mechanisms regulate multiple catenin proteins:

canonical Wnt signals and components modulate p120-catenin isoform-1 and additional p120 subfamily members. *J Cell Sci* **123**, 4351-65.

**Hong, J. Y., Park, J. I., Cho, K., Gu, D., Ji, H., Artandi, S. E. and McCreary, P. D.** (2010). Shared molecular mechanisms regulate multiple catenin proteins: canonical Wnt signals and components modulate p120-catenin isoform-1 and additional p120 subfamily members. *J Cell Sci* **123**, 4351-65.

**Hosking, C. R., Ulloa, F., Hogan, C., Ferber, E. C., Figueroa, A., Gevaert, K., Birchmeier, W., Briscoe, J. and Fujita, Y.** (2007). The transcriptional repressor Glis2 is a novel binding partner for p120 catenin. *Mol Biol Cell* **18**, 1918-27.

**Hou, J. C., Shigematsu, S., Crawford, H. C., Anastasiadis, P. Z. and Pessin, J. E.** (2006). Dual regulation of Rho and Rac by p120 catenin controls adipocyte plasma membrane trafficking. *J Biol Chem* **281**, 23307-12.

**Huber, A. H., Nelson, W. J. and Weis, W. I.** (1997). Three-dimensional structure of the armadillo repeat region of beta-catenin. *Cell* **90**, 871-82.

**Hunter, I., McGregor, D. and Robins, S. P.** (2001). Caspase-dependent cleavage of cadherins and catenins during osteoblast apoptosis. *J Bone Miner Res* **16**, 466-77.

**Ide, N., Hata, Y., Deguchi, M., Hirao, K., Yao, I. and Takai, Y.** (1999). Interaction of S-SCAM with neural plakophilin-related Armadillo-repeat protein/delta-catenin. *Biochem Biophys Res Commun* **256**, 456-61.

**Iguchi, Y., Katsuno, M., Niwa, J., Yamada, S., Sone, J., Waza, M., Adachi, H., Tanaka, F., Nagata, K., Arimura, N. et al.** (2009). TDP-43 depletion

induces neuronal cell damage through dysregulation of Rho family GTPases. *J Biol Chem* **284**, 22059-66.

**Iioka, H., Doerner, S. K. and Tamai, K.** (2009). Kaiso is a bimodal modulator for Wnt/beta-catenin signaling. *FEBS Lett* **583**, 627-32.

**Ishizaki, Y., Jacobson, M. D. and Raff, M. C.** (1998). A role for caspases in lens fiber differentiation. *J Cell Biol* **140**, 153-8.

**Israely, I., Costa, R. M., Xie, C. W., Silva, A. J., Kosik, K. S. and Liu, X.** (2004). Deletion of the neuron-specific protein delta-catenin leads to severe cognitive and synaptic dysfunction. *Curr Biol* **14**, 1657-63.

**Izawa, I., Nishizawa, M., Ohtakara, K. and Inagaki, M.** (2002). Densin-180 interacts with delta-catenin/neural plakophilin-related armadillo repeat protein at synapses. *J Biol Chem* **277**, 5345-50.

**Jeanes, A., Gottardi, C. J. and Yap, A. S.** (2008). Cadherins and cancer: how does cadherin dysfunction promote tumor progression? *Oncogene* **27**, 6920-9.

**Johnson, E., Theisen, C. S., Johnson, K. R. and Wheelock, M. J.** (2004). R-cadherin influences cell motility via Rho family GTPases. *J Biol Chem* **279**, 31041-9.

**Jones, S. B., Lanford, G. W., Chen, Y. H., Morabito, M., Kim, K. and Lu, Q.** (2002). Glutamate-induced delta-catenin redistribution and dissociation from postsynaptic receptor complexes. *Neuroscience* **115**, 1009-21.

**Kawamura, Y., Fan, Q. W., Hayashi, H., Michikawa, M., Yanagisawa, K. and Komano, H.** (1999). Expression of the mRNA for two isoforms of neural

plakophilin-related arm-repeat protein/delta-catenin in rodent neurons and glial cells. *Neurosci Lett* **277**, 185-8.

**Keil, R., Wolf, A., Huttelmaier, S. and Hatzfeld, M.** (2007). Beyond regulation of cell adhesion: local control of RhoA at the cleavage furrow by the p0071 catenin. *Cell Cycle* **6**, 122-7.

**Keller, R.** (2005). Cell migration during gastrulation. *Curr Opin Cell Biol* **17**, 533-41.

**Keller, R., Davidson, L. A. and Shook, D. R.** (2003). How we are shaped: the biomechanics of gastrulation. *Differentiation* **71**, 171-205.

**Kessler, T. and Muller, H. A.** (2009). Cleavage of Armadillo/beta-catenin by the caspase DrlCE in Drosophila apoptotic epithelial cells. *BMC Dev Biol* **9**, 15.

**Kim, H., Han, J. R., Park, J., Oh, M., James, S. E., Chang, S., Lu, Q., Lee, K. Y., Ki, H., Song, W. J. et al.** (2007). delta -Catenin induced dendritic morphogenesis: An essential role of p190RhoGEF interaction through Akt1 mediated phosphorylation. *J Biol Chem*.

**Kim, H., Han, J. R., Park, J., Oh, M., James, S. E., Chang, S., Lu, Q., Lee, K. Y., Ki, H., Song, W. J. et al.** (2008a). Delta-catenin-induced dendritic morphogenesis. An essential role of p190RhoGEF interaction through Akt1-mediated phosphorylation. *J Biol Chem* **283**, 977-87.

**Kim, H., Oh, M., Lu, Q. and Kim, K.** (2008b). E-Cadherin negatively modulates delta-catenin-induced morphological changes and RhoA activity reduction by competing with p190RhoGEF for delta-catenin. *Biochem Biophys*

*Res Commun* **377**, 636-41.

**Kim, J. S., Bareiss, S., Kim, K. K., Tatum, R., Han, J. R., Jin, Y. H., Kim, H., Lu, Q. and Kim, K.** (2006). Presenilin-1 inhibits delta-catenin-induced cellular branching and promotes delta-catenin processing and turnover. *Biochem Biophys Res Commun* **351**, 903-8.

**Kim, K., Oh, M., Ki, H., Wang, T., Bareiss, S., Fini, M. E., Li, D. and Lu, Q.** (2008c). Identification of E2F1 as a positive transcriptional regulator for delta-catenin. *Biochem Biophys Res Commun* **369**, 414-20.

**Kim, K., Pang, K. M., Evans, M. and Hay, E. D.** (2000). Overexpression of beta-catenin induces apoptosis independent of its transactivation function with LEF-1 or the involvement of major G1 cell cycle regulators. *Mol Biol Cell* **11**, 3509-23.

**Kim, K., Sirota, A., Chen Yh, Y. H., Jones, S. B., Dudek, R., Lanford, G. W., Thakore, C. and Lu, Q.** (2002). Dendrite-like process formation and cytoskeletal remodeling regulated by delta-catenin expression. *Exp Cell Res* **275**, 171-84.

**Kim, S. W., Park, J. I., Spring, C. M., Sater, A. K., Ji, H., Otchere, A. A., Daniel, J. M. and McCrea, P. D.** (2004). Non-canonical Wnt signals are modulated by the Kaiso transcriptional repressor and p120-catenin. *Nat Cell Biol* **6**, 1212-20.

**Kolbus, A., Pilat, S., Husak, Z., Deiner, E. M., Stengl, G., Beug, H. and Baccarini, M.** (2002). Raf-1 antagonizes erythroid differentiation by restraining caspase activation. *J Exp Med* **196**, 1347-53.



**Kornbluth, S. and Evans, E. K.** (2001). Analysis of apoptosis using Xenopus egg extracts. *Curr Protoc Cell Biol* **Chapter 11**, Unit 11 12.

**Kosik, K. S., Donahue, C. P., Israely, I., Liu, X. and Ochiishi, T.** (2005). Delta-catenin at the synaptic-adherens junction. *Trends Cell Biol* **15**, 172-8.

**Kowalczyk, A. P. and Reynolds, A. B.** (2004). Protecting your tail: regulation of cadherin degradation by p120-catenin. *Curr Opin Cell Biol* **16**, 522-7.

**Kumar, S.** (2007). Caspase function in programmed cell death. *Cell Death Differ* **14**, 32-43.

**Kuranaga, E. and Miura, M.** (2007). Nonapoptotic functions of caspases: caspases as regulatory molecules for immunity and cell-fate determination. *Trends Cell Biol* **17**, 135-44.

**Lampugnani, M. G., Zanetti, A., Breviario, F., Balconi, G., Orsenigo, F., Corada, M., Spagnuolo, R., Betson, M., Braga, V. and Dejana, E.** (2002). VE-cadherin regulates endothelial actin activating Rac and increasing membrane association of Tiam. *Mol Biol Cell* **13**, 1175-89.

**Laura, R. P., Witt, A. S., Held, H. A., Gerstner, R., Deshayes, K., Koehler, M. F., Kosik, K. S., Sidhu, S. S. and Lasky, L. A.** (2002). The Erbin PDZ domain binds with high affinity and specificity to the carboxyl termini of delta-catenin and ARVCF. *J Biol Chem* **277**, 12906-14.

**Le, S. S., Loucks, F. A., Udo, H., Richardson-Burns, S., Phelps, R. A., Bouchard, R. J., Barth, H., Aktories, K., Tyler, K. L., Kandel, E. R. et al.** (2005). Inhibition of Rac GTPase triggers a c-Jun- and Bim-dependent

mitochondrial apoptotic cascade in cerebellar granule neurons. *J Neurochem* **94**, 1025-39.

**Lee, A., Morrow, J. S. and Fowler, V. M.** (2001). Caspase remodeling of the spectrin membrane skeleton during lens development and aging. *J Biol Chem* **276**, 20735-42.

**Levesque, G., Yu, G., Nishimura, M., Zhang, D. M., Levesque, L., Yu, H., Xu, D., Liang, Y., Rogueva, E., Ikeda, M. et al.** (1999). Presenilins interact with armadillo proteins including neural-specific plakophilin-related protein and beta-catenin. *J Neurochem* **72**, 999-1008.

**Lien, W. H., Klezovitch, O. and Vasioukhin, V.** (2006). Cadherin-catenin proteins in vertebrate development. *Curr Opin Cell Biol* **18**, 499-506.

**Ling, Y., Zhong, Y. and Perez-Soler, R.** (2001). Disruption of cell adhesion and caspase-mediated proteolysis of beta- and gamma-catenins and APC protein in paclitaxel-induced apoptosis. *Mol Pharmacol* **59**, 593-603.

**Liu, W., Sato, A., Khadka, D., Bharti, R., Diaz, H., Runnels, L. W. and Habas, R.** (2008). Mechanism of activation of the Formin protein Daam1. *Proc Natl Acad Sci U S A* **105**, 210-5.

**Lockshin, R. A. and Zakeri, Z.** (2007). Cell death in health and disease. *J Cell Mol Med* **11**, 1214-24.

**Logan, C. Y. and Nusse, R.** (2004). The Wnt signaling pathway in development and disease. *Annu Rev Cell Dev Biol* **20**, 781-810.

**Looman, C., Abrink, M., Mark, C. and Hellman, L.** (2002). KRAB zinc finger proteins: an analysis of the molecular mechanisms governing their

increase in numbers and complexity during evolution. *Mol Biol Evol* **19**, 2118-30.

**Lu, J. P., Zhang, J., Kim, K., Case, T. C., Matusik, R. J., Chen, Y. H., Wolfe, M., Nopparat, J. and Lu, Q.** Human homolog of Drosophila Hairy and enhancer of split 1, Hes1, negatively regulates delta-catenin (CTNND2) expression in cooperation with E2F1 in prostate cancer. *Mol Cancer* **9**, 304.

**Lu, Q.** (2010). delta-Catenin dysregulation in cancer: interactions with E-cadherin and beyond. *J Pathol* **222**, 119-23.

**Lu, Q., Dobbs, L. J., Gregory, C. W., Lanford, G. W., Revelo, M. P., Shappell, S. and Chen, Y. H.** (2005). Increased expression of delta-catenin/neural plakophilin-related armadillo protein is associated with the down-regulation and redistribution of E-cadherin and p120ctn in human prostate cancer. *Hum Pathol* **36**, 1037-48.

**Lu, Q., Mukhopadhyay, N. K., Griffin, J. D., Paredes, M., Medina, M. and Kosik, K. S.** (2002). Brain armadillo protein delta-catenin interacts with Abl tyrosine kinase and modulates cellular morphogenesis in response to growth factors. *J Neurosci Res* **67**, 618-24.

**Lu, Q., Paredes, M., Medina, M., Zhou, J., Cavallo, R., Peifer, M., Orecchio, L. and Kosik, K. S.** (1999). delta-catenin, an adhesive junction-associated protein which promotes cell scattering. *J Cell Biol* **144**, 519-32.

**Lu, Q., Zhang, J., Allison, R., Gay, H., Yang, W. X., Bhowmick, N. A., Frelix, G., Shappell, S. and Chen, Y. H.** (2008). Identification of extracellular delta-catenin accumulation for prostate cancer detection. *Prostate*.

**Lyons, J. P., Miller, R. K., Zhou, X., Weidinger, G., Deroo, T., Denayer,**

**T., Park, J. I., Ji, H., Hong, J. Y., Li, A. et al.** (2009). Requirement of Wnt/beta-catenin signaling in pronephric kidney development. *Mech Dev* **126**, 142-59.

**Mackie, S. and Aitken, A.** (2005). Novel brain 14-3-3 interacting proteins involved in neurodegenerative disease. *Febs J* **272**, 4202-10.

**Maeda, M., Johnson, E., Mandal, S. H., Lawson, K. R., Keim, S. A., Svoboda, R. A., Caplan, S., Wahl, J. K., 3rd, Wheelock, M. J. and Johnson, K. R.** (2006). Expression of inappropriate cadherins by epithelial tumor cells promotes endocytosis and degradation of E-cadherin via competition for p120(ctn). *Oncogene* **25**, 4595-604.

**Magie, C. R., Pinto-Santini, D. and Parkhurst, S. M.** (2002). Rho1 interacts with p120ctn and alpha-catenin, and regulates cadherin-based adherens junction components in *Drosophila*. *Development* **129**, 3771-82.

**Martinez, M. C., Ochiishi, T., Majewski, M. and Kosik, K. S.** (2003). Dual regulation of neuronal morphogenesis by a delta-catenin-cortactin complex and Rho. *J Cell Biol* **162**, 99-111.

**Matter, C., Pribadi, M., Liu, X. and Trachtenberg, J. T.** (2009). Delta-catenin is required for the maintenance of neural structure and function in mature cortex in vivo. *Neuron* **64**, 320-7.

**McCrea, P. D. and Gu, D.** (2010). The catenin family at a glance. *J Cell Sci* **123**, 637-42.

**McCrea, P. D., Gu, D. and Balda, M. S.** (2009). Junctional Music that the Nucleus Hears: Cell-Cell Contact Signaling and the Modulation of Gene Activity. *Cold Spring Harb Perspect Biol* **1**, a002923.

**McCrea, P. D. and Park, J. I.** (2007). Developmental functions of the P120-catenin sub-family. *Biochim Biophys Acta* **1773**, 17-33.

**McCusker, C. D. and Alfandari, D.** (2009). Life after proteolysis: Exploring the signaling capabilities of classical cadherin cleavage fragments. *Commun Integr Biol* **2**, 155-7.

**Medina, M., Marinescu, R. C., Overhauser, J. and Kosik, K. S.** (2000). Hemizyosity of delta-catenin (CTNND2) is associated with severe mental retardation in cri-du-chat syndrome. *Genomics* **63**, 157-64.

**Morishita, H., Makishima, T., Kaneko, C., Lee, Y. S., Segil, N., Takahashi, K., Kuraoka, A., Nakagawa, T., Nabekura, J., Nakayama, K. et al.** (2001). Deafness due to degeneration of cochlear neurons in caspase-3-deficient mice. *Biochem Biophys Res Commun* **284**, 142-9.

**Munoz, J. P., Huichalaf, C. H., Orellana, D. and Maccioni, R. B.** (2007). cdk5 modulates beta- and delta-catenin/Pin1 interactions in neuronal cells. *J Cell Biochem* **100**, 738-49.

**Muro, I., Berry, D. L., Huh, J. R., Chen, C. H., Huang, H., Yoo, S. J., Guo, M., Baehrecke, E. H. and Hay, B. A.** (2006). The Drosophila caspase Ice is important for many apoptotic cell deaths and for spermatid individualization, a nonapoptotic process. *Development* **133**, 3305-15.

**Myster, S. H., Cavallo, R., Anderson, C. T., Fox, D. T. and Peifer, M.** (2003). Drosophila p120catenin plays a supporting role in cell adhesion but is not an essential adherens junction component. *J Cell Biol* **160**, 433-49.

**Nelson, C. M. and Chen, C. S.** (2003). VE-cadherin simultaneously

stimulates and inhibits cell proliferation by altering cytoskeletal structure and tension. *J Cell Sci* **116**, 3571-81.

**Noren, N. K., Liu, B. P., Burridge, K. and Kreft, B.** (2000). p120 catenin regulates the actin cytoskeleton via Rho family GTPases. *J Cell Biol* **150**, 567-80.

**Nutt, S. L., Bronchain, O. J., Hartley, K. O. and Amaya, E.** (2001). Comparison of morpholino based translational inhibition during the development of *Xenopus laevis* and *Xenopus tropicalis*. *Genesis* **30**, 110-3.

**O'Geen, H., Squazzo, S. L., Iyengar, S., Blahnik, K., Rinn, J. L., Chang, H. Y., Green, R. and Farnham, P. J.** (2007). Genome-wide analysis of KAP1 binding suggests autoregulation of KRAB-ZNFs. *PLoS Genet* **3**, e89.

**Oh, M., Kim, H., Yang, I., Park, J. H., Cong, W. T., Baek, M. C., Bareiss, S., Ki, H., Lu, Q., No, J. et al.** (2009). GSK-3 phosphorylates delta-catenin and negatively regulates its stability via ubiquitination/proteasome-mediated proteolysis. *J Biol Chem* **284**, 28579-89.

**Paffenholz, R. and Franke, W. W.** (1997). Identification and localization of a neurally expressed member of the plakoglobin/armadillo multigene family. *Differentiation* **61**, 293-304.

**Paredes, J., Correia, A. L., Ribeiro, A. S. and Schmitt, F.** (2007). Expression of p120-catenin isoforms correlates with genomic and transcriptional phenotype of breast cancer cell lines. *Cell Oncol* **29**, 467-76.

**Parisiadou, L., Fassa, A., Fotinopoulou, A., Bethani, I. and Efthimiopoulos, S.** (2004). Presenilin 1 and cadherins: stabilization of cell-cell adhesion and proteolysis-dependent regulation of transcription. *Neurodegener*

*Dis* **1**, 184-91.

**Park, J. I., Ji, H., Jun, S., Gu, D., Hikasa, H., Li, L., Sokol, S. Y. and McCrea, P. D.** (2006). Frdo links Dishevelled to the p120-catenin/Kaiso pathway: distinct catenin subfamilies promote Wnt signals. *Dev Cell* **11**, 683-95.

**Park, J. I., Kim, S. W., Lyons, J. P., Ji, H., Nguyen, T. T., Cho, K., Barton, M. C., Deroo, T., Vleminckx, K., Moon, R. T. et al.** (2005). Kaiso/p120-catenin and TCF/beta-catenin complexes coordinately regulate canonical Wnt gene targets. *Dev Cell* **8**, 843-54.

**Pettitt, J., Cox, E. A., Broadbent, I. D., Flett, A. and Hardin, J.** (2003). The *Caenorhabditis elegans* p120 catenin homologue, JAC-1, modulates cadherin-catenin function during epidermal morphogenesis. *J Cell Biol* **162**, 15-22.

**Popoff, M. R. and Geny, B.** (2009). Multifaceted role of Rho, Rac, Cdc42 and Ras in intercellular junctions, lessons from toxins. *Biochim Biophys Acta* **1788**, 797-812.

**Qian, J., Steigerwald, K., Combs, K. A., Barton, M. C. and Groden, J.** (2007). Caspase cleavage of the APC tumor suppressor and release of an amino-terminal domain is required for the transcription-independent function of APC in apoptosis. *Oncogene* **26**, 4872-6.

**Revankar, C. M., Vines, C. M., Cimino, D. F. and Prossnitz, E. R.** (2004). Arrestins block G protein-coupled receptor-mediated apoptosis. *J Biol Chem* **279**, 24578-84.

**Reynolds, A. B.** (2007). p120-catenin: Past and present. *Biochim*

*Biophys Acta* **1773**, 2-7.

**Reynolds, A. B. and Carnahan, R. H.** (2004). Regulation of cadherin stability and turnover by p120ctn: implications in disease and cancer. *Semin Cell Dev Biol* **15**, 657-63.

**Reynolds, A. B. and Roczniak-Ferguson, A.** (2004). Emerging roles for p120-catenin in cell adhesion and cancer. *Oncogene* **23**, 7947-56.

**Ridley, A. J.** (2001a). Rho family proteins: coordinating cell responses. *Trends Cell Biol* **11**, 471-7.

**Ridley, A. J.** (2001b). Rho GTPases and cell migration. *J Cell Sci* **114**, 2713-22.

**Rodova, M., Kelly, K. F., VanSaun, M., Daniel, J. M. and Werle, M. J.** (2004). Regulation of the rapsyn promoter by kaiso and delta-catenin. *Mol Cell Biol* **24**, 7188-96.

**Salazar, N. C., Chen, J. and Rockman, H. A.** (2007). Cardiac GPCRs: GPCR signaling in healthy and failing hearts. *Biochim Biophys Acta* **1768**, 1006-18.

**Schreiber, E., Matthias, P., Muller, M. M. and Schaffner, W.** (1989). Rapid detection of octamer binding proteins with 'mini-extracts', prepared from a small number of cells. *Nucleic Acids Res* **17**, 6419.

**Schulte, G. and Bryja, V.** (2007). The Frizzled family of unconventional G-protein-coupled receptors. *Trends Pharmacol Sci* **28**, 518-25.

**Semina, E. V., Rubina, K. A., Rutkevich, P. N., Voyno-Yasenetskaya, T. A., Parfyonova, Y. V. and Tkachuk, V. A.** (2009). T-cadherin activates Rac1



and Cdc42 and changes endothelial permeability. *Biochemistry (Mosc)* **74**, 362-70.

**Senthivinayagam, S., Mishra, P., Paramasivam, S. K., Yallapragada, S., Chatterjee, M., Wong, L., Rana, A. and Rana, B.** (2009). Caspase-mediated cleavage of beta-catenin precedes drug-induced apoptosis in resistant cancer cells. *J Biol Chem* **284**, 13577-88.

**Silverman, J. B., Restituto, S., Lu, W., Lee-Edwards, L., Khatri, L. and Ziff, E. B.** (2007). Synaptic anchorage of AMPA receptors by cadherins through neural plakophilin-related arm protein AMPA receptor-binding protein complexes. *J Neurosci* **27**, 8505-16.

**Sive, H. L., Grainger, R. M. and Harland, R. M.** (2000). Early Development of *Xenopus laevis*: A Laboratory Manual. *Cold Spring Harbor Laboratory Press*.

**Solary, E., Eymin, B., Droin, N. and Haugg, M.** (1998). Proteases, proteolysis, and apoptosis. *Cell Biol Toxicol* **14**, 121-32.

**Solnica-Krezel, L.** (2006). Gastrulation in zebrafish -- all just about adhesion? *Curr Opin Genet Dev* **16**, 433-41.

**Steinhusen, U., Badock, V., Bauer, A., Behrens, J., Wittman-Liebold, B., Dorken, B. and Bommert, K.** (2000). Apoptosis-induced cleavage of beta-catenin by caspase-3 results in proteolytic fragments with reduced transactivation potential. *J Biol Chem* **275**, 16345-53.

**Steinhusen, U., Weiske, J., Badock, V., Tauber, R., Bommert, K. and Huber, O.** (2001). Cleavage and shedding of E-cadherin after induction of

apoptosis. *J Biol Chem* **276**, 4972-80.

**Suzanne, M. and Steller, H.** (2009). Letting go: modification of cell adhesion during apoptosis. *J Biol* **8**, 49.

**Tada, M., Concha, M. L. and Heisenberg, C. P.** (2002). Non-canonical Wnt signalling and regulation of gastrulation movements. *Semin Cell Dev Biol* **13**, 251-60.

**Tanahashi, H. and Tabira, T.** (1999). Isolation of human delta-catenin and its binding specificity with presenilin 1. *Neuroreport* **10**, 563-8.

**Tao, Q., Yokota, C., Puck, H., Kofron, M., Birsoy, B., Yan, D., Asashima, M., Wylie, C. C., Lin, X. and Heasman, J.** (2005). Maternal wnt11 activates the canonical wnt signaling pathway required for axis formation in *Xenopus* embryos. *Cell* **120**, 857-71.

**Tseng, A. S., Adams, D. S., Qiu, D., Koustubhan, P. and Levin, M.** (2007). Apoptosis is required during early stages of tail regeneration in *Xenopus laevis*. *Dev Biol* **301**, 62-9.

**Urrutia, R.** (2003). KRAB-containing zinc-finger repressor proteins. *Genome Biol* **4**, 231.

**van Hengel, J. and van Roy, F.** (2007). Diverse functions of p120ctn in tumors. *Biochim Biophys Acta* **1773**, 78-88.

**van Roy, F. M. and McCrea, P. D.** (2005). A role for Kaiso-p120ctn complexes in cancer? *Nat Rev Cancer* **5**, 956-64.

**Vize, P. D., Jones, E. A. and Pfister, R.** (1995). Development of the *Xenopus* pronephric system. *Dev Biol* **171**, 531-40.

**Wallingford, J. B., Fraser, S. E. and Harland, R. M.** (2002). Convergent extension: the molecular control of polarized cell movement during embryonic development. *Dev Cell* **2**, 695-706.

**Wang, T., Chen, Y. H., Hong, H., Zeng, Y., Zhang, J., Lu, J. P., Jeansonne, B. and Lu, Q.** (2008). Increased nucleotide polymorphic changes in the 5'-untranslated region of delta-catenin (CTNND2) gene in prostate cancer. *Oncogene*.

**Webb, S. J., Nicholson, D., Bubb, V. J. and Wyllie, A. H.** (1999). Caspase-mediated cleavage of APC results in an amino-terminal fragment with an intact armadillo repeat domain. *Faseb J* **13**, 339-46.

**Weiske, J. and Huber, O.** (2005). Fate of desmosomal proteins in apoptotic epidermal cells. *Methods Mol Biol* **289**, 175-92.

**Wildenberg, G. A., Dohn, M. R., Carnahan, R. H., Davis, M. A., Lobdell, N. A., Settleman, J. and Reynolds, A. B.** (2006). p120-catenin and p190RhoGAP regulate cell-cell adhesion by coordinating antagonism between Rac and Rho. *Cell* **127**, 1027-39.

**Willert, K. and Jones, K. A.** (2006). Wnt signaling: is the party in the nucleus? *Genes Dev* **20**, 1394-404.

**Xiao, K., Oas, R. G., Chiasson, C. M. and Kowalczyk, A. P.** (2007). Role of p120-catenin in cadherin trafficking. *Biochim Biophys Acta* **1773**, 8-16.

**Xing, Y., Takemaru, K., Liu, J., Berndt, J. D., Zheng, J. J., Moon, R. T. and Xu, W.** (2008). Crystal structure of a full-length beta-catenin. *Structure* **16**, 478-87.

**Yanagisawa, M., Huvelde, D., Kreinest, P., Lohse, C. M., Cheville, J. C., Parker, A. S., Copland, J. A. and Anastasiadis, P. Z.** (2008). A p120 catenin isoform switch affects Rho activity, induces tumor cell invasion, and predicts metastatic disease. *J Biol Chem* **283**, 18344-54.

**Yap, A. S. and Kovacs, E. M.** (2003). Direct cadherin-activated cell signaling: a view from the plasma membrane. *J Cell Biol* **160**, 11-6.

**Yun, S. I., Yoon, H. Y. and Chung, Y. S.** (2009). Glycogen synthase kinase-3beta regulates etoposide-induced apoptosis via Bcl-2 mediated caspase-3 activation in C3H10T1/2 cells. *Apoptosis* **14**, 771-7.

**Zeng, Y., Abdallah, A., Lu, J. P., Wang, T., Chen, Y. H., Terrian, D. M., Kim, K. and Lu, Q.** (2009). delta-Catenin promotes prostate cancer cell growth and progression by altering cell cycle and survival gene profiles. *Mol Cancer* **8**, 19.

**Zermati, Y., Garrido, C., Amsellem, S., Fishelson, S., Bouscary, D., Valensi, F., Varet, B., Solary, E. and Hermine, O.** (2001). Caspase activation is required for terminal erythroid differentiation. *J Exp Med* **193**, 247-54.

**Zhang, J., Lu, J. P., Suter, D. M., Krause, K. H., Fini, M. E., Chen, B. and Lu, Q.** (2010a). Isoform- and dose-sensitive feedback interactions between paired box 6 gene and delta-catenin in cell differentiation and death. *Exp Cell Res* **316**, 1070-81.

**Zhang, J. Y., Wang, Y., Zhang, D., Yang, Z. Q., Dong, X. J., Jiang, G. Y., Zhang, P. X., Dai, S. D., Dong, Q. Z., Han, Y. et al.** (2010b). delta-Catenin promotes malignant phenotype of non-small cell lung cancer by non-competitive

binding to E-cadherin with p120ctn in cytoplasm. *J Pathol*.

**Zheng, G., Lyons, J. G., Tan, T. K., Wang, Y., Hsu, T. T., Min, D., Succar, L., Rangan, G. K., Hu, M., Henderson, B. R. et al.** (2009). Disruption of E-cadherin by matrix metalloproteinase directly mediates epithelial-mesenchymal transition downstream of transforming growth factor-beta1 in renal tubular epithelial cells. *Am J Pathol* **175**, 580-91.

**Zhou, J., Liyanage, U., Medina, M., Ho, C., Simmons, A. D., Lovett, M. and Kosik, K. S.** (1997). Presenilin 1 interaction in the brain with a novel member of the Armadillo family. *Neuroreport* **8**, 2085-90.

## VITA

Dongmin Gu was born in Changshu, People's Republic of China, on September 30, 1977 to Jianchang Gu and Chuanzhen Dai. After attending Changshu No. 1 Middle School, he pursued a Bachelor of Medicine degree in Medicine from Nanjing Medical University in Nanjing, China, and he earned the degree in 2000. He continued to study for a Master of Science from the same university in Department of Biochemistry and Molecular Biology, where he conducted research on Transaldolase. After obtaining his master degree in 2003, Dongmin joined the same department as a junior faculty and taught biochemistry courses to undergraduate and graduate students. In 2004, Dongmin entered the United States of America to pursue his degree of Doctor of Philosophy in Biomedical Sciences from the University of Texas Health Science Center at Houston, Graduate School of Biomedical Sciences. Dongmin currently lives with his wife, Ying Liu, M.D., M.S. and daughter Grace L. Gu in Houston, Texas.

Permanent address:

7900 Cambridge St., Apt. 2-1A, Houston, Texas 77054